



PARIS
REINFORCE



PARIS
REINFORCE

28/11/2020

**D4.2 FIRST PORTFOLIO ANALYSIS OF
TECHNOLOGICAL AND POLICY MIXES**

WP4 – ROBUSTIFICATION & SOCIO-TECHNICAL
ANALYSIS TOOLBOX

Version: 1.00

www.paris-reinforce.eu



Disclaimer

The sole responsibility for the content of this publication lies with the authors. It does not necessarily reflect the opinion of the European Union. Neither the EASME nor the European Commission is responsible for any use that may be made of the information contained therein.

Copyright Message

This report, if not confidential, is licensed under a Creative Commons Attribution 4.0 International License (CC BY 4.0); a copy is available here: <https://creativecommons.org/licenses/by/4.0/>. You are free to share (copy and redistribute the material in any medium or format) and adapt (remix, transform, and build upon the material for any purpose, even commercially) under the following terms: (i) attribution (you must give appropriate credit, provide a link to the license, and indicate if changes were made; you may do so in any reasonable manner, but not in any way that suggests the licensor endorses you or your use); (ii) no additional restrictions (you may not apply legal terms or technological measures that legally restrict others from doing anything the license permits).

Grant Agreement Number	820846		Acronym	Paris Reinforce
Full Title	Delivering on the Paris Agreement: A demand-driven, integrated assessment modelling approach			
Topic	LC-CLA-01-2018			
Funding scheme	Horizon 2020, RIA – Research and Innovation Action			
Start Date	June 2019	Duration	36 Months	
Project URL	https://www.paris-reinforce.eu/			
EU Project Officer	Frederik Accoe			
Project Coordinator	National Technical University of Athens – NTUA			
Deliverable	D4.2 – First portfolio analysis of technological and policy mixes			
Work Package	WP4 – Robustification & Socio-Technical Analysis Toolbox			
Date of Delivery	Contractual	30/11/2020	Actual	28/11/2020
Nature	Report	Dissemination Level	Confidential	
Lead Beneficiary	NTUA			
Responsible Author	Alexandros Nikas	Email	anikas@epu.ntua.gr	
		Phone	+302107723612	
Contributors	Konstantinos Koasidis, Haris Doukas (NTUA); Dirk-Jan Van de Ven (BC3)			
Reviewer(s)	Ajay Gambhir (Imperial); Vangelis Marinakis (HOLISTIC); Alecos Kelemenis (NTUA)			
Keywords	Portfolio analysis, portfolio theory, multi-objective programming, uncertainty analysis, integrated assessment models, AUGMECON-R, Eastern Africa, COVID-19, recovery, Sustainable Development Goals, robustness			



EC Summary Requirements

1. Changes with respect to the DoA

No changes with respect to the work described in the DoA.

2. Dissemination and uptake

This deliverable aims to serve as a scientific framework for assessing integrated assessment modelling results throughout the PARIS REINFORCE project, in work packages WP5-WP7, against different types of uncertainty while looking into progress along non-climate sustainable development goals. It can also be used by policymakers and other stakeholders in Eastern Africa and the EU, showcasing optimal technological subsidy mixes in different contexts: achieving emissions cuts, along with health and access to energy co-benefits in the first case; and making the best of the announced COVID recovery plans in Europe, by achieving additional emissions cuts while creating new jobs in the energy sector and supporting the pandemic-impacted employment.

3. Short summary of results (<250 words)

As a starting point, this report establishes a multiple-uncertainty analysis framework for integrated assessment modelling of several Sustainable Development Goals (SDGs). It introduces a two-level integration of climate-economy modelling and portfolio analysis, to simulate technological subsidisation with implications for multiple SDGs, across socioeconomic trajectories, and considering different levels of uncertainties. The framework is validated in a real-world case study, applied in Sub-Saharan Africa, where it builds on the GCAM model and the well-established AUGMECON-2 multi-objective programming algorithm, to optimise technology subsidisation portfolios that achieve sustainable energy use, while contributing to SDGs 3 (air pollution-related mortality), 7 (access to clean energy), and 13 (climate change mitigation) in an uncertain future. Acknowledging the weaknesses of the selected multi-objective programming algorithm, the report then documents the development of a novel, enhanced and more robust variant of the method, AUGMECON-R, allowing to quickly resolve significantly more complex problems with any number of objectives. The enhanced framework is then applied on top of the first model inter-comparison exercise of the PARIS REINFORCE project, in line with its “where are we headed?” scenario logic, seeking to identify the optimal allocation of the green part of the announced recovery packages in the EU, with the aim to both achieve extra emissions reductions and lead to employment co-benefits in the entire energy sector.









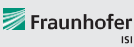









4. Evidence of accomplishment

This report, the three peer-reviewed publications (in Environmental Research Letters, Environmental Modelling & Software, and Operational Research), and the presentation of the EU case study results in the EASME knowledge sharing event (November 27, 2020).



Preface

PARIS REINFORCE will develop a novel, demand-driven, IAM-oriented assessment framework for effectively supporting the design and assessment of climate policies in the European Union as well as in other major emitters and selected less emitting countries, in respect to the Paris Agreement. By engaging policymakers and scientists/modellers, PARIS REINFORCE will create the open-access and transparent data exchange platform I2AM PARIS, in order to support the effective implementation of Nationally Determined Contributions, the preparation of future action pledges, the development of 2050 decarbonisation strategies, and the reinforcement of the 2023 Global Stocktake. Finally, PARIS REINFORCE will introduce innovative integrative processes, in which IAMs are further coupled with well-established methodological frameworks, in order to improve the robustness of modelling outcomes against different types of uncertainties.

NTUA - National Technical University of Athens	GR	
BC3 - Basque Centre for Climate Change	ES	
Bruegel - Bruegel AISBL	BE	
Cambridge - University of Cambridge	UK	
CICERO - Cicero Senter Klimaforskning Stiftelse	NO	
CMCC - Fondazione Centro Euro-Mediterraneo sui Cambiamenti Climatici	IT	
E4SMA - Energy Engineering Economic Environment Systems Modeling and Analysis	IT	
EPFL - École polytechnique fédérale de Lausanne	CH	
Fraunhofer ISI - Fraunhofer Institute for Systems and Innovation Research	DE	
Grantham - Imperial College of Science Technology and Medicine - Grantham Institute	UK	
HOLISTIC - Holistic P.C.	GR	
IEECP - Institute for European Energy and Climate Policy Stichting	NL	
SEURECO - Société Européenne d'Economie SARL	FR	
CDS/UnB - Centre for Sustainable Development of the University of Brasilia	BR	
CUP - China University of Petroleum-Beijing	CN	
IEF-RAS - Institute of Economic Forecasting - Russian Academy of Sciences	RU	
IGES - Institute for Global Environmental Strategies	JP	
TERI - The Energy and Resources Institute	IN	



Executive Summary

As a starting point, this report establishes a multiple-uncertainty analysis framework for integrated assessment modelling of several Sustainable Development Goals (SDGs). It introduces a two-level integration of climate-economy modelling and portfolio analysis, to simulate technological subsidisation with implications for multiple SDGs, across socioeconomic trajectories, and considering different levels of uncertainties. The framework is validated in a real-world case study, applied in Sub-Saharan Africa, where it builds on the GCAM model and the well-established AUGMECON-2 multi-objective programming algorithm, to optimise technology subsidisation portfolios that achieve sustainable energy use, while contributing to SDGs 3 (air pollution-related mortality), 7 (access to clean energy), and 13 (climate change mitigation) in an uncertain future. Acknowledging the weaknesses of the selected multi-objective programming algorithm, the report then documents the development of a novel, enhanced and more robust variant of the method, AUGMECON-R, allowing to quickly resolve significantly more complex problems with any number of objectives. The enhanced framework is then applied on top of the first model inter-comparison exercise of the PARIS REINFORCE project, in line with its “where are we headed?” scenario logic, seeking to identify the optimal allocation of the green part of the announced recovery packages in the EU, with the aim to both achieve extra emissions reductions and lead to employment co-benefits in the entire energy sector.

In particular, the pandemic has had a significant impact on the European economy, with approximately 1.8 million EU citizens losing their jobs between September 2019 and September 2020. Towards facilitating a recovery, the EU launched the Recovery and Resilience Facility (RRF) to provide €672.5 billion of financial support to Member States in the coming years. In line with the European Green Deal and climate efforts, 37% of investments in national plans requesting RRF financing must focus on a “green” transition. Integrated within the first PARIS REINFORCE model inter-comparison scenario logic of exploring “where the world is headed” based on current policies and pledges, we seek the optimal allocation of renewable energy subsidies from the COVID-19 recovery package in the EU. Towards further mitigating emissions and creating new jobs in the green transition, on top of a current policies scenario, we use budgets aligned with announced plans, and couple integrated assessment modelling with a technological portfolio analysis. We find that, for a €100-200 billion investment budget in 2021-2025, about 230-432k new jobs can be created by 2025 in the energy sector. The support package could also bring the EU (only slightly) closer to the new 2030 climate target: 50-233 MtCO_{2e} can be cut by 2030, corresponding to a 0.2-1% drop further down from the current policies scenario. Biofuels, wind, and biogas appear to be the most optimal technologies to subsidise against the two criteria, with small geothermal investments complementing portfolios. As solar energy already reaches high levels of penetration in a current policies scenario, additional subsidies push emissions higher due to increasing gas use for balancing grid load, while electric vehicles display expensive emissions cuts for negligible new jobs. Wind-based portfolios prioritising employment gains appear more robust against uncertainties; this shifts in favour of biofuels if larger investment capacity is assumed, maximising emissions reductions.



Contents

1	A multiple-uncertainty analysis framework for integrated assessment modelling of several sustainable development goals.....	9
1.1	Introduction.....	9
1.2	Methods.....	12
1.2.1	The Global Change Assessment Model	12
1.2.2	Multi-objective optimisation and portfolio analysis	15
1.2.3	A cross-scenario framework	16
1.2.4	Stochastic uncertainty analysis.....	18
1.2.5	A validation framework.....	18
1.3	Validation and Discussion.....	20
1.3.1	Context of the case study	20
1.3.2	Cost-effectiveness of technology subsidies and SDG progress	21
1.3.3	Robust subsidy portfolios in each individual SSP	24
1.3.4	Robust subsidy portfolios across all three SSPs	26
1.3.5	Empirical findings, discussion and results.....	27
1.4	Conclusions.....	28
2	A robust augmented ϵ-constraint method (AUGMECON-R) for finding exact solutions of multi-objective linear programming problems	31
2.1	Introduction.....	31
2.2	A brief overview of the augmented ϵ -constraint method	31
2.3	AUGMECON-R.....	33
2.3.1	Motivation.....	33
2.3.2	An improved search algorithm.....	34
2.3.3	Source code.....	38
2.4	Comparative analysis and discussion.....	39
2.4.1	Reference benchmark problems.....	39
2.4.2	Complex benchmark problems	41
2.5	Conclusions.....	46
3	Optimal allocation of renewable energy subsidies from the COVID-19 recovery package: Mitigating emissions and creating new jobs	47
3.1	Introduction.....	47
3.2	Methods.....	49
3.3	Results and Discussion.....	51
3.3.1	Portfolios with budget of €100 billion	51
3.3.2	Portfolios with budget of €150 billion	53
3.3.3	Portfolios with budget of €200 billion	55
3.3.4	Discussion	56
3.4	Key takeaways	57



Bibliography	59
Appendix A: Source code of AUGMECON-R	71
Appendix B: Datasets used for the complex problems	79
<i>B.1 Dataset of the 4kp40 problem</i>	79
<i>B.2 Dataset of the 4kp50 binary problem</i>	81
<i>B.3 Dataset of the 5kp40 binary problem</i>	84
<i>B.4 Dataset of the 6kp50 binary problem</i>	86

Table of Figures

Figure 1 Methodological Framework.....	12
Figure 2 GCAM - PA model integration (inputs and outputs).....	14
Figure 3 The PA optimisation problem formulation.....	17
Figure 4 Impact of energy technology subsidies in terms of energy access levels for the different SSPs by 2020, 2030 and 2040.	22
Figure 5 Impact of energy technology subsidies in terms of GHG emissions for the different SSPs by 2020, 2030 and 2040.....	23
Figure 6 Impact of energy technology subsidies in terms of mortality for the different SSPs, by 2020, 2030 and 2040.....	24
Figure 7 Technology subsidy portfolios that are Pareto-optimal in terms of simultaneously avoiding GHG emissions, premature deaths and improving energy access per SSP in 2020. Size of dots illustrates robustness against stochastic uncertainty of modelling parameters.....	25
Figure 8 Technology subsidy portfolios that are Pareto-optimal in terms of simultaneously avoiding GHG emissions, premature deaths and improving energy access per SSP in 2030. Size of dots illustrates robustness against stochastic uncertainty of modelling parameters.....	25
Figure 9 Technology subsidy portfolios that are Pareto-optimal in terms of simultaneously avoiding GHG emissions, premature deaths and improving energy access per SSP in 2040. Size of dots illustrates robustness against stochastic uncertainty of modelling parameters.....	26
Figure 10 Technology subsidy portfolios that are Pareto-optimal in terms of simultaneously avoiding GHG emissions, premature deaths and improving energy access in 2020, 2030 and 2040. Size of dots illustrates robustness against SSP uncertainty.....	27
Figure 11 Flowchart of the AUGMECON-R algorithm.....	38
Figure 12 The Pareto front of the 4kp40 problem.	42
Figure 13 The Pareto front of the 4kp50 problem.	43
Figure 14 The Pareto front of the 5kp40 problem.	45
Figure 15 The Pareto front of the 6kp50 problem.	45
Figure 16: Optimal Portfolios and technologies participation (€100 billion).....	52
Figure 17: Technologies participation in the Monte Carlo simulations (€100 billion)	52
Figure 18: Pareto Front of robust portfolios (€100 billion)	53
Figure 19: Optimal Portfolios and technologies participation (€150 billion).....	53
Figure 20: Technologies participation in the Monte Carlo simulations (€150 billion)	54
Figure 21: Pareto Front of robust portfolios (€150 billion)	55
Figure 22: Optimal Portfolios and technologies participation (€200 billion).....	55



Figure 23: Technologies participation in the Monte Carlo simulations (€200 billion)	56
Figure 22: Pareto Front of robust portfolios (€200 billion)	56

Table of Tables

Table 1 Uncertainty boundaries (ranges of the uniform distribution) for a timepoint.....	19
Table 2 Example of SSP-based uncertainty boundaries for robustness (technology #1) for 2020. Each row represents a different subsidy level.....	19
Table 3 Evolution of key SSP parameters in GCAM	20
Table 4 Decrease in GCAM output ranges between SSPs for each of the three SDGs when selecting a portfolio of higher robustness score.....	27
Table 5 Ranges of total impact and contributions per technology for the most robust Pareto optimal subsidy portfolios across SSPs.....	28
Table 6 Payoff table of example problem.....	35
Table 7 Grid points of the example problem.....	36
Table 8 Performance comparison between AUGMECON 2 (AUGM 2) and AUGMECON-R (AUGM-R) for the 3kpY problems.	39
Table 9 Comparison ratios of performance of AUGMECON 2 over AUGMECON-R for the 3kpY problems.....	40
Table 10 Performance comparison between AUGMECON 2 (AUGM 2) and AUGMECON-R (AUGM-R) for the 3kpY problems with lower bounds.	40
Table 11 Performance comparison between AUGMECON 2 and AUGMECON-R for the 4kp40 problem, with the true nadir points (4kp40) and with lower bounds (4kp40*).....	42
Table 12 Performance comparison between AUGMECON 2 and AUGMECON-R for the 4kp50 problem, with the true nadir points (4kp50) and with lower bounds (4kp50*).....	43
Table 13 Performance comparison between AUGMECON 2 and AUGMECON-R for the 5kp40 problem, with the true nadir points (5kp40) and with lower bounds (5kp40*).....	44
Table 14 Performance comparison between AUGMECON 2 and AUGMECON-R for the 6kp50 problem, with the true nadir points (6kp50) and with lower bounds (6kp50*).....	45
Table 15 Job Assumptions per technology	50



1 A multiple-uncertainty analysis framework for integrated assessment modelling of several sustainable development goals

This section builds on the PARIS REINFORCE publication in Environmental Research Letters (Van de Ven et al., 2019) and has been peer-reviewed and published in Environmental Modelling & Software (Forouli et al., 2020).

1.1 Introduction

Integrated Assessment Models (IAMs) are a core element of the scientific processes that comprise the “best available science” (Peters, 2016), when it comes to analysing energy system transitions within the context of climate change mitigation and sustainable socioeconomic development (Nikas et al., 2019; Pietzcker et al., 2017; Schwanitz, 2013; Janssen et al., 2009). These tools are applied to analyse adaptive energy–environment–economy systems in the global scientific and policy arena (Ewert et al., 2015; Gidden et al., 2018; Estrada et al., 2019), advance scientific understanding of the potential to combat climate change and underlying dynamics towards robust and sustainable development (Huppmann et al., 2019; Warren et al., 2019), and evaluate the various technologies, initiatives and policy options that ensure clean and sustainable energy transition (Wyrwa, 2015; Shi et al., 2017; Liu et al., 2019).

In particular, these models constitute a well-established scientific tool aimed at understanding feedbacks and influences between different system components, including the social, economic and ecological implications of different natural or anthropogenic factors, especially with regard to interlinkages between the human and the natural system (Calvin and Bond-Lamberty, 2018; Gidden et al., 2018). The core advantage of these complex models is that they provide an integrated system perspective to study the dauntingly complex interactions between energy, economy, land use, water, and climate systems (Scott et al., 1999; Weyant, 2017). Through such an integration, IAMs combine multiple and diverse components across their social, organisational and conceptual boundaries to provide a comprehensive analysis of the problem (Collins et al., 2015; Jakeman and Letcher, 2003). For this purpose, different modules or components are coupled with one other, usually including but not limited to the economy, the environment, the energy system and the climate feedbacks or economic impacts of changes among them (Giupponi et al., 2013). Modelling results are widely used to, inter alia, directly influence decisions and taken stock of towards advising policymakers, as is the case of the assessment reports of the Intergovernmental Panel on Climate Change (IPCC). Recent examples of publications where IAMs contribute to providing background information on possible energy and climate futures, and to scientifically underpinning international climate policy negotiations are the IPCC’s special report on the impacts of global warming of 1.5 °C above pre-industrial levels (IPCC, 2018), the World Energy Outlook 2018 (International Energy Agency, 2018), or the European Union (EU) Energy Roadmap 2050 (EC COM, 2016). In this respect, decision makers are based on IAM-driven policy prescriptions to develop policies that contribute to managing environmental resources and assets in a way that delivers acceptable environmental and socioeconomic outcomes. More details on IAMs can be found in Krey (2014), Weyant (2017) and Nikas et al (2019), which review energy – economic models, including or focusing on IAMs, and provide a categorisation of them based on parameters like their degree of integration and mathematical underpinnings, as well as highlight the challenges associated with these modelling frameworks.

Given their strengths and weaknesses (Hamilton et al., 2015), however, analyses based exclusively on these formalised frameworks alone are usually not sufficient to address the broad spectrum of challenges associated with climate change and policy assessment (Doukas et al., 2018), and recent advances and paradigms call for



and/or apply complementing them with other methods and tools (Turnheim et al., 2015; Geels et al., 2016). In this direction, IAMs have recently been coupled with a diversity of tools, towards enhancing scientific processes and leading to more pragmatic policy prescriptions, including but not limited to life cycle analyses (Arvesen et al., 2018), fuzzy cognitive mapping (Nikas et al., 2020; Antosiewicz et al., 2020), and multiple criteria decision aid frameworks (Baležentis and Streimikiene, 2017; Shmelev and Van den Bergh, 2016). One of these tools, which has been established in the climate policy domain (Doukas and Nikas, 2020) in diverse applications (Allan et al., 2011; Bistline, 2016; Odeh et al., 2018; Zhang et al., 2018) and long been coupled with IAMs (e.g. Baker and Solak, 2011; Pugh et al., 2011; Forouli et al., 2019a; Forouli et al., 2019b; del Granado et al., 2019), is portfolio theory.

In fact, energy planning decisions are often portfolio building problems, in which the task is to find a viable mix of actions to meet the overall objectives, targets, and constraints. Therefore, today, as many energy-related decisions fall into this category, portfolio decision analysis methods and tools are seen as the next step in energy decision support (Marinoni et al., 2011; Vilkkumaa et al., 2014). Through such tools, decision makers are able to consider a set of actions and create policy incorporating relevant concerns and interests in a balanced way. Typically, decision makers have to consider the overall performance of a portfolio across many relevant dimensions or criteria, such as techno-economic, socio-political and environmental impacts (Huang and Wu, 2008; Muñoz et al., 2009). Portfolio analysis (PA) addresses the need to consider multiple objectives and constraints, and further contributes to identifying promising candidate actions and examining interactions among them.

Portfolio decision models were first applied on risk diversification in financial investments and have their roots to the work of Markowitz (1952). Markowitz proposed a mean-variance model to support investment decisions in light of uncertainty associated with the future returns of financial assets. Today, there is a range of portfolio modelling approaches, which offer modelling and optimisation support to find the most preferred portfolio of actions, and which are applicable to energy and environmental modelling. Lahtinen et al. (2017) provide a detailed, comparative description of portfolio modelling approaches. Among the most common ones are the value–cost (or benefit–cost) approach, where actions are prioritised according to the value–cost ratio until a budget cap is reached (Hajkowicz et al., 2008; Marinoni et al., 2011). The disadvantage of this method is that, in case of synergies or interactions between the actions, optimality is not guaranteed. As interactions play a critical role in energy-and/or climate-economy problems, this approach is often not sufficient. An approach that incorporates the risk parameter into the evaluation is the modern portfolio theory approach where the optimal resource allocation for each risk level is identified (Crowe and Parker, 2008; Paydar and Qureshi, 2012).

From the above, we understand that PA and IAMs are widely used in policy analysis and evaluation of pathways for the transformation of the human and earth systems. The interconnectedness of our world is broadly acknowledged to require integrated rather than piecemeal approaches to resolving complex environmental issues, particularly in view of the increasing speed and pervasiveness of connections associated with globalisation. With the interaction of Sustainable Development Goals (SDGs) with climate change and action gaining increasing prominence at the interface of science and policy, developing computational tools and models that operate across academic disciplines and methodologies becomes ever more important.

In this paper, we use a multi-objective optimisation approach where the result is a set of non-dominated portfolios. Through this approach, interactions among the set of actions and portfolio constraints can be considered. The goal is to generate non-dominated combinations of actions, in terms of comparing between the evaluation criteria. As required by portfolio modelling, and in order to generate the non-dominated portfolios, all candidate actions are simultaneously considered and optimised in the same portfolio optimisation model. The goal is to identify optimal portfolios of actions or a set of non-dominated portfolios that best meet multiple objectives while satisfying the problem constraints. Decision makers can then select a portfolio among the non-



dominated ones, tailored to their needs and preferences. To understand the term of portfolio dominance, a portfolio is said to be dominated, if there exists another portfolio of actions that performs better in some attribute (criterion) and at least equally good in all other attributes. The model-based portfolio generation process proposed here supports the consideration of multiple objectives and constraints, and interactions among the actions, while acknowledging the vital role of uncertainty.

In particular, the first goal of this paper is to create an efficient scientific workflow and a two-way technical integration of integrated assessment modelling and portfolio optimisation outcomes. To this end, at first, we simulate future policy under policy-relevant socioeconomic scenarios, such as the Shared Socioeconomic Pathways (SSPs) (O'Neill et al., 2014). The Global Change Assessment Model (GCAM) is used as the implementation integrated assessment model¹. The outputs from each policy scenario are translated into progress parameters relevant to three SDGs of the United Nations' 2030 Agenda for Sustainable Development and fed into a PA model. These parameters include air pollution-related mortality (SDG3), access to clean energy (SDG7) and greenhouse gas emissions (SDG13). The optimisation problem formulation is run for selecting the optimal combinations of subsidy levels for six technologies, which simultaneously maximise progress in each of the selected SDGs. This is the first step of IAM-PA integration.

Moreover, acknowledging that uncertainty is widely accepted to be pervasive in any attempt to manage and understand environmental problems (Uusitalo et al., 2015), a robustness analysis is incorporated in the proposed framework. Depending on the discipline and context of application, uncertainty of data or model components can be interpreted in different ways, varying from measures of performance, bounds, alternative scenarios (Fuss et al., 2012; Trachanas et al., 2018) or probability distributions (Lin and Beck, 2012). In this approach, the propagation of uncertainties through the integrated models involves determining the effect on the output of changes in the inputs and is expressed stochastically, by means of a probability distribution, and deterministically, with the use of scenarios. Probabilistic uncertainty is incorporated in the portfolio analysis model to find robust Pareto-optimal portfolios of technologies in each of SSPs. Deterministic uncertainty, referring to specific scenarios with clearly determined datasets (Nikas et al., 2019), is used to assess the robustness of the modelling results across different socioeconomic pathways and timescales (Van Groenendaal and Kleijnen, 2002). This is done primarily by using different SSPs, which represent epistemic uncertainty (Hanger-Kopp et al., 2019) but constitute reference single futures of deterministic nature, on which modelling exercises anchor to cover a broad spectrum of possible future socioeconomic states of the world (van Ruijven et al., 2014). The second goal of this paper is to simulate an "SSP robustness" scenario, by defining SSP-based uncertainty bounds as boundaries for robustness and simulate probabilistic uncertainty among the socioeconomic pathways. Results of the "SSP robustness" scenario are compared with results of the distinct socioeconomic pathways analysis.

The second step of IAM-PA integration is achieved by feeding the PA results back to GCAM. The SSP-robust subsidy portfolios are re-run in the GCAM model with each SSP, to check whether portfolios that are found to be robust to SSP-based uncertainty are also translated to more homogeneity between the SSPs with respect to the portfolio's impact on SDG progress. The identification of technological portfolios that are robust among the different SSPs can be helpful for stakeholders to make decisions and formulate policies that will be optimal, independently of the realisation of different SSPs in the future, providing a useful tool to handle SSP-based uncertainty.

¹ The updated GCAM documentation website includes a specific section describing the SSP implementation throughout the model: <https://github.com/JGCRI/gcam-doc/blob/gh-pages/ssp.md>



Validation of the methodological framework, which is outlined in Figure 1, is achieved by means of a case study in Eastern Africa, in Section 3.

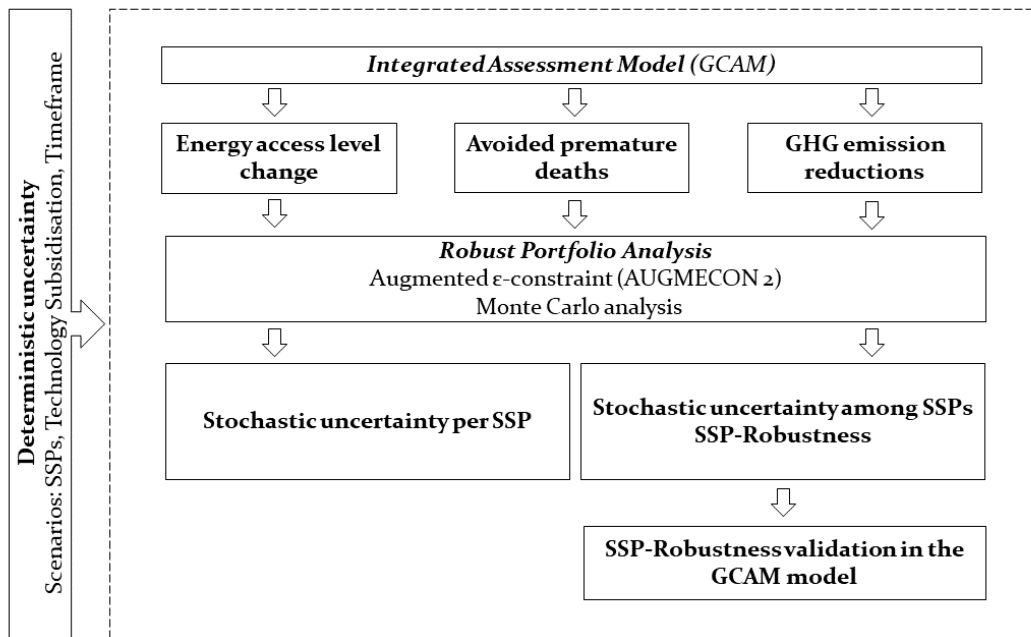


Figure 1 Methodological Framework

1.2 Methods

1.2.1 The Global Change Assessment Model

GCAM is a dynamic-recursive, partial equilibrium model connecting socioeconomics, energy, land use and climate systems, and can be used to investigate the consequences of climate change mitigation policies, including carbon taxes, carbon trading, regulations and accelerated deployment of energy technology (JGCRI, 2017). GCAM and its predecessors have been used in applications investigating future emission scenarios and energy technology pathways (Edmonds et al., 1994; Rao et al., 2017). GCAM is one of the four models chosen to develop the Representative Concentration Pathways of the IPCC's 5th Assessment Report (Pachauri et al., 2015) and has been included in almost all major climate/energy assessments over the last few decades. The model covers the entire world, dividing it into 32 regions, and runs in 5-year time steps from 1990 to 2100, simulating future emission paths for 24 greenhouse gases and short-lived species, including CO₂ (from fossil fuel combustion and land use change), CH₄, N₂O, NO_x, SO₂, BC, OC, CO and NMVOC.

For the purposes of this study, GCAM version 4.4 is used as a base. Within this model, the case study region in the model (eastern Africa, see section 3.1) has been adjusted for a more informed reflection of modern, real-world conditions (Van de Ven et al., 2019). In particular, urban energy demand has been separated from rural energy demand (Yu et al., 2014); and specific residential energy demands, such as cooking, lighting, refrigeration and TVs, separated from other residential energy uses. Especially demand for cooking has been modelled in more detail, improving realistic projections into future cooking energy use, and its impacts on indoor and outdoor air quality. These impacts on air quality are quantified by measuring the premature deaths that air pollution (both indoor and outdoor) is projected to cause in future scenarios. Indoor mortality is estimated by extrapolating a historical causal



relationship between indoor PM2.5 and mortality measured by the Global Burden of Disease (Forouzanfar et al, 2016). Outdoor mortality is measured through the air quality model TM5-FASST (Van Dingenen et al., 2018). Furthermore, additional costs have been added to the provision of centrally generated electricity to rural areas, representing the required extensions in transmission and distribution networks, while mini-grids have been added as an alternative for rural energy demand. This novelty allows for projecting more realistic future scenarios in terms of household energy access, which has been measured on a household level using the “Tier framework” (World Bank, 2015). See Van de Ven et al (2019) for all details on how GCAM outputs are translated to SDG progress indicators.

The inputs used to run the GCAM model and the outputs retrieved to be utilised as input in the portfolio analysis (PA) model are presented in Figure 2. Inputs to GCAM include socioeconomic data for different SSPs, such as population, gross domestic product (GDP), rate of urbanisation, energy demand, food demand, household discount rates, agricultural yields, energy resource productivity and emission factors. Outputs, to be used in the PA model, include energy access tier changes, avoided premature deaths and GHG emission reductions as a result of different subsidy levels for a number of sustainable technologies, per SSP and time point (2020, 2030 and 2040).



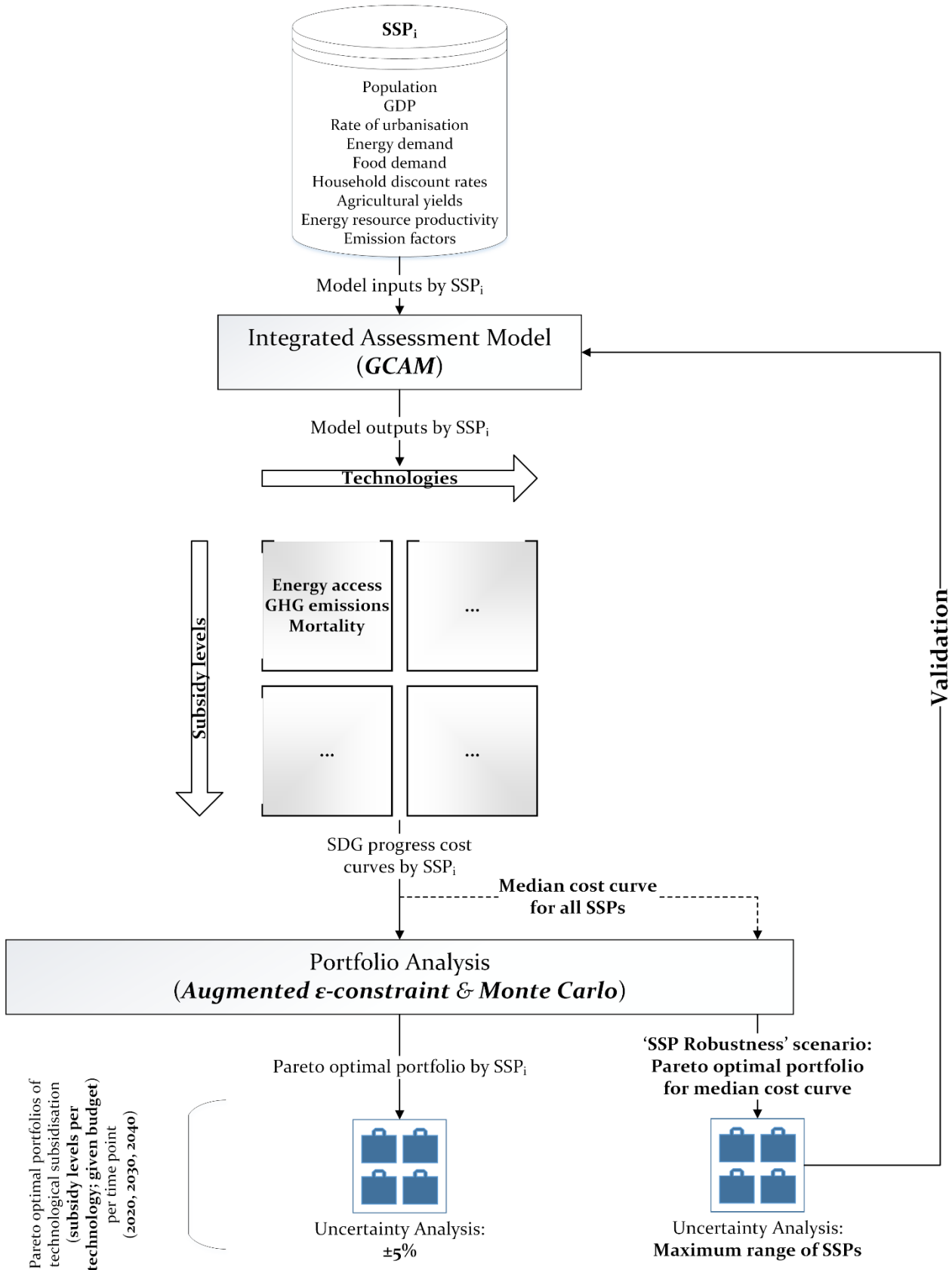


Figure 2 GCAM - PA model integration (inputs and outputs)

1.2.2 Multi-objective optimisation and portfolio analysis

Multi-objective optimisation refers to the simultaneous optimisation (i.e. minimisation or maximisation) of multiple, usually conflicting, objective functions. Once such a problem is posed, it is of the practitioner's interest to obtain/approximate and view the set of all trade-off, or compromise, solutions of the problem. The set of trade-off solutions is referred to, in the current article, as the Pareto front of the problem. As environmental problems are driven by multiple objectives and criteria, a single optimal solution very rarely exists. Rather, a Pareto set of solutions can be identified, within which no single solution is strictly better than any other and a trade-off is required between the competing objectives.

If the variables of a multi-objective optimisation problem take values from a continuous set, then we refer to that problem as a multi-objective continuous optimisation problem. On the other hand, if the variables take values from a set of integers, then the problem is referred to as a multi-objective integer programming (MOIP) problem. In this paper we model and solve a MOIP problem.

The most widely used methods concerning the identification of Pareto optimal solutions are the weighting and ϵ -constraint methods. Especially in cases of integer programming the ϵ -constraint method has better performance and certain advantages over the weighting generation methods (Steuer, 1989). In the principle of the ϵ -constraint method lies the optimisation of one of the objective functions (p) using the other objective functions ($p - 1$) as constraints. Only portfolios that are non-dominated (i.e. when none of the objective functions can be improved in performance without degrading one or more of the other objective function values) can be considered as portfolios that represent the optimal trade-off between objectives. For the purpose of identifying the non-dominated, or 'Pareto-optimal' solutions to the mathematical optimisation formulation, here the use of an extension of the ϵ -constraint method, namely the augmented ϵ -constraint (AUGMECON 2) (Mavrotas and Florios, 2013) algorithm is suggested. The AUGMECON 2 method guarantees the generation of all Pareto optimal solutions, while avoiding the generation of other, non-optimal solutions. The AUGMECON 2 method can deal with multiple objectives simultaneously and has been successful in recent optimisation studies in a variety of fields concerning municipal solid waste management (Mavrotas et al., 2013), energy efficiency policies evaluation (Forouli et al., 2019b), power generation technology portfolio optimisation (Forouli et al., 2019a), equity portfolio construction and selection (Xidonas et al., 2010), biopharmaceutical processes (Vieira et al., 2017), surface mounting devices machines component allocation (Torabi et al., 2013), etc.

In the AUGMECON 2 method the problem to be solved is of the following form:

$$\max (f_1(x) + eps * \left(\frac{S_2}{r_2} + 10^{-1} * \frac{S_3}{r_3} + \dots + 10^{-(p-2)} * \frac{S_p}{r_p} \right))$$

with the following constraints:

Subject to:

$$X \in F$$

$$f_k(X) - S_k = e_k, k = 2..p$$

where

$f_k(X)$ is the objective function to be maximised

F is the feasible region

$$eps \in [10^{-6}, 10^{-3}]$$

e_k is the right-hand side of the corresponding constraint for the objective function k .



r_k is the range of the objective function k .

S_k is a surplus variable for objective function k .

The optimisation process is driven by the parametrical variation in the right-hand side of the constrained objective functions (e_k).

At first, the range r_k of objective functions 2.. p that will be used as constraints is calculated, from the payoff table (the table with the results from the individual optimisation of the p objective functions). The AUGMECON 2 method proposes the use of lexicographic optimisation for every objective function in order to construct the payoff table with only Pareto optimal solutions.

The range of the k – th objective function is divided to g_k intervals using $g_k - 1$ intermediate equidistant grid points. Thus, we have in total $g_k + 1$ grid points that are used to vary parametrically the right-hand side (e_k) of the k th objective function. The step for the variation of e_k for objective function k will be:

$$step_k = \frac{r_k}{g_k}$$

And the right-hand side of the corresponding constraint in the i th iteration for objective function k will be:

$$e_k = fmin_k + i_k * step_k$$

$fmin_k$ is the minimum from the payoff table of objective function k

The optimisation process is solved iteratively for the different e_k , which correspond to the different grid points, and so the number of runs are $(g_2 + 1) * (g_3 + 1) * ... * (g_p + 1)$. Supposing we first begin to optimise by adding $step_2$ to e_2 . In each iteration we compare the surplus variable (S_2) of objective function f_2 that corresponds to the innermost objective function (i.e. the first of the p objective functions from which we begin) with $step_2$. When the surplus variable S_2 is larger than $step_2$, it is implied that in the next iteration the same solution will be obtained with the only difference being the surplus variable, which will now have the value $S_2 - step_2$. This makes the iteration redundant and therefore we can bypass it as no new Pareto optimal solution is generated. We then calculate the new e'_2 by moving forward by $step_2$, until all grid points of f_2 are either assessed or bypassed. Then we repeat the same procedure by varying the right-hand side of f_3 , namely e_3 , and the iterations are repeated for the p objecting functions. Following the above calculation procedure, we obtain the exact Pareto set of optimal solutions.

For a more in-depth description on finding the exact pareto set in multi-objective integer programming problems with the use of the augmented ϵ -constraint, the reader is referred to (Mavrotas and Florios, 2013). The portfolio optimisation problem is solved in the General Algebraic Modelling System (GAMS). The portfolio analysis parameters coming from GCAM (Section 2.1) include the three parameters relevant to progress across three different SDGs: energy access tier change, GHG emission cuts, and avoided premature deaths due to air pollution (Figure 2).

1.2.3 A cross-scenario framework

To understand the impact of technology subsidies, the GCAM modelling exercise considers subsidies for different energy technology packages, in combination with three different socioeconomic pathways. In the context of the region of the case study focus, i.e. Eastern Africa, SSPs 3 and 5 can be seen as extreme scenarios of respectively low and high development and are expected to represent the margins of uncertainty for policy implementation, drawing from both the narratives associated with the SSP framework (O'Neill et al., 2017) and the GCAM outputs. In a few situations, however, the average conditions as represented in SSP 2, which reflects a possible future



following historic patterns, translate to the highest (or lowest, depending on the technology) cost-effectiveness of technological subsidisation. Results for SSP 1 ('Sustainability') and SSP 4 ('Inequality') are assumed to lie in most cases within the margins of the three modelled SSPs, and therefore neither of these two scenarios have been modelled explicitly. The optimisation portfolio analysis problem (Figure 3) is thus run separately for each of the three SSPs (2, 3, and 5).

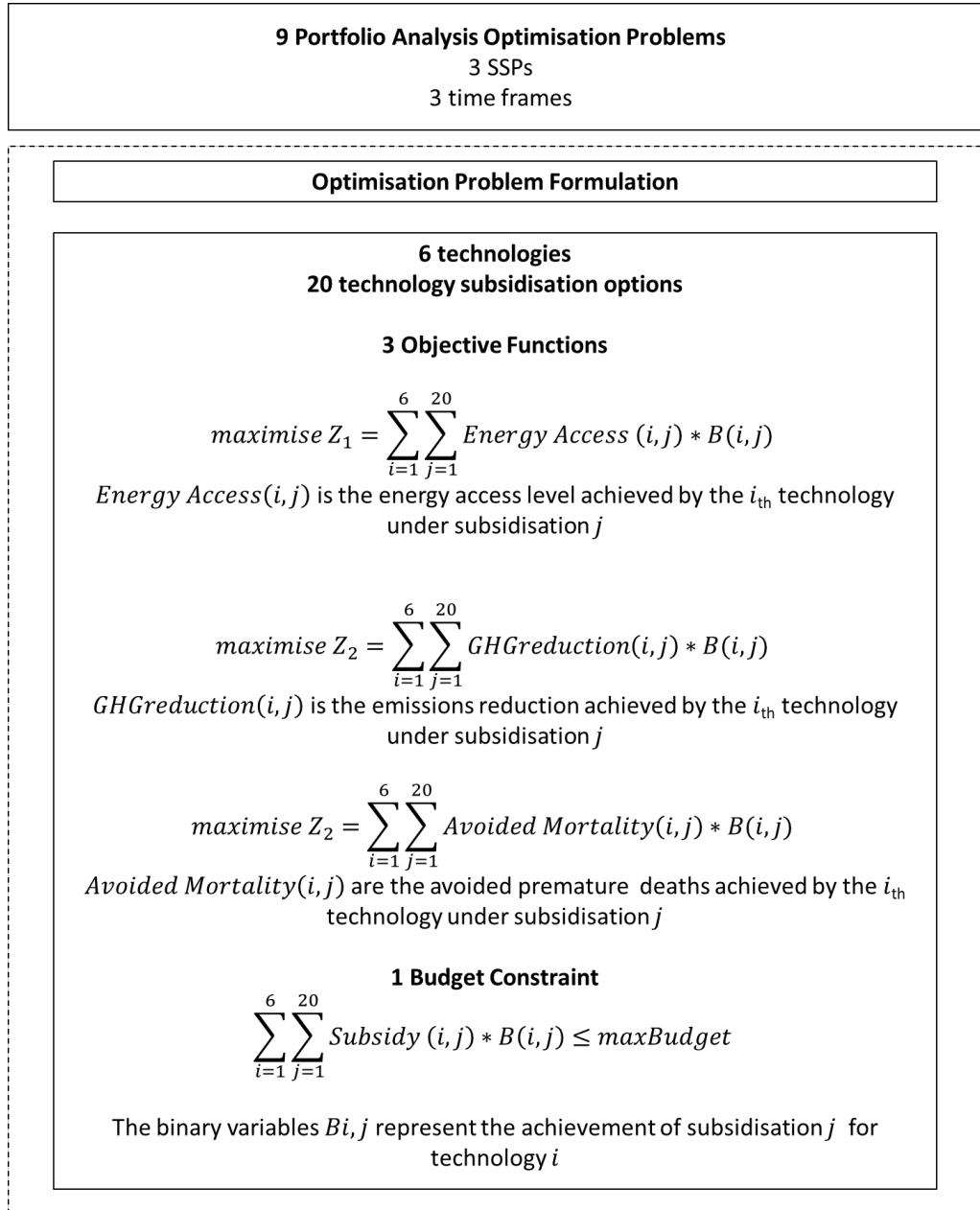


Figure 3 The PA optimisation problem formulation

We identify three evaluation criteria or objectives to optimise and thus we formulate a tri-objective optimisation problem. The evaluation criteria include the maximisation of GHG emission reductions, the maximisation of energy access tier improvement, and the maximisation of avoided premature deaths; corresponding to SDG13 ('climate action'), SDG7 ('affordable and clean energy'), and SDG 3 ('good health and well-being'), respectively. The three different time points are reflected as differences in the values of the portfolio analysis input data. Last but not



least, the model considers a subsidy budget constraint in order to ensure that the overall cost of the approved applications does not exceed a predefined value. Ultimately, nine portfolio optimisation problems are solved: three for each of the different timescales (2020, 2030 and 2040), for each of the three SSPs (SSP2, SSP3 and SPP5).

1.2.4 Stochastic uncertainty analysis

The proposed approach examines the effects of both deterministic and stochastic (non-deterministic) uncertainty in order to effectively assess the robustness of the resulting optimal portfolios. Deterministic uncertainty is expressed by means of the above-described scenario analysis: we consider different scenarios in terms of technology performance in each of the three time frames but, more importantly, the optimality of solutions is stress-tested across the three socioeconomic scenarios. Regarding stochastic uncertainty, which is inherent in these parameters, this is incorporated into the model by running a Monte Carlo simulation. The uncertain model parameters, namely the performance of the assumed technologies in terms of maximising emission reductions, energy access and health benefits, are treated as of stochastic nature, by sampling their values using a uniform distribution. At first, we run the model using deterministic values for all the uncertain parameters and the “no uncertainty” Pareto front is determined. Then, Monte Carlo simulation is performed iteratively to sample random values for the uncertain parameters from the uniform distributions, and the model is solved to generate the set of Pareto-optimal portfolios. Eventually, the execution of multiple Monte Carlo iterations results in many differentiated Pareto fronts, which are analysed to draw conclusions over the robustness of the portfolios shaping the Pareto front when no uncertainty is considered. We perform 1,000 Monte Carlo iterations.

As discussed above, the GCAM model is run for the three SSP scenarios separately for every subsidy level. The SSPs are seen here as an uncertain set of conditions that affect the performance of every technological subsidy policy. For the three major optimisation problems run to identify the optimal portfolios separately for each of the three considered SSPs, the mean value for the uniform distributions is set equal to the estimated values as obtained from the runs of the GCAM model, and the deviation of the Monte Carlo iterations is set equal to $\pm 5\%$, as in Forouli et al. (2019a).

1.2.5 A validation framework

In order to perform a robustness analysis on the modelling results of the individual SSPs, we introduce the “SSP robustness” scenario. The “SSP robustness” scenario is not run in the GCAM model as a new scenario, and there is no intention to introduce a new scenario to “replace” or simulate any of the SSPs. As already mentioned, GCAM is run for the individual SSPs and generates results per SSP, regarding the impact of each technology subsidisation option on the three parameters: energy access change, GHG emissions reductions, and avoided deaths associated to air pollution. This impact is different per SSP. Our purpose is to define robust subsidy portfolios regardless of what SSP our world will resemble in the future. The “SSP robustness” scenario uses the mid-point of the SSP scenario outcomes on the cost effectiveness for progress along these parameters corresponding to the three SDGs and uses the range along the three SSP outcomes to perform a robustness analysis. Uncertainty over which SSP is expected to be realised in the future is therefore incorporated in the portfolio analysis, as a range for the cost-effectiveness of the technologies in achieving progress to each of the SDGs (Van de Ven et al., 2019). In this way, the range of the GCAM SSP simulation outcomes, which are different for each technology, define the ranges of the uniform distribution, which is used for Monte Carlo simulation. Uncertainty ranges differ among the considered technologies: the higher the range of the SSP outcomes is, the broader the range of uncertainty in the uniform distribution is considered. A portfolio analysis problem, in which technologies with narrow uncertainty boundaries are optimised, is thus expected to be more robust among the different SSPs, compared to one with a larger uncertainty range, depicting higher vulnerability to the SSP simulation outcomes. To better clarify this, in the



extreme scenario where the resulting performance of a technology is identical among the different SSPs, portfolios resulting from the optimisation will be completely robust, when uncertainty is examined in terms of different SSP realisation. The ranges of the uniform distributions (SSP-based uncertainty boundaries) and an example of calculating the SSP-based uncertainty boundaries based on the mid-point of the performances across the three SSPs are presented in Tables 1-2.

Table 1 Uncertainty boundaries (ranges of the uniform distribution) for a timepoint.

Uncertainty boundaries (ranges of the uniform distribution)			
Technology	Indicator #1	Indicator #2	Indicator #3
Technology #1	[0.99,1.01]	[0.98,1.02]	[0.98,1.02]
Technology #2	[0.98, 1.02]	[0.99, 1.01]	[0.95, 1.05]
Technology #3	[0.98, 1.02]	[0.99, 1.01]	[0.89, 1.11]
Technology #4	[0.89, 1.11]	[0.90, 1.10]	[0.90, 1.10]
Technology #5	[0.97, 1.03]	[0.96, 1.04]	[0.91, 1.09]
Technology #6	[0.72, 1.28]	[0.61, 1.39]	[0.93, 1.07]

Table 2 Example of SSP-based uncertainty boundaries for robustness (technology #1) for 2020. Each row represents a different subsidy level

Mid-point of the performances across three SSPs			Range of performances across the three SSPs			% Range of performances across the three SSPs		
Indicator #1	Indicator #2	Indicator #3	Indicator #1	Indicator #2	Indicator #3	Indicator #1	Indicator #2	Indicator #3
0.000439	62.9566	0.17109	4.2E-06	0.436791	0.001689	0.96%	0.69%	0.99%
0.003189	455.108	1.24059	2.25E-05	2.955247	0.016963	0.71%	0.65%	1.37%
0.00579	825.195	2.25515	3.66E-05	12.78863	0.033728	0.63%	1.55%	1.50%
0.161016	23751.5	59.9151	0.00087	746.8392	1.943537	0.54%	3.14%	3.24%
Uncertainty boundaries (ranges of the uniform distribution) = distance from avg. of the % Range of performances across the 3 SSPs						[0.99,1.01]	[0.98,1.02]	[0.98,1.02]

In order to verify if the robustness of SSP uncertainty bounds leads to more robust solutions among the different SSPs, optimal portfolios of the "SSP robustness" scenario differing in their robustness score are selected and reiterated in the GCAM model. The reiteration is applied across the three different SSPs. New results on the contribution of the technologies to each of the SDGs are retrieved and the goal is to test whether the results of a more robust portfolio are indeed more homogeneous between the different SSPs compared to a less robust one. This is quantified by measuring the ranges of performances across the three SDGs, among the SSPs, and verifying that they are smaller in case of a more robust portfolio.

To summarise the information flow into, between and out of the two models (Figure 2), the GCAM model is initially fed with socioeconomic data from three SSPs and its outputs are used to calculate avoided premature mortality due to air pollution, GHG emissions cuts and energy access levels associated with different subsidisation levels for a number of sustainable technologies. The latter, along with a given total budget, are fed into the PA model, which calculates the most robust near-optimal technology subsidisation portfolios for three timescales (2020, 2030 and 2040) per SSP, carrying out Monte Carlo analysis within a $\pm 5\%$ uncertainty range for each of the three SDG-relevant parameters. At the same time, an additional subsidy dataset is developed, based on the midpoint of the



extreme GCAM-resulting outcomes in terms of cost-effectiveness of technology subsidies for SDG progress (separately for each technology and SDG impact); Monte Carlo analysis for this extra scenario is performed in a different uncertainty range that is defined by the extreme values of each parameter for each subsidy level and technology. Finally, optimal subsidy levels for each technology, from selected portfolios of this scenario of various robustness scores, are fed back into GCAM, in order to validate whether portfolios with higher robustness scores are indeed more robust to the impact of SSP-related modelling inputs on outputs in terms of the cost-effectiveness of SDG progress.

1.3 Validation and Discussion

1.3.1 Context of the case study

Three different SSP datasets (O'Neill et al., 2014) have been modelled in GCAM for the purposes of a case study focusing on twelve Eastern African countries (Burundi, Comoros, Djibouti, Eritrea, Ethiopia, Kenya, Madagascar, Rwanda, Somalia, Sudan, South-Sudan and Uganda), aggregated and assessed as one region. These datasets include SSP 2 ('Middle of the Road'), SSP 3 ('Regional Rivalry') and SSP 5 ('Fossil-fuelled Development'). Specifically, the GCAM inputs that have been adapted to each of these SSPs are (global) population, GDP, rate of urbanisation, energy and food demand, household discount rates, agricultural yields, energy resource productivity, and emission factors² (Riahi et al., 2017). Table 3 shows the assumed evolution from 2010 to 2040 of the SSP inputs, regionally for Eastern Africa, that have most influence on the GCAM outputs: population, GDP and urbanisation.

Table 3 Evolution of key SSP parameters in GCAM

	2010	2020	2030	2040		2010	2020	2030	2040		2010	2020	2030	2040
	Population (Million inhabitants) (Samir and Lutz, 2017)					GDP per capita (\$ (2015) annually) (Dellink et al., 2017)					Urban population share (%) (Jiang and O'Neill, 2017)			
SSP2	259	327	399	468		732	965	1438	2173		22.9	27.7	32.6	37.7
SSP3	259	335	425	521		732	951	1248	1547		22.9	24.8	26.7	28.4
SSP5	259	319	373	419		732	980	1833	3893		22.9	31.0	40.0	49.2

The candidate actions are six technological subsidisation pathways revolving around liquefied petroleum gas (LPG), photovoltaics (PV), biogas, ethanol, charcoal and fuelwood, i.e. technologies likely to be adopted in the twelve developing countries of Eastern Africa (based on their action pledges, as reflected in their Nationally Determined Contributions), while contributing to the three predefined SDGs. The GCAM-generated parameters for the three SDGs showcase the contribution of each technology pathway to each of the objective functions under twenty subsidy levels. For each of the four major optimisation problems different time frames are applied and results for the years 2020, 2030 and 2040 are extracted.

The budget constraint starts from \$3.5 billion (USD at 2015 values) in 2020 and increases by 5% per year until 2030 and 2040.

² <https://github.com/JGCRI/gcam-doc/blob/gh-pages/ssp.md>



1.3.2 Cost-effectiveness of technology subsidies and SDG progress

The first step in the proposed methodological framework is to simulate future socioeconomic scenarios through the GCAM model and translate outputs from each policy scenario into progress parameters relevant to SDGs. This is done by applying six different pathways of technology subsidies, up to 2040, and then measuring the impact of these subsidies on progress towards each of the three SDGs.

Results on the cost-effectiveness of technology subsidies for SDG progress (Figures 4-6) show that subsidies for biogas systems are the most cost-effective for each of the indicators, scenarios and years. On the contrary, subsidies for fuelwood pathways are only reasonably cost-effective in the short-term. For charcoal pathways, we observe that cost effectiveness is highly dependent on the invested subsidies. When examining progress on the different timescales we see that more subsidies are required for achieving the same impact in the long-term, at least for energy access and premature mortality indicators. In addition, in the medium- and long-term, technologies like fuelwood, charcoal and ethanol show an even negative impact for the examined subsidies. Between the different SSPs, cost-effectiveness remains in the same levels for each technology, with some differences observed in the short-term for biogas and the GHG emissions indicator, as well as on charcoal for reducing GHG emissions in the medium- and long-term. Overall, more subsidies are required to achieve a positive impact in the three SDGs when SSP 5 is realised. Generally, we notice that depending on the scenario and the point in time, some technology pathways are more cost-effective than others for a specific SDG and some result in negative outcomes (and thus not incorporated in Figures 4-6). Thus, the need to identify technological portfolios that are both Pareto-optimal in terms of contributing simultaneously to the three SDGs and, most importantly, robust among the different scenarios is more than prominent.



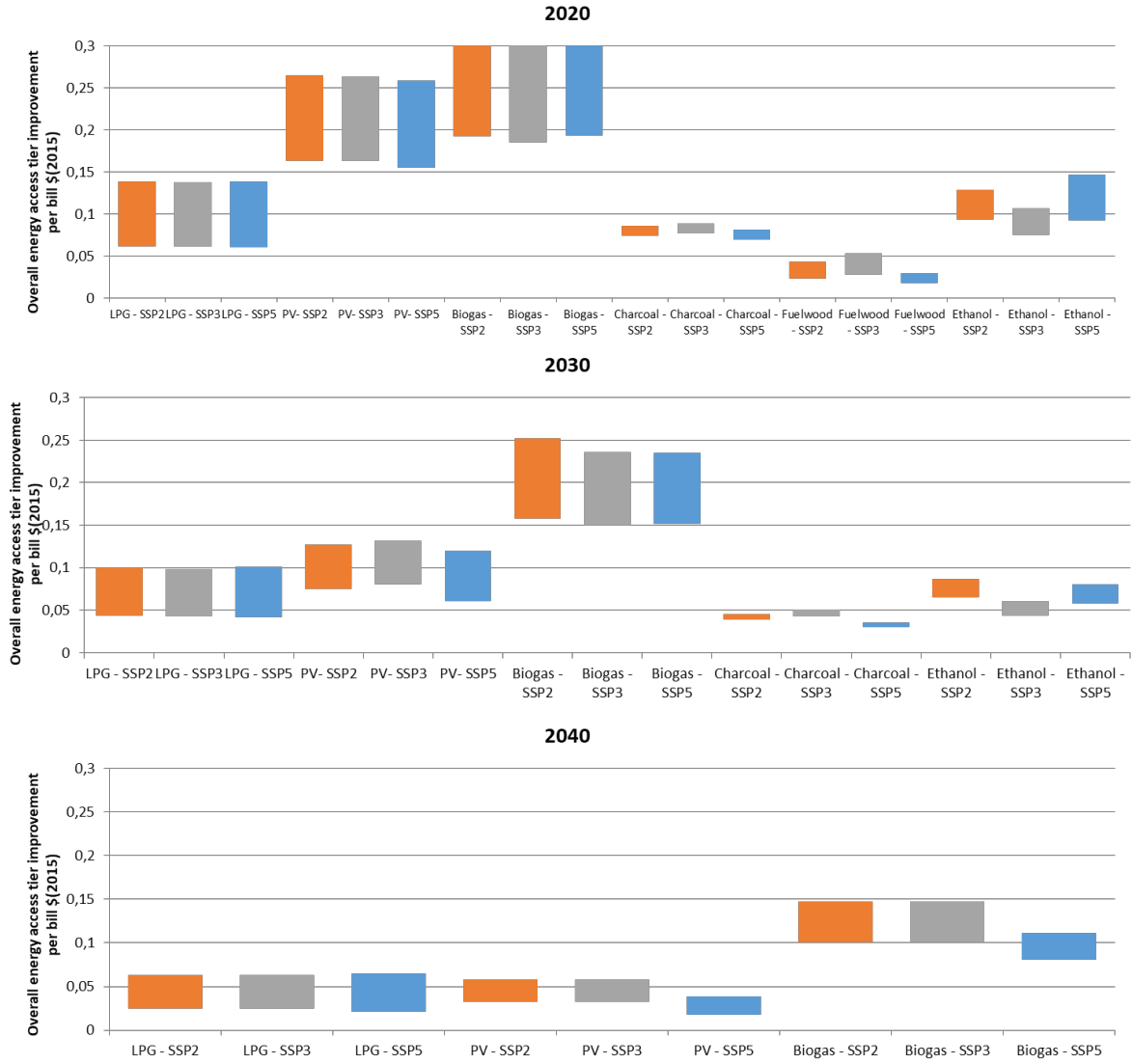


Figure 4 Impact of energy technology subsidies in terms of energy access levels for the different SSPs by 2020, 2030 and 2040.



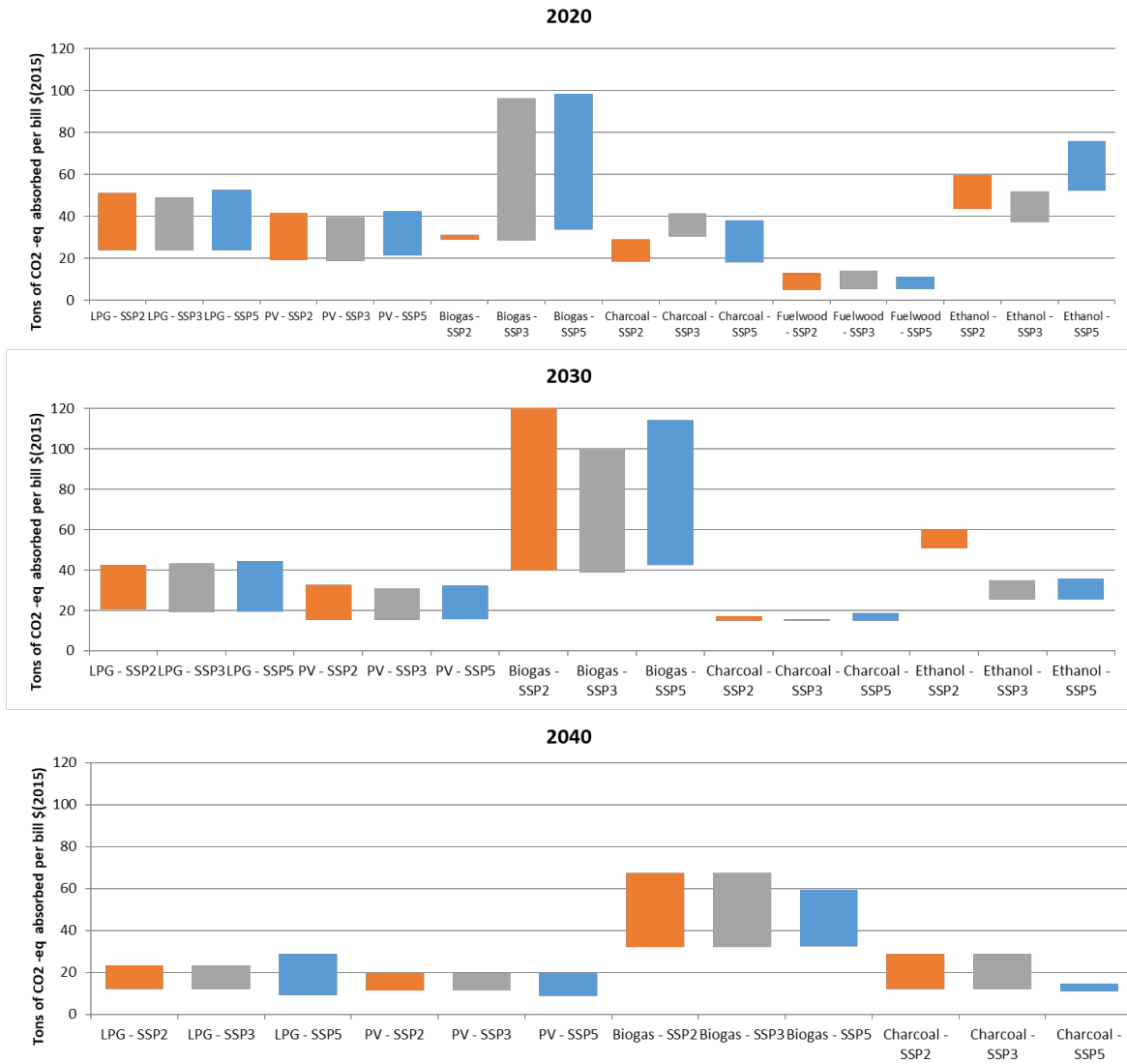


Figure 5 Impact of energy technology subsidies in terms of GHG emissions for the different SSPs by 2020, 2030 and 2040.



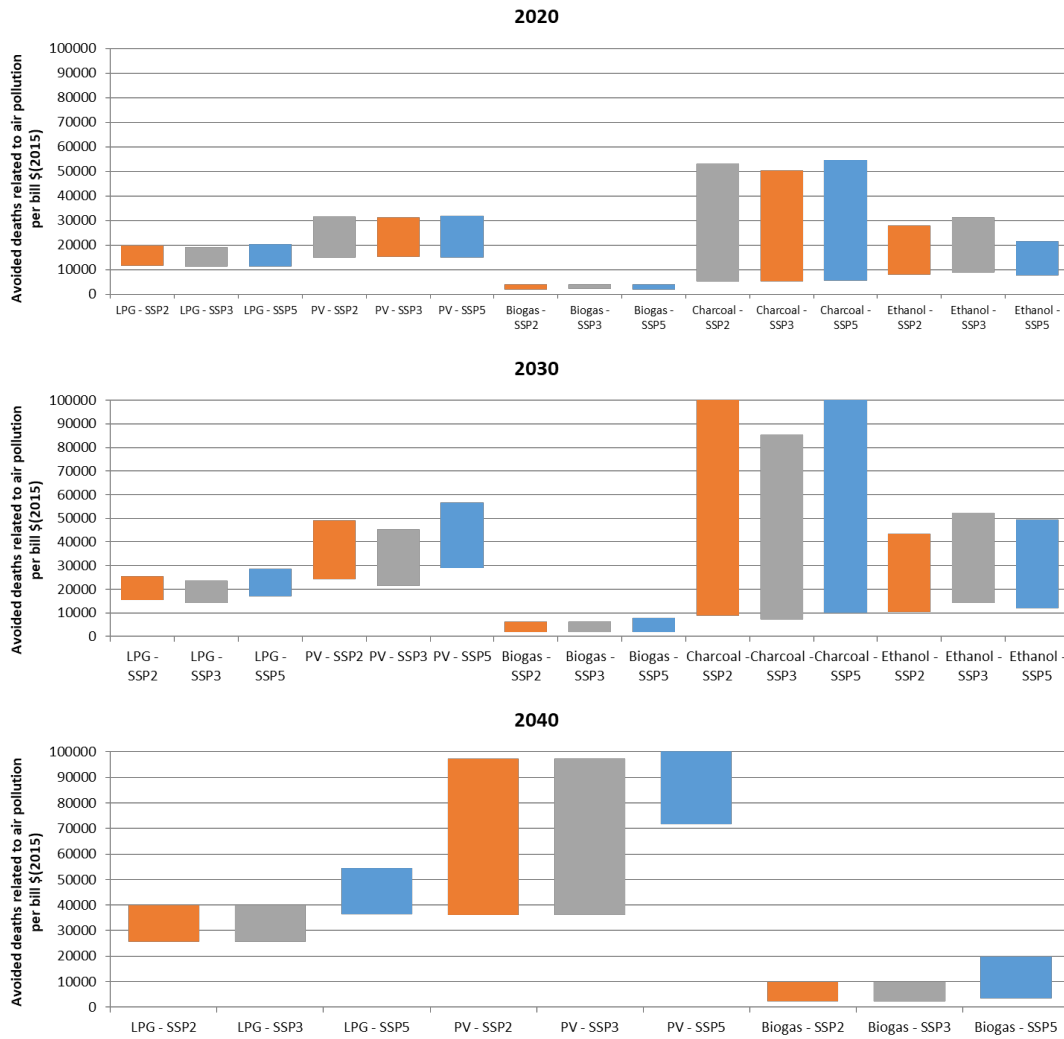


Figure 6 Impact of energy technology subsidies in terms of mortality for the different SSPs, by 2020, 2030 and 2040.

1.3.3 Robust subsidy portfolios in each individual SSP

The second goal of this research is to identify optimal technology portfolios that are robust in each of the different socioeconomic pathways, when probabilistic uncertainty in the model parameters is imposed. The results of the portfolio optimisation, incorporating the robustness information produced by the Monte Carlo runs, are shown per policy scenario in Figures 7-9, where we can see the set of solutions that represent the best possible trade-offs between the three SDGs. A comparison of results among the different SSPs can be easily retrieved. In each figure, differences on technological performance among the SSPs are mainly observed in SSP 5 for the years 2030 and 2040. In more detail, SSP 2 can prove more progress-friendly in achieving the three SDGs in the short-term, among all different socioeconomic pathways. In the medium- and long-term, SSP 3 leads to better results for the energy access and health criteria, while for the goal of reducing emissions, SSP 2 performs better. SSP 5 features the lowest contribution to the optimisation objectives for all considered time scales, which is fairly consistent with its intended narrative. SSP 5 is characterised by higher incomes and urbanisation, which increase access to high-quality energy sources, such as LPG, even without subsidisation. Due to this more “positive” counterfactual, technology subsidisation in SSP5 is found less cost-effective. The reasoning on how policy implications affect the



adoption of technologies can be found in Van de Ven et al. (2019).

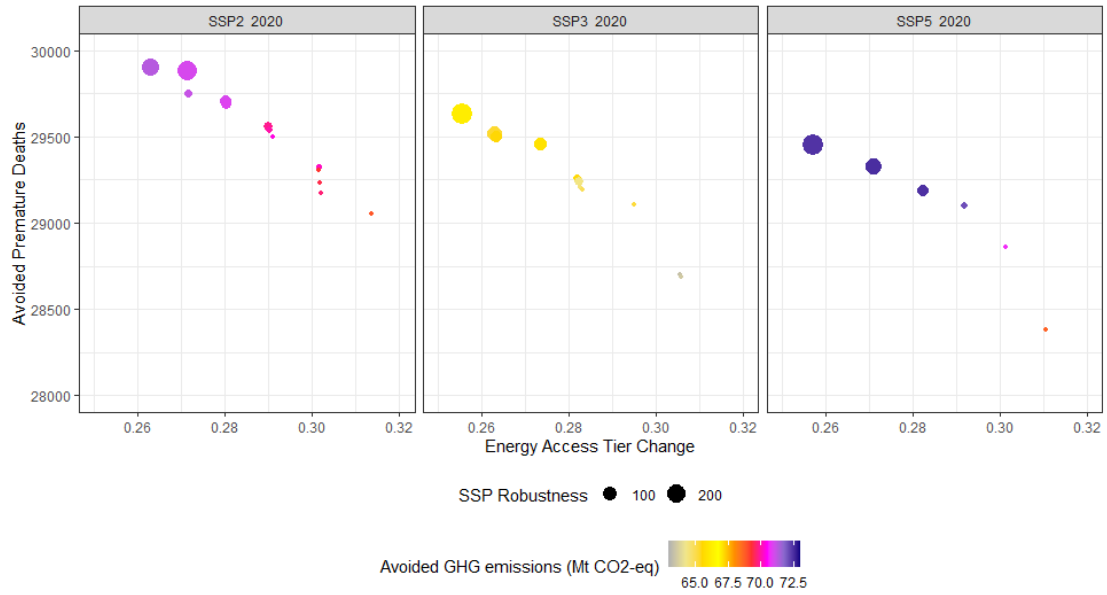


Figure 7 Technology subsidy portfolios that are Pareto-optimal in terms of simultaneously avoiding GHG emissions, premature deaths and improving energy access per SSP in 2020. Size of dots illustrates robustness against stochastic uncertainty of modelling parameters.

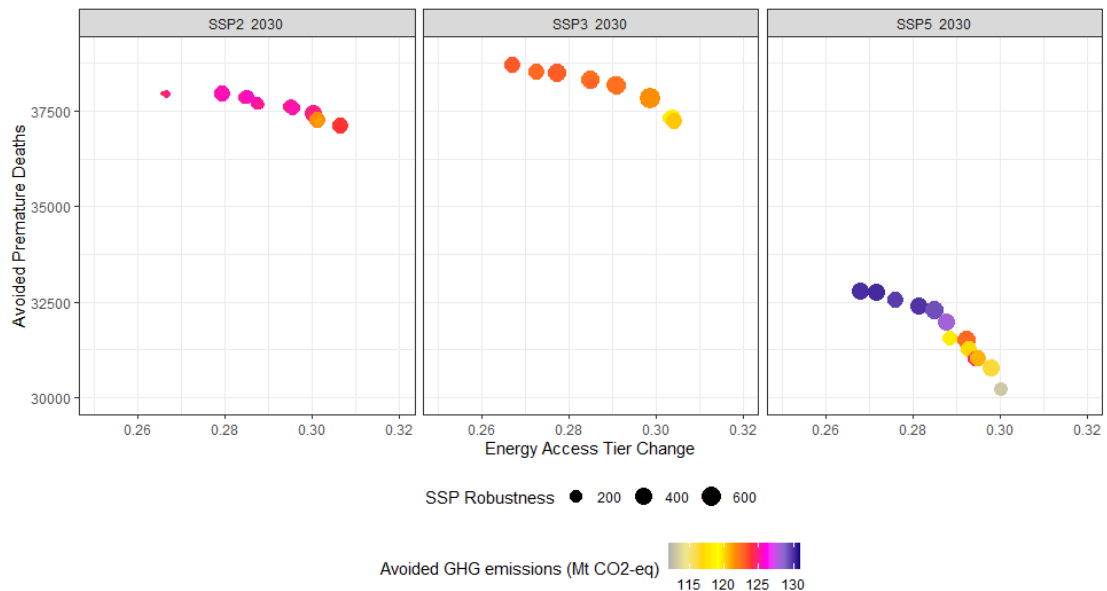


Figure 8 Technology subsidy portfolios that are Pareto-optimal in terms of simultaneously avoiding GHG emissions, premature deaths and improving energy access per SSP in 2030. Size of dots illustrates robustness against stochastic uncertainty of modelling parameters.

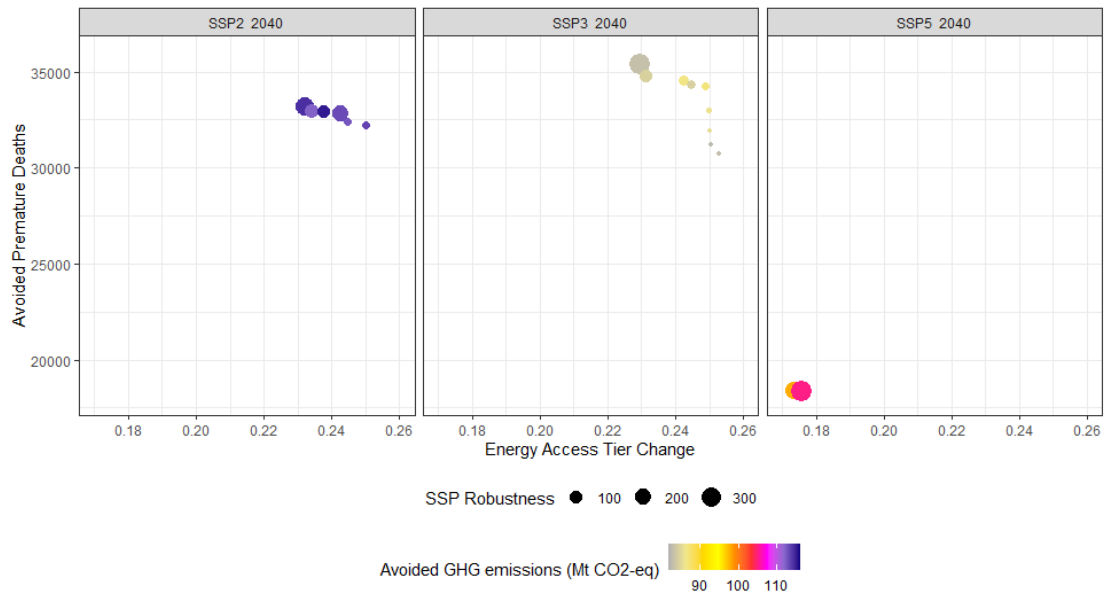


Figure 9 Technology subsidy portfolios that are Pareto-optimal in terms of simultaneously avoiding GHG emissions, premature deaths and improving energy access per SSP in 2040. Size of dots illustrates robustness against stochastic uncertainty of modelling parameters.

1.3.4 Robust subsidy portfolios across all three SSPs

In this section the goal is to define robust subsidy portfolios for any of the three SSPs (2, 3 and 5). To evaluate the robustness of the results, an analysis that applies the ranges of the GCAM simulation outcomes between SSPs as its boundaries for robustness is introduced and carried out. Figure 10 illustrates the Pareto fronts of the optimal solutions, while giving information on the robustness of the results, which is represented by the size of dots: the bigger the dots, the higher the robustness.

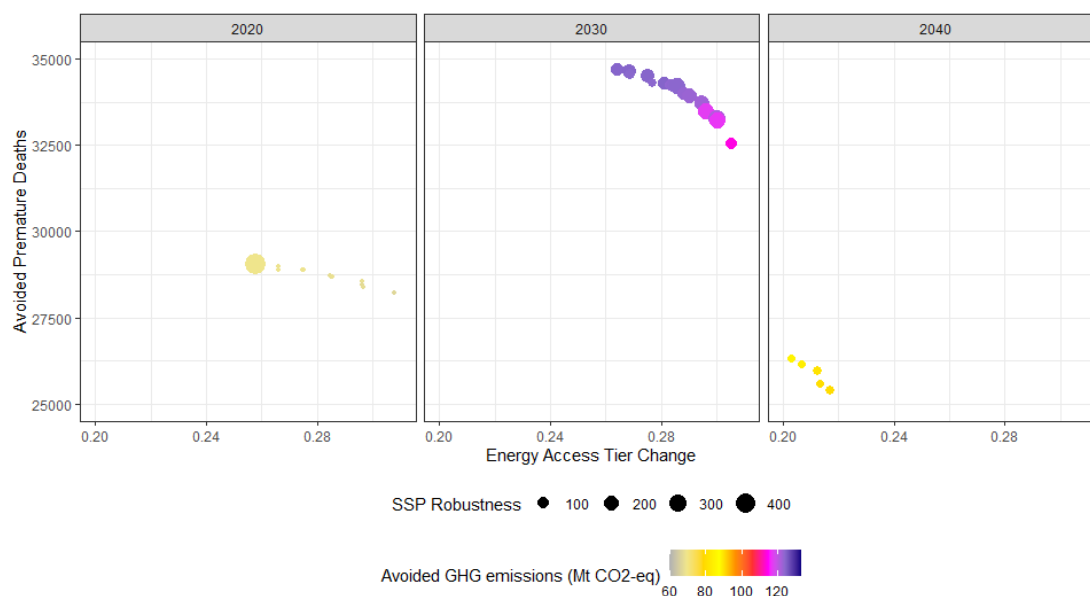


Figure 10 Technology subsidy portfolios that are Pareto-optimal in terms of simultaneously avoiding GHG emissions, premature deaths and improving energy access in 2020, 2030 and 2040. Size of dots illustrates robustness against SSP uncertainty.

The behaviour of the optimal solutions across the different timescales shows homogeneity with the analysis provided for the different SSPs. What is important is to additionally verify if the robustness of SSP uncertainty bounds leads to more robust solutions among the different SSPs. To achieve that, we select two optimal portfolios for each of the six Pareto curves of Figure 10, one with a higher robustness score and one with a lower robustness score. The robustness score indicates the number of Monte Carlo iterations within which a portfolio remains optimal. We re-iterate these portfolios in the GCAM model to test whether the results of a more robust portfolio are indeed more homogeneous between the different SSPs, i.e. that the ranges of SDG performances across the SSPs are smaller in case of a more robust portfolio. The results shown in Table 4 suggest that in the majority of the scenarios we can confirm a smaller output range between SSPs, if a portfolio with a higher robustness score is chosen. The range in outcomes decreases by up to 16% for the baseline scenario in 2020.

Table 4 Decrease in GCAM output ranges between SSPs for each of the three SDGs when selecting a portfolio of higher robustness score.

	Decrease in output ranges between SSPs		
	GHG Emissions	Mortality	Energy Access
Baseline 2020	-1%	-4%	-16%
Baseline 2030	-4%	1%	-1%
Baseline 2040	2%	-1%	-11%

1.3.5 Empirical findings, discussion and results

Table 5 shows how the realisation of the different SSPs affects the total impact and contributions per technology for the most robust Pareto-optimal subsidy portfolios. The robustness of the optimisation process is examined for each of the SSPs separately, assuming that the performance of the assumed technologies in terms of maximising



emission reductions, energy access and health benefits is stochastically uncertain.

Consistent with the analysis on the cost-effectiveness of the technology subsidies, biogas is the technology with the higher participation in the robust portfolios. This is evident across the different SSPs and timescales. The use of LPG and PV systems also have a high contribution to progress in the three SDGs. Charcoal kilns, and ethanol technologies reach their maximum potential, which though corresponds to a much lower subsidy and impact level compared to LPG, PV and biogas. Fuelwood is the least attractive technology. The policy context on how the different policy scenarios affect subsidisation and effectiveness of the technologies is provided in Van de Ven et al. (2019). Here the SSPs are assumed as an uncertain set of conditions that affect the performance of every technological subsidy policy and we focus on how the realisation of the different SSPs will ultimately affect the participation of technologies in the robust portfolios.

For the year 2020, technologies show a stable share of participation in the robust portfolios. In 2030, a high increase in the contribution of ethanol is observed for SSP 5, where ethanol is subsidised up to 11%, in contrast to SSPs 2 and 3 where subsidisation for ethanol is less than 2%. The realisation of different SSPs has an overall bigger effect on SDG progress in 2040.

Table 5 Ranges of total impact and contributions per technology for the most robust Pareto optimal subsidy portfolios across SSPs

SC	Technology	Energy Access	GHG	Mortality	Subsidy
2020	LPG	20-23%	28-34%	15-18%	34-40%
	PV	16-21%	7-8%	3-4%	8-10%
	Biogas	49-53%	50-52%	73-75%	42%
	Charcoal	1-8%	2%	2%	3%
	Fuelwood	0.02-0.2%	0.10%	0%	1%
	Ethanol	3-10%	5-14%	2-7%	4-13%
2030	LPG	10-14%	10-15%	7-10%	13-22%
	PV	18-28%	9-13%	5-7%	18-23%
	Biogas	58-62%	70-72%	78-81%	56%
	Charcoal	1%	1%	1-2%	2-3%
	Ethanol	1-11%	2-10%	1-8%	2-11%
2040	LPG	35-42%	29-51%	24-31%	48-57%
	PV	7-26%	6-20%	3-10%	8-21%
	Biogas	33-55%	29-65%	60-73%	22-43%
	Charcoal	0.00%	0.10%	0%	0%

1.4 Conclusions

This research presents a two-level integration of an integrated assessment model, namely GCAM, and a portfolio analysis model, based on AUGMECON 2 and Monte Carlo simulations, with the aim to provide policymakers with a comprehensive tool to address environmental and energy-related issues, facilitating the exchange of input data and model results across different methodologies. The integration is applied to a case study focusing on technological portfolio optimisation among different plausible socioeconomic futures in Eastern Africa. Initially, the GCAM model is run to simulate future socioeconomic scenarios for six relatively sustainable technologies. Outputs from each scenario are translated into progress parameters relevant to SDGs and are fed into a PA model. The portfolio optimisation model leads to the identification of Pareto fronts of optimal portfolios and allows



comparison among different SSPs. The results show how resource allocation must be shared among the technologies to achieve optimal trade-offs on the simultaneous achievement of three goals: increase of energy access (SDG7), reduced exposure to air pollution and avoidance of related mortality (SDG3) and mitigation of global warming (SDG13). Biogas is the technology with the higher participation in the robust portfolios, across all SSPs and timescales, while fuelwood is the least attractive technology. A comparison between the SSPs shows that differences in the technological performances among the SSPs are mainly observed in SSP 5 for the years 2030 and 2040.

In order to hedge uncertainty concerning the realisation of different SSPs, an analysis that applies the ranges of the GCAM simulation outcomes between SSPs as its boundaries for robustness is introduced. The second link between the PA and GCAM models is achieved by feeding the GCAM model with the results of the portfolio optimisation analysis, to verify if the robustness of SSP uncertainty boundaries leads to more robust solutions across the different SSPs. We selected for each Pareto front a portfolio of high robustness and a portfolio with lower robustness score and reiterated these portfolios in the GCAM model to retrieve results for the technologies' impact for each SSP. This is to test whether the resulting ranges of SDG performances between the SSPs are smaller in case of a more SSP-robust portfolio. The results confirm that all portfolios show a smaller output range between SSPs, if a portfolio with a higher robustness score is chosen, showcasing the advantage of the proposed methodology.

A limitation of our proposed methodology related to the "SSP robustness" scenario lies on the initial choice of the mid-point between the range of SSP results in terms of the impact of each technology on SDG progress, for identifying the Pareto front of the optimal portfolio. The proposed idea is not to imply that the SSPs have the same probability of occurrence, as no rational assessment of probabilities of various representative scenarios can conclude equal likelihood (Kinzig and Starrett, 2003) hence justifying the use of a mean value; but rather to assess the uncertainty of the results across the entire spectrum of the resulting values, as defined by the individual SSP results. Even though we do apply the full SSP-related uncertainty range when calculating the robustness of the individual portfolios on the Pareto front, it could be that the election of a different point within the SSP outcome range would yield a slightly different Pareto front, and hence alter the portfolio outcome. However, we think that the difficulty to select a justifiable "mid-value" within an SSP-related outcome range poses a limitation that is a necessary evil, which enables the stochastic identification of optimal technology portfolios against all, or most, potential outcomes (Grübler and Nakicenovic, 2001) of technological subsidisation, regardless of our capacity to envisage a future world state that leads to these outcomes, and especially since these outcomes are forecasts of a single model (Allen, 2003).

Nevertheless, acknowledging this limitation and understanding the knowledge gaps reflected in this broad spectrum, against which the resulting technological subsidisation portfolios are assessed, may allow science both to reduce uncertainties in a systematic manner and to convey to policymakers the need to manage and integrate uncertainty into the policymaking process (Schneider, 2003). Along those lines, it is also important to note, that although the policy assumptions of the paper are carefully selected based on published research (Van de Ven et al., 2019), policy-relevance of results is highly dependent on the assumptions applied when modelling the policy scenarios, and these must be carefully considered when interpreting the results. Without overlooking this limitation, the novel methodology introduced in this research can be useful for stakeholders to manage the uncertainty prominent in the future states of the world, according to different adaptation and mitigation challenges. Both core elements of the methodology, namely the GCAM model and the portfolio analysis model can be extended to include more parameters (i.e. technologies) than the ones represented in the current application. However, we must consider the limitations in terms of time and processing requirements, that the solution of more complex problems i.e. of numerous objective functions, more Monte Carlo simulations may



require; this limitation can in the future be overcome, by using an enhanced algorithm for solving the portfolio analysis model, like AUGMECON-R, which is a more advanced version of AUGMECON 2 with significantly faster resolution performance (Nikas et al., 2020). Further prospects towards enriching the proposed methodological framework include the selection of variables with implications for a broader set of SDGs, and the integration of the models with participatory tools, to actively involve stakeholders in the case study; participation of stakeholders in policy analysis has been found to improve system understanding and scoping risks associated with climate policy and technologies (van Vliet et al., 2020).



2 A robust augmented ϵ -constraint method (AUGMECON-R) for finding exact solutions of multi-objective linear programming problems

This section has been peer-reviewed and published in *Operational Research* (Nikas et al., 2020).

2.1 Introduction

Despite rapid technological advancements in software and hardware performance, many problems featuring numerous evaluation criteria or objective functions (Wiedemann, 1978), multiple constraints of different nature and hundreds to thousands of decision variables remain challenging to solve (Carrizosa et al., 2019). Several methods have been developed to solve multi-objective linear programming problems, each of which features strengths and weaknesses (Sylva and Crema, 2007). Among these, the ϵ -constraint method, along with its variants, has been used in many systems and applications (e.g. Liu and Papageorgiou, 2013; Paul et al., 2017; Zhou et al., 2018; Jenkins et al., 2019), reported as a powerful way to solve multi-objective linear programming problems and preferred over competing techniques (Kadziński et al., 2017; Jabbarzadeh et al., 2019).

In this study, we focus on one of the most widely used improvements of ϵ -constraint, the AUGMECON method (Mavrotas, 2009) as subsequently improved in AUGMECON 2 (Mavrotas and Florios, 2013). By looking at its main novelties, its core weaknesses are identified and discussed in detail, serving as a motivation for developing a new model that effectively overcomes them. These weaknesses, although dependent on various characteristics and processes of the method, can be summarised in the ineffective handling of the true nadir points of the objective functions of a problem and, most notably, in the significant amount of time required to apply it as more objective functions are added to a problem, which can even make a problem practically insolvable. Drawing on these, we introduce AUGMECON-R, a powerful and robust improvement that addresses these weaknesses, and apply it in comparison with its predecessor, in both a set of reference problems from the literature and a series of significantly more complex problems of four to six objective functions.

The rest of the paper is organised as follows. Section 2 carries out a brief overview of the ϵ -constraint, AUGMECON and AUGMECON 2 methods, by highlighting their characteristics of significance to introducing AUGMECON-R in Section 3. Section 4 performs a comparative analysis between AUGMECON-R and its predecessor (AUGMECON 2). Finally, Section 5 draws conclusions and outlines prospects for future work.

2.2 A brief overview of the augmented ϵ -constraint method

According to Hwang et al. (1980), Multiple-Objective Mathematical Programming (MOMP) solving algorithms can be organised in three groups: a priori methods, in which the decision makers have the capacity to express their preferences or objective function weights prior to solving the problem; interactive methods, which feature an ongoing dialogue between analysts and decision makers, eventually leading to preferences converging with solutions; and a posteriori methods, in which the problem is solved and the effective Pareto solutions are found, allowing the decision makers to select among these based on their preferences. Given the infrequency of early knowledge and quantification capacity of the decision makers' preference model, which is prerequisite to a priori methods, and the difficulty in the decision makers having complete overview of (an approximation of) the Pareto front, associated with interactive methods, this paper orients on a posteriori methods to solving a MOMP problem of the form:



$$\max\{f_1(x), f_2(x), \dots, f_p(x)\}$$

$$s. t. : x \in S$$

where: x is the vector of decision variables, $f_1(x), f_2(x), \dots, f_p(x)$ are the p objective functions, and S is the space of efficient solutions.

Among these methods, the ϵ -constraint algorithm aims at optimising one objective function, while considering all other objective functions as constraints. The model, widely applied for multi-objective linear programming problems (Mavrotas et al., 2011; Sakar and Koksalan, 2013), is thus transformed to:

$$\max\{f_1(x)\}$$

$$s. t. :$$

$$f_2(x) \geq e_2$$

$$f_3(x) \geq e_3$$

...

$$f_p(x) \geq e_p$$

$$x \in S$$

By changing the right-hand side of the constrained objective functions (e_i), efficient solutions are obtained. The problem is solved on a step-by-step basis on an $N_2 \times N_3 \times \dots \times N_p$ grid, where N_i is the integer range of the objective function f_i .

One of the method's main advantages is that the number of efficient solutions can be controlled, by appropriately adjusting the number of grid points, on which each optimisation is solved, along the range of each objective function. However, this range must be calculated; it cannot be secured that solutions are not weak but effective; and solving any problem with more than two objective functions is very time-consuming.

These weaknesses motivated the development of augmented ϵ -constraint or AUGMECON (Mavrotas, 2009), which transforms the problem into the following:

$$\max\{f_1(x) + eps \times (s_2 + s_3 + \dots + s_p)\}, eps \in (10^{-6}, 10^{-3})$$

$$s. t. :$$

$$f_2(x) - s_2 = e_2$$

$$f_3(x) - s_3 = e_3$$

...

$$f_p(x) - s_p = e_p$$

$$x \in S$$

In essence, AUGMECON introduces the following modifications to the original ϵ -constraint method, to ensure that only effective Pareto solutions are obtained: (i) all constraints corresponding to the $p - 1$ objective functions become strict inequalities; and (ii) slack (or surplus) variables are introduced both to the primary objective function and to the constrained ones.

Another significant novelty of AUGMECON is that it exploits cases where the problem is infeasible, leading to an early exit from the nested loop of the step increase function: the algorithm initially sets lower bounds to the constrained objective functions, which gradually become stricter; if the problem becomes infeasible, i.e. the model



cannot be solved for the given constraint of an objective function, after a specific grid point increase, there is no point in strengthening the constraints and the algorithm exits from the innermost loop and continues to the next grid point of said objective function. This way AUGMECON contributes to faster model solution, especially when the problem features more than two objective functions.

AUGMECON has been employed in various applications and systems, including supply chain management (Torabi et al., 2013; Bootaki et al., 2014; Bootaki et al., 2016; Canales-Bustos et al., 2017; Musavi and Bozorgi-Amiri, 2017; Ravat et al., 2017; Vieira et al., 2017; Sazvar et al., 2018; Ehrenstein et al., 2019; Oiu et al., 2019; Shekarjan et al., 2019; Xin et al., 2019), energy planning (Hombach and Walther, 2015; Tartibu et al., 2015; Arancibia et al., 2016; Cambero and Sowlati, 2016; Cambero et al., 2016; Mohammadkhani et al., 2018; Rabbani et al., 2018; Sedighizadeh et al., 2018; Razm et al., 2019), waste management (Mavrotas et al., 2013; Mavrotas et al., 2015; Inghels et al., 2016), portfolio analysis (Xidonas et al., 2011; Khalili-Damghani et al., 2012; Xidonas et al., 2010), transportation (Resat and Turkay, 2015; Babakeik et al., 2018) and others (Khalili-Damghani and Amiri, 2012; Aras and Yurdakul, 2016; Yu et al., 2018; Behmanesh and Zandieh, 2019; Zhang et al., 2019; Xiong et al., 2019); and has been combined with or compared against evolutionary algorithms (Khalili-Damghani et al., 2013; Dabiri et al., 2017; Wang et al., 2018; Mohammadi et al., 2019).

Mavrotas and Florios (2013) further extended this algorithm in AUGMECON 2, by introducing a bypass coefficient as well as a type of lexicographic optimisation to all objective functions, the order of which was insignificant in AUGMECON:

$$\max\{f_1(x) + eps \times (s_2/r_2 + 10^{-1}s_3/r_3 + \dots + 10^{-(p-2)}s_p/r_p)\}$$

By means of the bypass coefficient, AUGMECON 2 makes use of the information provided by the slack/surplus variables of the constrained objective functions to avoid unnecessary iterations and accelerate solution. The jumps made in the innermost loop to help accelerate grid scanning allow for decreasing the step of the process and therefore increasing the grid points; by doing so, the exact Pareto set can be identified. But, in order to do so, (a) the objective function coefficients must be integer and (b) the nadir points of the Pareto set must be known.

To deal with the first limitation, non-integer coefficients can be multiplied by the appropriate power of 10, as necessary, which can however significantly expand the grid and increase the grid points, leading to very large solution times. Regarding the second limitation, adding steps to accurately calculate the nadir points of the Pareto set can also increase the algorithm's complexity, so the AUGMECON 2 algorithm only uses an underestimation (overestimation), i.e. a lower (upper) bound, in cases of maximisation (minimisation) objectives.

Despite its weaknesses, which are analysed in detail below, AUGMECON 2 has significantly better performance over AUGMECON, and this is why it has also been applied in a wide range of problem domains since its introduction, including supply chain management (Gavranis and Kozanidis, 2017; Bal and Satoglu, 2018; Attia et al., 2019; Habibi et al., 2019; Resat and Unsal, 2019; Roshan et al., 2019; Saedinia et al., 2019; Vafaenezhad et al., 2019; Mohammed and Duffuaa, 2020), project selection (Mavrotas et al., 2015; Schaeffer and Cruz-Reyes, 2016), and network optimisation and planning (Florios and Mavrotas, 2014; Oke and Siddiqui, 2015; Mousazadeh et al., 2018; Rahimi et al., 2019), as well as in policy-related problems, such as energy and climate action (Forouli et al., 2019a; Forouli et al., 2019b; Van de Ven et al., 2019; Doukas and Nikas, 2020).

2.3 AUGMECON-R

2.3.1 Motivation

Although AUGMECON 2 constitutes a significant upgrade to AUGMECON and a powerful algorithm for solving



multi-objective integer programming (MOIP) problems and finding the exact Pareto set of a problem, it features certain weaknesses, the need to overcome which has motivated the development of AUGMECON-R.

First, the solution time for large-scale problems of more than two objective functions is still high, since jumps only occur in the innermost loop and not across the grid and for all nested loops, which represent the constrained objective functions: a problem of m objective functions of average range n would have an AUGMECON 2 complexity of $O(n^{m-1})$, which is relatively large for programs running in environments like GAMS. For example, a 6kpY problem (a knapsack problem of 6 objective functions, 6 constraints and Y decision variables), with an average integer range of 1,000 for each objective function, would feature a complexity of $O(10^{15})$, or slightly less given the iterations avoided due to the bypass coefficient of the innermost loop. The more objective functions a problem has, the more time-consuming AUGMECON 2 becomes for solving said problem.

Second, AUGMECON 2 requires that objective function coefficients be integer. If this is not the case, non-integer coefficients are multiplied by the appropriate power of 10, thereby also increasing the complexity accordingly: a problem of m objective functions of average range n and an average number of decimals k would have an AUGMECON 2 complexity of $O(n^{m-1} \times 10^{k \times (m-1)})$.

Third, implementing AUGMECON 2 requires a priori knowledge of the nadir points of the objective functions. Nadir point calculation algorithms are usually complex, hard to program and could require writing chunks of code larger than those of AUGMECON 2 itself; are generally capable of solving problems of up to three objective functions; and their running time is comparable to the one required by AUGMECON 2 (Alves and Costa, 2009). This is why AUGMECON 2 opts for underestimation of nadir points, i.e. the use of lower bounds of the objective functions, thereby only slightly increasing computation time. This process of approximating the nadir points, in AUGMECON 2, takes place in the problem's payoff table where the lowest values, which in theory are equal to or greater than the nadir points, are multiplied by an arbitrary coefficient (e.g. 90%), resulting in what is hopefully an underestimation of the actual nadir points. Academically speaking, one heuristic approach around this would be the calculation of all payoff tables, considering all possible orders of the constrained objective functions; this would expectedly give a closer approximation to the actual nadir points, allowing tightening the arbitrary coefficient, e.g. to 95%, hopefully ensuring that the nadir point would be included in the new, smaller grid. However, this approach would simply improve computation time, without avoiding either the arbitrary or the hopeful nature of the approximation process.

Fourth, the correlation between the order of constrained objective functions across loops and computation time is a weakness by itself: AUGMECON 2 features a bypass coefficient only for the innermost loop of the process, resulting in getting rid of only those unnecessary grid point checks that can be avoided within the innermost loop. In order to maximise the number of unnecessary iterations avoided as much as possible, after calculating the payoff table, the algorithm should be in a position to switch order of constrained objective functions accordingly, so that the objective function of the largest range could be placed in the innermost loop.

These four limitations associated with AUGMECON 2 constitute the motivation of developing a new algorithm that can significantly improve computation time and efficiency, as well as allow for easily solving problems that have so far been hard or practically impossible to solve.

2.3.2 An improved search algorithm

Reading through (Mavrotas and Florios, 2013) and the performance recorded for AUGMECON 2, there appears to be a large deviation between the number of models solves and the solutions included in the Pareto front. For example, in the case of the 3kp100 problem—i.e. of a knapsack problem of three objective functions, three constraints and a hundred decision variables—there are 103,049 models solved, which is approximately sixteen



times the number of the solutions included in the Pareto Front (6,500). However, given that this is a MOIP problem and AUGMECON 2 calculates the exact Pareto set by using a unity step to explore all possible integer values of the objective functions across the grid, one would expect that the models solved would be equal or at least close to the number of Pareto front solutions, which is not the case.

This large number of unnecessary optimisations computed can be attributed to the use of only one bypass coefficient in the innermost loop and, in addition, to the large number of infeasibilities that could have otherwise been to some extent foreseen and avoided.

In this direction, AUGMECON-R introduces a novelty that is largely based on the existing notion of the bypass coefficient, by incorporating to the model as many bypass coefficients as objective functions, which would be of the form:

$$b_2 = \text{int}(s_2/\text{step}_2)$$

$$b_3 = \text{int}(s_3/\text{step}_3)$$

...

$$b_p = \text{int}(s_p/\text{step}_p)$$

where: $\text{int}()$ is the function that returns the integer part of a real number, and s_i is the slack/surplus variable for an objective function i , and step_i is the discretisation step for this objective function:

$$\text{step}_i = r_i/q_i$$

where: r_i is the range of the objective function i , and q_i the number of equal intervals that the range is divided to formulate the grid, so that the latter comprise $q_i + 1$ grid points.

This way, instead of having one bypass coefficient acting at the innermost loop like AUGMECON 2, AUGMECON-R features an active bypass coefficient in each one of the outer loops as well. In every iteration, bypass coefficients $b_i = \text{int}(s_i/\text{step}_i)$ are calculated. When $s_i > \text{step}_i$, in the next iteration for b_i' corresponding to $e_i' = e_i + \text{step}_i$ the optimisation will again lead to the same solution, with $s_i' = s_i - \text{step}_i$, making the iteration unnecessary. The b_i bypass coefficient indicates how many iterations should be bypassed, provided that these iterations concern the i^{th} objective function and the right-hand sides of all other constrained objective functions remain constant. The new process introduced in the proposed algorithm can be shown with a simple example. Assume that we have a four-objective problem with the following payoff table as shown in Table 1 (all objective functions to be maximised):

Table 6 Payoff table of example problem.

	f1	f2	f3	f4
max f1(x)	105	102	77	50
max f2(x)	95	112	80	53
max f3(x)	100	108	87	46
max f4(x)	100	110	80	56

From the payoff table, we have $r_2 = r_3 = r_4 = 10$, which are divided into ten equal intervals, with a unity step of $\text{step}_2 = \text{step}_3 = \text{step}_4 = 1$. AUGMECON-R includes the following process:

For $i = 0 - 10$

$$e_4 = 46 + i$$

For $j = 0 - 10$



```

e3 = 77 + j
For k = 0 – 10
    e2 = 102 + k
    Solve(P)
Next k
Next j

```

Next i

The objective function $f_2(x)$ is represented in the innermost loop (k counter). Assume that we currently are at the 2nd iteration of the innermost loop ($k = 1$), the 4th iteration of the middle loop ($j = 3$) and the 3rd iteration of the outermost loop ($i = 2$), with $e_2 = 103$, $e_3 = 80$, and $e_4 = 48$, as displayed in brackets and bold in Table 2.

Table 7 Grid points of the example problem.

Objective function	Counter	Grid points										
		0	1	2	3	4	5	6	7	8	9	10
f ₂ (x)	k	102	[103]	104	105	106	107	108	109	110	111	112
f ₃ (x)	j	77	78	79	[80]	81	82	83	84	85	86	87
f ₄ (x)	i	46	47	[48]	49	50	51	52	53	54	55	56

After the optimisation, we obtain $s_2 = 4$, $s_3 = 3$, and $s_4 = 4$, meaning that $f_2 = 103 + 4 = 107$, $f_3 = 80 + 3 = 83$, and $f_4 = 48 + 4 = 52$ (and, for the sake of completeness, $f_1 = 97$). Hence, $b_2 = 4$, $b_3 = 3$, and $b_4 = 4$. While AUGMECON 2 would consider unnecessary only the four next iterations of the innermost loop, AUGMECON-R acknowledges that any combination of $k \in [1,5]$, $j \in [3,6]$, $i \in [2,6]$ would return the same solution. In this problem, AUGMECON-R would avoid 19 unnecessary iterations that AUGMECON 2 would not.

Assuming we have the capacity to store the values of the bypass coefficients b_i in optimisation h and defining as pure any optimisation that leads to a solution different from the one resulting from a unity decrease of any of the parameters for the right-hand side for a specific iteration drawn from the grid points of the objective functions, e_i , then AUGMECON-R can avoid:

$$\begin{aligned}
 & \sum_{h \in D} \{b_{3,h}\}, \text{ if } p = 3 \\
 & \sum_{h \in D} \{b_{3,h} + b_{4,h} * (b_{3,h} + 1)\}, \text{ if } p = 4 \\
 & \sum_{h \in D} \{b_{3,h} + b_{4,h} * (b_{3,h} + 1) + b_{5,h} * (b_{4,h} + 1)(b_{3,h} + 1)\}, \text{ if } p = 5 \\
 & \sum_{h \in D} \{b_{3,h} + b_{4,h}(b_{3,h} + 1) + b_{5,h}(b_{4,h} + 1)(b_{3,h} + 1) + \dots + b_{p,h}(b_{p-1,h} + 1)(b_{p-2,h} + 1) \dots (b_{3,h} + 1)\}, \text{ if } p \geq 6
 \end{aligned}$$

iterations compared to AUGMECON 2, where: h is a pure optimisation and D is the sum of all pure optimisations.

In order to achieve this for any problem of p objective functions, as suggested above, the AUGMECON-R algorithm requires that a $(p - 1)$ -dimensional array be introduced to store integer flag values, $flag[(N_2 + 1) \times (N_3 + 1) \times \dots \times (N_p + 1)]$, where N_i is the integer range of the objective function f_i . The array is initialised with zero values and, prior to any optimisation, the algorithm examines if the corresponding value of the array is zero or not; if it is zero, the optimisation is performed, otherwise the algorithm jumps in the innermost loop as many steps as the array value indicates.

By introducing the flag array and the notion of pure optimisations, AUGMECON-R can at the same time avoid any



unnecessary optimisations due to infeasibilities: if, for any value of $e_2^*, e_3^*, \dots, e_p^*$ of the right-hand side of the constrained objective functions, there lies an infeasibility, then for an increase of any of e_2, e_3, \dots, e_p with all others equal to or greater than $e_2^*, e_3^*, \dots, e_p^*$ an infeasibility will also be reached. Therefore, for $\delta_i \in N$, any $\{e_i^* + \delta_i\}$ combination on the right-hand side of the constrained objective functions will return an infeasibility; while AUGMECON 2 would only avoid infeasibilities for $\{e_2^* + \delta_2, e_3^*, \dots, e_p^*\}, \delta_2 > 0$, AUGMECON-R avoids all infeasibilities for $\{e_2^* + \delta_2, e_3^* + \delta_3, \dots, e_p^* + \delta_p\}$.

The proposed algorithm can, therefore, avoid all iterations, for which all right-hand sides of the constrained objective functions are equal to or greater than the e_i^* values that led to an infeasibility.

The flow chart of AUGMECON-R is shown in Figure 1.



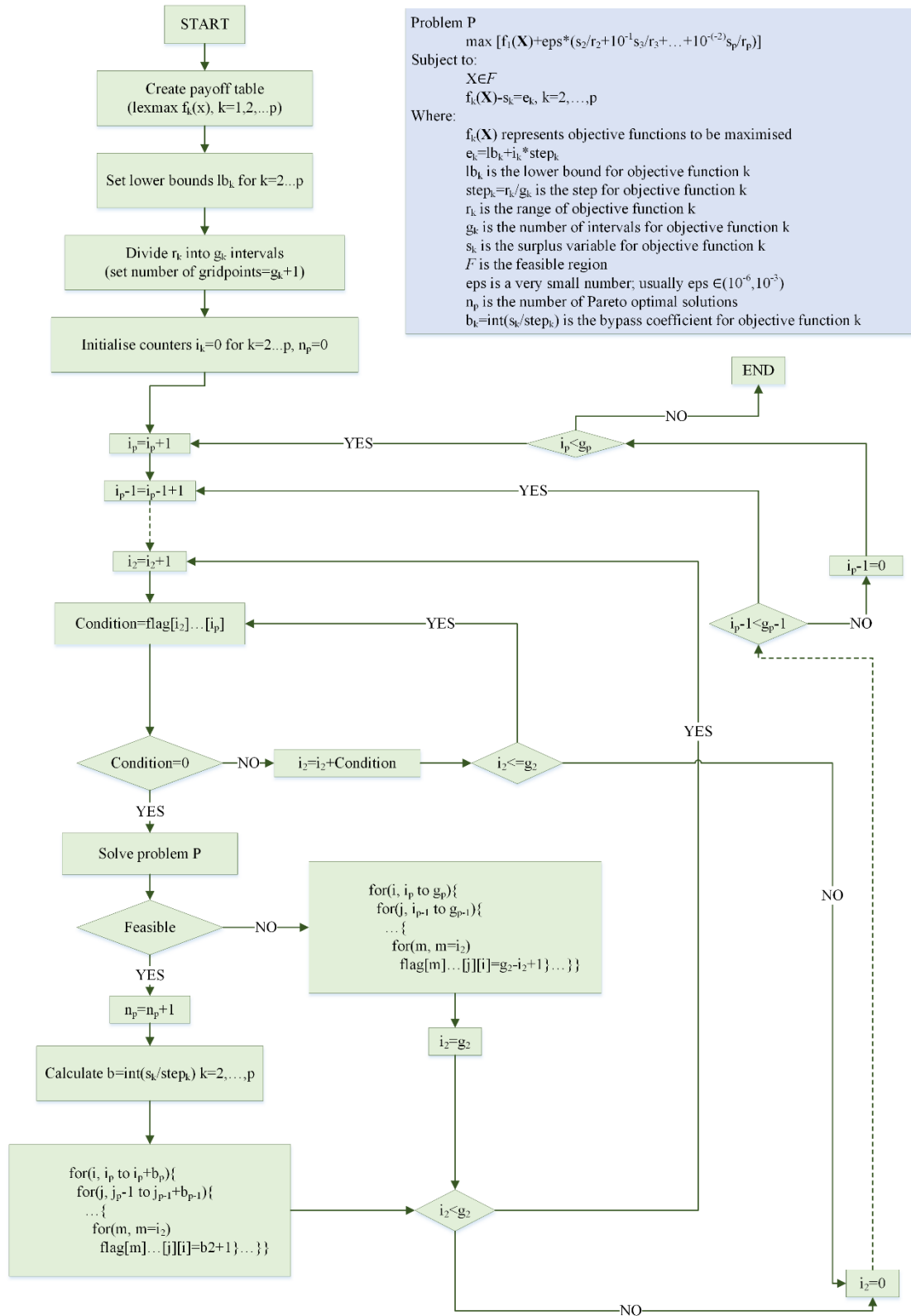


Figure 11 Flowchart of the AUGMECON-R algorithm.

2.3.3 Source code

The code for AUGMECON-R customised for a representative model of a 4kp40 problem, freely available on



GitHub³, has largely been based on the AUGMECON 2 source code and is presented in Appendix A.

2.4 Comparative analysis and discussion

In this section, AUGMECON-R is employed for numerous problems and its performance is compared against the performance of AUGMECON 2. Initially, the benchmark problems presented by Mavrotas and Florios (2013) are solved, acting as a reference, followed by a series of random, more challenging in terms of objective functions and density problems; for the latter, AUGMECON 2 was also used by the authors, to provide for a comparative analysis.

It must be noted that all problems presented in the section have been solved in GAMS version 23.5, using CPLEX 12.2, a 64-bit Windows 10 operating system, a 2.7 GHz i5-6400 processor and an 8GB RAM memory.

2.4.1 Reference benchmark problems

Here, given that AUGMECON-R was designed as an upgrade to AUGMECON 2, we use as reference the 3kpY problems Mavrotas and Florios (2013) used to compare the performance of and establish AUGMECON 2 against AUGMECON; these include a 3kp100, a 3kp50 and a 3kp40 problem, i.e. selected knapsack problems of three objective functions, three constraints, and 100, 50 and 40 decision variables respectively. The 2kpY problems used in the same study were disregarded since, based on the proposed model outlined in Section 3.2, AUGMECON-R is identical to AUGMECON2 when dealing with only two objective functions.

It should also be noted that, in their study, Mavrotas and Florios (2013) do not use their originally proposed AUGMECON 2 algorithm, but a programming modification of it that arbitrarily avoids certain optimisations at the initial stages, both in the innermost loop and in the outer loop. This is noteworthy as, although the use of this modification does not significantly change the order of the resulting difference (cf. the performance reported in Mavrotas and Florios, 2013), here the performance of AUGMECON-R is compared against the original AUGMECON 2 algorithm, and not against the ad hoc modified one. Table 3 summarises the performance between the two algorithms, in terms of the CPU time needed, the grid points per objective function, the total models solved, the infeasibilities found, the number of models solved multiple times ('duplicate solutions'), the dominated solutions and the solutions found in the Pareto front.

Table 8 Performance comparison between AUGMECON 2 (AUGM 2) and AUGMECON-R (AUGM-R) for the 3kpY problems.

	3kp100		3kp50		3kp40	
	AUGM 2	AUGM-R	AUGM 2	AUGM-R	AUGM 2	AUGM-R
CPU Time	23 h	268 min	113 min	695 sec	42 min	220 sec
Grid points per objective function	1236	1236	846	846	540	540
Models solved	103652	11727	25245	1951	11098	746
Infeasibilities	1093	137	564	78	420	34
Duplicate solutions	96020	5071	23630	823	10287	321
Dominated solutions	39	19	3	2	2	2
Solutions in the Pareto	6500	6500	1048	1048	389	389

³ Github link (to be included after acceptance, to ensure double-blind review process).



front						
-------	--	--	--	--	--	--

Our findings suggest that, for the same number of solutions in the Pareto front, AUGMECON-R is multiple times faster and solves significantly less models, leading to significantly fewer infeasibilities and duplicate solutions (Table 4). To make up for potential randomness in CPU times due to different levels of CPU core availability, the CPU times presented are average times after a series of model runs, so that comparison can be considered unbiased and representative. This is also why the number of models solved is highlighted as a comparison metric, indicating similar ratios. It should be noted that the differences in CPU time ratios and models solved can be attributed to the time needed by AUGMECON-R to perform the bypass condition checks. Furthermore, the differences of ratios among the three problems can be attributed to the different density of the problems, i.e. the ratio of the number of solutions included in the Pareto front over the number of models solved: the denser the problem, the smaller the time difference between the two algorithms, as fewer iterations are avoided in the loops outside the innermost loop.

Table 9 Comparison ratios of performance of AUGMECON 2 over AUGMECON-R for the 3kpY problems.

Problem	CPU Time Ratio	Models solved Ratio	Infeasibilities Ratio	Duplicate solutions Ratio
3kp100	5.15	8.84	7.98	18.93
3kp50	9.75	12.94	7.23	28.71
3kp40	11.45	14.88	12.35	32.05

To highlight the enhanced performance of AUGMECON-R over AUGMECON 2, the arbitrary selection of the lower bounds loosens, to maximise the probability of including the actual nadir points in the analysis and ensure that no solution is missed. So, instead of multiplying the nadir values of the payoff tables by 95%, as was the case in the problems above, we reiterate our analysis of these three problems, by multiplying the nadir values by 5%, leading to an emphatically larger grid, in order to evaluate how this impacts the performance of the two algorithms in comparison (Table 5).

Table 10 Performance comparison between AUGMECON 2 (AUGM 2) and AUGMECON-R (AUGM-R) for the 3kpY problems with lower bounds.

	3kp100*		3kp50*		3kp40*	
	AUGM 2	AUGM-R	AUGM 2	AUGM-R	AUGM 2	AUGM-R
CPU Time	62 h	274 min	230 min	737 sec	130 min	234 sec
Grid points per objective function	3940	3940	1880	1880	1560	1560
Models solved	417809	11768	61442	1953	39648	748
Infeasibilities	1093	137	564	78	420	34
Duplicate solutions	410138	5090	59827	825	38836	322
Dominated solutions	78	41	3	2	3	3
Solutions in the Pareto front	6500	6500	1048	1048	389	389

Although the difference of the two algorithms is now more evident for the case of significantly lower bounds, by looking at Tables 3 and 5, it is worth pointing out that this problem modification led to a CPU time increase of 2.24%, 6.00% and 6.40% for AUGMECON-R, compared to a CPU time increase of 170.00%, 103.50% and 209.52% for AUGMECON 2, for 3kp100, 3kp50 and 3kp40 respectively. Similar findings can be observed for all other relevant



metrics; for example, the additional models solved by AUGMECON-R are negligible in all three problems (41, 2 and 2), the same cannot be said for AUGMECON 2 (314157, 36197 and 28550 respectively).

2.4.2 Complex benchmark problems

Here, we implement both algorithms to evaluate AUGMECON-R in problems of more than three objective functions. Before doing so, however, we distinguish between uncorrelated and weakly correlated problems (Martello and Monaci, 2020; Shah and Reed, 2011): uncorrelated problems assume no correlation between elements of the objective function coefficient matrix and those of the constraint coefficient matrix, while weakly correlated problems assume a weak correlation between these elements. This weak correlation makes their solution significantly more difficult, as the solver requires more time resources, and given the time requirements for AUGMECON 2 to solve such problems, only uncorrelated problems are assumed in this study.

We define the following problems:

A 4kp40 problem, with 155, 119 and 121 being the true nadir points of the three constrained objective functions and 123, 127 and 140 being their ranges respectively.

A 4kp40* problem, which is identical with the 4kp40 problem but without a priori knowledge of nadir points, hence with the consideration of significantly lower bounds: 15, 11 and 13 being the lower bounds and 263, 235 and 248 the range respectively.

A 4kp50 binary problem, with objective function coefficients resulting from a uniform distribution $U[0,1]$ and constraint coefficients from a uniform distribution $U[50,70]$, with 718, 735 and 713 being the true nadir points, and 51, 35 and 44 being the ranges respectively.

A 4kp50* binary problem, which is identical with the 4kp50 binary problem but after extending the range of the objective functions by assigning new lower bounds at 70, 69 and 57.

A 5kp40 problem, with objective function coefficients resulting from a uniform distribution $U[50,40]$ and constraint coefficients from a uniform distribution $U[2,10]$, with 29, 32, 27 and 27 being the true nadir points of the four constrained objective functions, and 21, 21, 27 and 25 being the ranges respectively.

A 5kp40* problem, which is identical with the 5kp40 problem but after extending all ranges to 45, to make sure we include the now unknown true nadir points, with 5, 8, 9 and 7 being the new lower bounds.

A 6kp50 binary problem, with objective function coefficients resulting from a uniform distribution $U[0,1]$ and constraint coefficients from a uniform distribution $U[0,5]$, with 38, 37, 31, 27 and 30 being the true nadir points of the five constrained objective functions, and 21, 24, 26, 30 and 22 being the ranges respectively.

A 6kp50* problem, which is identical with the 6kp50 binary problem but after extending all ranges to 50, to make sure we include the now unknown true nadir points, with 9, 11, 7, 7 and 2 being the new lower bounds.

The matrices of the objective function and constraint coefficients are provided in Appendix B, for all of the above pairs of problems, i.e. for 4kp40 – 4kp40*, 4kp50 – 4kp50*, 5kp40 – 5kp40* and 6kp50 – 6kp50*.

Table 6 summarises the performance differences between AUGMECON 2 and AUGMECON-R, for the problems 4kp40 and 4kp40*, while Figure 2 visualises the Pareto front of the problem.



Table 11 Performance comparison between AUGMECON 2 and AUGMECON-R for the 4kp40 problem, with the true nadir points (4kp40) and with lower bounds (4kp40*).

	4kp40		4kp40*	
	AUGMECON 2	AUGMECON-R	AUGMECON 2	AUGMECON-R
CPU Time	1214 min	56 min	85 hours	59 min
Models solved	290443	14735	1431195	10846
Infeasibilities	14735	359	35363	359
Duplicate solutions	272530	7324	1392653	7315
Dominated solutions	6	0	7	0
Solutions in the Pareto front	3172	3172	3172	3172

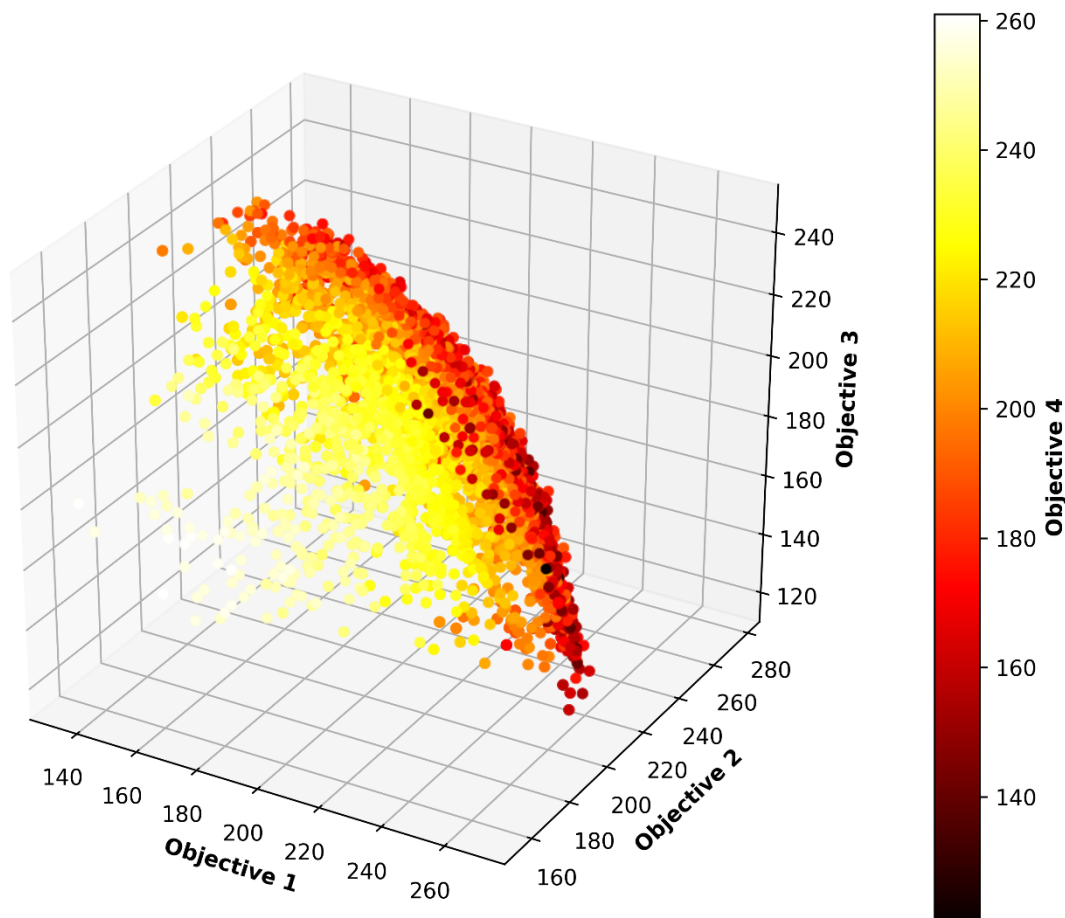


Figure 12 The Pareto front of the 4kp40 problem.

It is evident, from Table 4, that AUGMECON-R is almost 21 times faster than its predecessor, with the latter solving almost 26 times more models, in the problem where the actual nadir points are known a priori; this ratio difference is, as discussed above, due to the number of checks made by AUGMECON-R in its *flag* array. When considering the case of the true nadir points being unknown and thus extending the grid to secure that the actual nadir points are included in the analysis and that no solution is missed, AUGMECON-R outperforms AUGMECON 2 by solving about 131 times less models, more than 85 times faster. One odd finding is that AUGMECON-R now solves even

less models than before; given how small the lower bounds are, the surplus variables are significantly larger, and this circumstantially leads to less models. This, however, does not bear any negative impacts on the accuracy of the algorithm, as it stumbles upon equally as many infeasibilities.

Similarly, Table 7 summarises the performance differences between AUGMECON 2 and AUGMECON-R, for the binary problems 4kp50 and 4kp50*, while Figure 3 visualises the Pareto front of the problem.

Table 12 Performance comparison between AUGMECON 2 and AUGMECON-R for the 4kp50 problem, with the true nadir points (4kp50) and with lower bounds (4kp50*).

	4kp50		4kp50*	
	AUGMECON 2	AUGMECON-R	AUGMECON 2	AUGMECON-R
CPU Time	1021 sec	31 sec	161 hours	939 sec
Models solved	6296	176	>4000000	161
Infeasibilities	1211	28	-	28
Duplicate solutions	5039	102	-	87
Dominated solutions	0	0	-	0
Solutions in the Pareto front	46	46	46	46

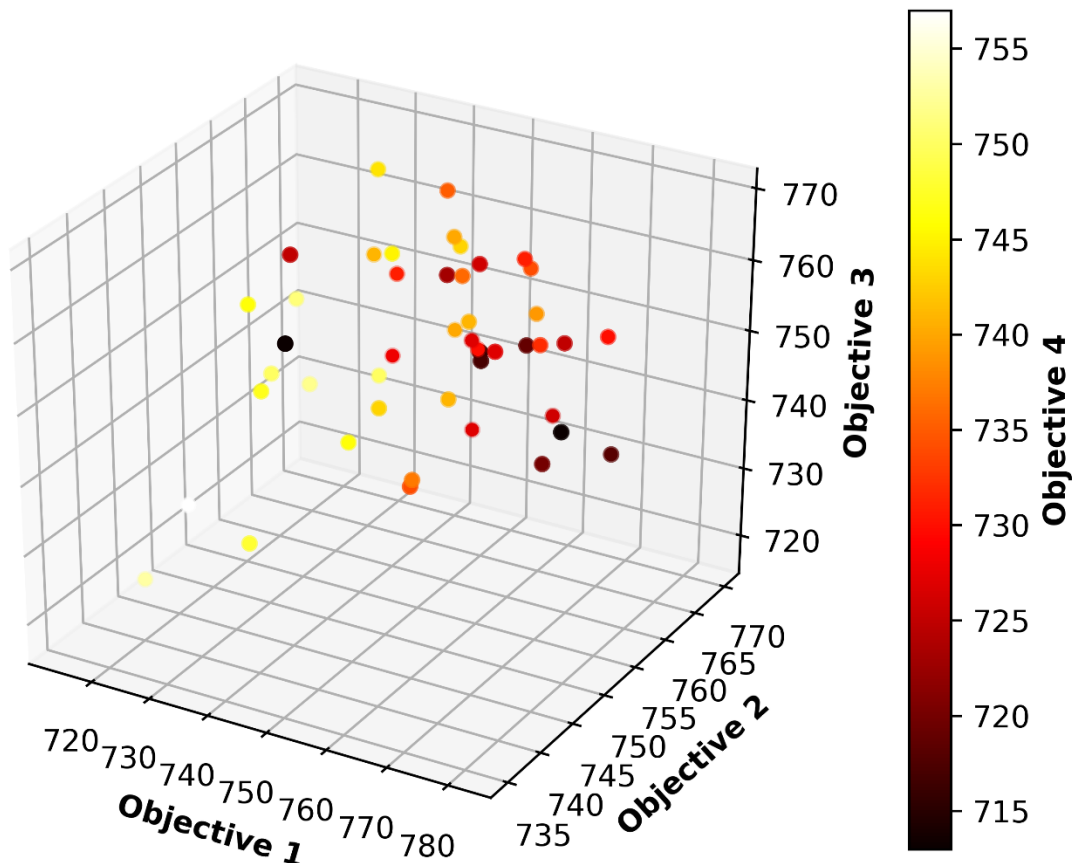


Figure 13 The Pareto front of the 4kp50 problem.

Again, AUGMECON-R solves the 4kp50 problem almost 32 times faster, having solved about 35 times less models. But what is strikingly interesting is that, when considering the 4kp50* problem, AUGMECON 2 required 161 hours and solved more than four million models. These findings clearly indicate that AUGMECON-R has the capacity to timely solve time-wise non-viable, complex problems, ensuring accuracy and assuring no solution is missed.

Moving onto a five-objective problem, Table 8 summarises the performance differences between AUGMECON 2 and AUGMECON-R, for the problems 5kp40 and 5kp40*, while Figure 4 visualises the Pareto front of the problem.

Table 13 Performance comparison between AUGMECON 2 and AUGMECON-R for the 5kp40 problem, with the true nadir points (5kp40) and with lower bounds (5kp40*).

	5kp40		5kp40*	
	AUGMECON 2	AUGMECON-R	AUGMECON 2	AUGMECON-R
CPU Time	12035 sec	175 sec	27 hours	194 sec
Models solved	52030	618	458760	622
Infeasibilities	9351	114	47521	114
Duplicate solutions	42553	378	411113	382
Dominated solutions	0	0	0	1
Solutions in the Pareto front	126	126	126	126

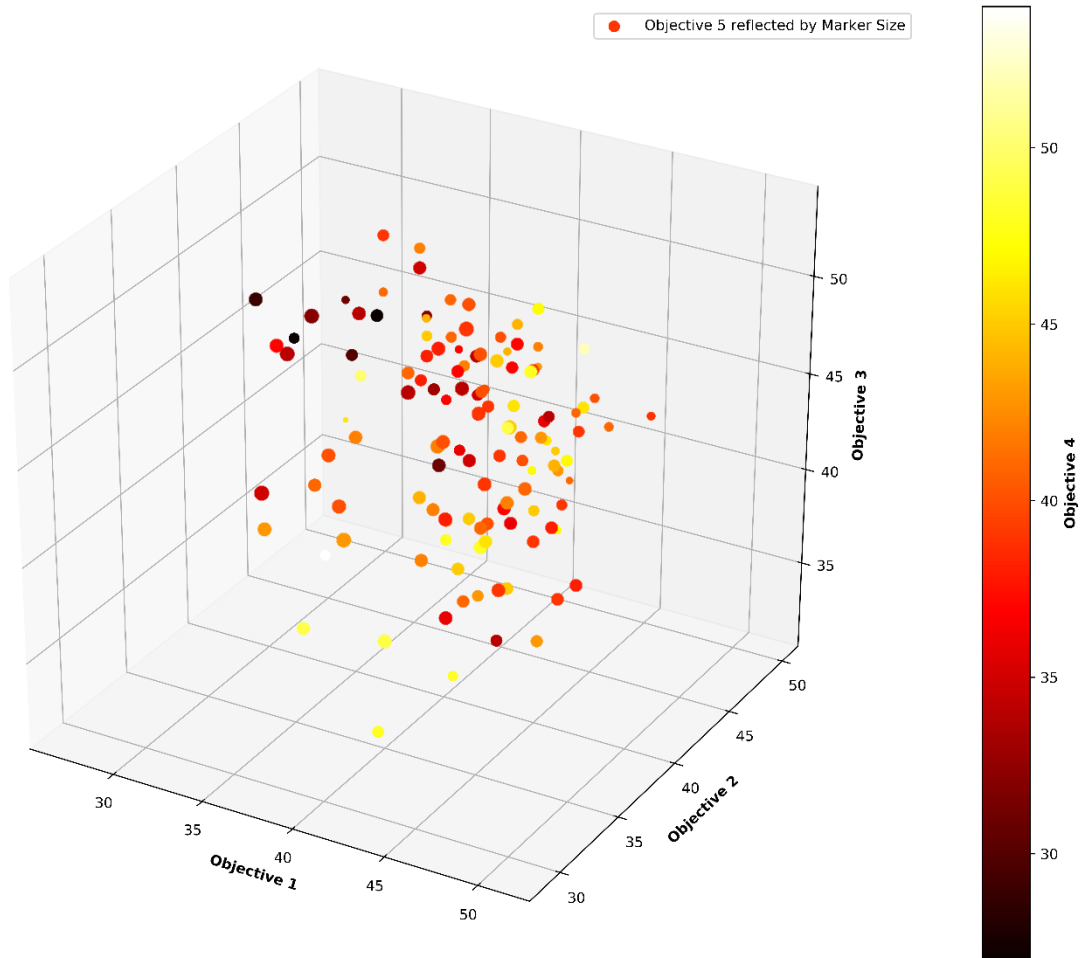


Figure 14 The Pareto front of the 5kp40 problem.

AUGMECON-R solved the 5kp40 problem almost 68 times faster, having solved about 83 times less models, while in the case of lack of a priori knowledge lower bounds considering the 4kp50* problem, these differences surge to 505 and 737 times respectively. In both cases, however, it is evident that AUGMECON-R outperforms AUGMECON 2 even more than in the previous two sets of problems of four objective functions; as previously discussed, the larger the number of objective functions is, the larger this outperformance is. This can be highlighted in the final problem of six objective functions, as follows in Table 9 and Figure 5.

Table 14 Performance comparison between AUGMECON 2 and AUGMECON-R for the 6kp50 problem, with the true nadir points (6kp50) and with lower bounds (6kp50*).

	6kp50		6kp50*	
	AUGMECON 2	AUGMECON-R	AUGMECON 2	AUGMECON-R
CPU Time	52 hours	1207 sec	-	4145 sec
Models solved	1104406	6269	-	6242
Infeasibilities	193612	863	-	863
Duplicate solutions	909949	4563	-	4536
Dominated solutions	2	0	-	0
Solutions in the Pareto front	843	843	843	843

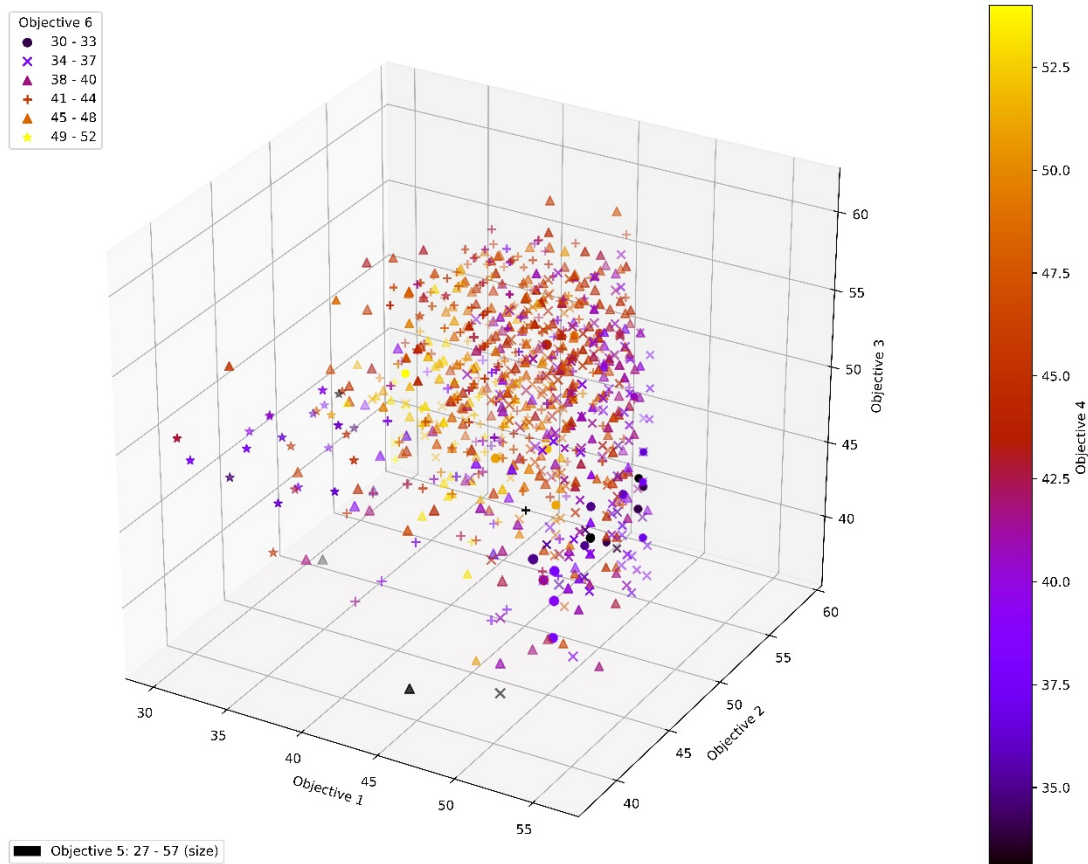


Figure 15 The Pareto front of the 6kp50 problem.



As with the 4kp50 binary problem, the 6kp50 binary problem solved by both AUGMECON 2 and AUGMECON-R emphasises the performance difference between the two methods. Given the significantly higher complexity that a sixth objective function adds to the problem, the CPU time and models solved ratios are even higher in this case, with AUGMECON 2 solving 175 more models 155 times slower. By extending the grid in order to ensure that the a priori unknown true nadir points are included in the analysis, AUGMECON 2 cannot solve the problem in a reasonable amount of time—it took the algorithm 47 hours to cross the grid once.

2.5 Conclusions

In this study, an improved version of the augmented ϵ -constraint method, AUGMECON-R, is introduced, allowing robust and timely optimisation of complex systems. Drawing from the weaknesses associated with its predecessor (AUGMECON 2), the concept and mathematical model of the proposed method is presented in detail and its code provided in Appendix A, before implementing both methods in comparison. The problems solved in Sections 4.1-4.2 suggest that the proposed method, AUGMECON-R, greatly outperforms its predecessor, AUGMECON 2, by solving significantly less models in emphatically less time and allowing us to easily and timely solve hard or even impossible, in terms of time and processing requirements, problems of multiple objective functions. AUGMECON-R, furthermore, solves the problem of unknown nadir points, by using very low or zero-value lower bounds without increasing the time requirements.

As with ϵ -constraint (e.g. Ehrgott and Ryan, 2002; Laumanns et al., 2006), there exist in the literature a few other attempts to identify weaknesses associated with and improve accordingly the AUGMECON 2 algorithm (e.g. Domínguez-Ríos et al., 2019), which however tend to perform a posteriori and numerous checks that potentially enhance complexity and time requirements, such as (Zhang and Reimann, 2014), which additionally is developed in Visual Studio Express instead of the usual operational research problem solving implementation platform, GAMS.

One limitation of the proposed method lies in the introduction of a *flag* array, the size of which is directly linked to the range of the objective functions and therefore can lead to occupy a large memory space that could be unavailable. To overcome this, AUGMECON-R could in the future be developed in an object-oriented language like C++, instead of GAMS, which allows for dynamic memory allocation. This would enable using virtual memory, avoiding the *flag* array initialisation with zero values and releasing memory space whenever a counter moves across the grid.

Given that even the slightest uncertainty in the data can render system optimality meaningless from a practical point of view (Bertsimas and Sim, 2004) and given recent advancements on robust linear optimisation (Bertsimas and Brown, 2009), other prospects for future research include the all-in-one integration of AUGMECON-R with uncertainty and robustness analysis methods (Van de Ven et al., 2019; Mastorakis and Siskos, 2016; Ben-Tal et al., 2010; Kadzinski et al., 2017; Witting et al., 2013), thereby avoiding the use of numerous methods, code scripts, or even implementation platforms.



3 Optimal allocation of renewable energy subsidies from the COVID-19 recovery package: Mitigating emissions and creating new jobs

3.1 Introduction

The outbreak of the COVID-19 pandemic at the end of 2019 and throughout 2020 has posed significant challenges to public health, as well as to medical and research communities in their efforts to battle the impacts of the global health crisis (Fauci et al., 2020). With many nations facing mandatory restrictions and lockdowns to mitigate the transmission of the virus, economic activities forcefully paused, causing an impending economic recession with multiple socio-economic implications (Nicola et al., 2020). The pandemic comes alongside the major ongoing threat of climate change, completing the triple front of challenges that humankind must face in the upcoming years: health, economic and environmental crises. Although no direct causality exists between the emergence of COVID-19 and climate change, human development and environmental malpractices, like deforestation, have been found to be the root of pandemics, due to the caused biodiversity losses and the destruction of natural habitats (Tollefson, 2020). On the other hand, it is highly unlikely that short-term positive environmental impacts that were observed due to the change in lifestyles, like reduced coal consumption and CO₂ emissions drop, can be maintained in the future (Saadat et al., 2020). With emissions forecasted to fully rebound post-crisis (Le Quéré et al., 2020; Nikas et al., 2020) and pandemics expected to increase in frequency unless biodiversity loss is reversed (IPBES, 2020), the two threats face important shared challenges (Manzanedo and Manning, 2020) that should be addressed co-dependently (Nikas et al., 2021).

Disruptive developments in the broader landscape, like COVID-19, tend to destabilise organisational structures and threaten reproduction of a system. Impulses for change then emerge that provide the choice for different pathways to be followed as the system evolves in light of these disruptions (Geels and Schot, 2007). In the post-pandemic future, most businesses will have to shift their models in line with corporate social responsibility including the introduction of more sustainable practices if they want to survive (He and Harris, 2020). Support from states is necessary in the process. In the UK, almost 9 million people constituting a quarter of the workforce financially depend on governmental assistance (Miles et al., 2020). At the same time, Eurostat reported that the unemployment rate in the EU in September 2020 was 7.5% while the corresponding rate for the euro area was 8.3% (Eurostat, 2020). This translates to 1.811 and 1.376 million jobs lost in the EU and the euro area respectively, compared to September 2019, with unemployment expected to rise as the second wave leads to more lockdowns. A key concern however remains on whether fiscal packages will accelerate the achievement of climate goals or lock-into a fossil fuel pathway (Hepburn et al., 2020). So far, COVID-19 has put sustainable transitions on hold. IRENA reports that the pandemic crisis resulted in both permanent job losses due to project cancellations and delays in supply chains with short-term effect: factory shutdowns in China, which dominates the wind power supply chain, and the lockdowns in Ecuador, responsible for almost 90% of global balsa production that is used in wind turbines, affected operations of supply chains, especially manufacturing of equipment (IRENA, 2020). With more jobs lost in the energy sector on top of the 160,000 coal jobs that are already at high risk (Alves Dias et al., 2018), the need for a sustainable and just transition that will create family-sustaining jobs is urgent (Henry et al., 2020). In the US, although the Green New Deal is surrounded by significant political controversy, the discussion is stirred towards the creation of sustainable jobs, with estimates expecting 18.3 additional million jobs to be created, out of which more than 2 million are "green" manufacturing jobs (Bezdek, 2020). Such a transition will require a carefully conceived plan to handle the shift of workforce and capital between the different sectors (Claeys et al.,



2019), since it is expected that 1.3% of EU jobs will be reallocated by 2050 (Fragkos and Paroussos, 2018). The renewable energy sector can play a pivotal role in the transition, both directly through renewable installation projects and indirectly to support other technologies, like “green” hydrogen (Levoyannis, 2021). A recent modelling study indicated that under a current policy scenario renewable energy can trigger more than 658,000 jobs especially in operation and maintenance and installation; however, in light of COVID-19, these expectations should be re-evaluated, considering that these sub-sectors are the most affected by the pandemic. Another issue that should also be considered is the ability of all member states to generate RES jobs, since results of the study show a concentration of these jobs in select few countries (Ortega et al., 2020).

To face these challenges and support the Member States’ economic recovery from the effects of COVID-19, the bloc has mobilised financial resources as part of the long-term budget of 2021-2027. As updated by the 23 April conference of the European Council and respective conclusions of the 21 July Council meeting, the available funds for the economic recovery amount to €2,364.3 billion, where €1,074.3 billion come from the Multiannual Financial Framework (MMF) 2021-2027, €750 billion constitute the NextGenerationEU program that is tailored to battle the impact of the pandemic, and €540 billion are funds already available from safety nets to support workers, businesses and member states (European Council, 2020). Based on recent pledges, 30% of the MMF and NextGenerationEU budgets, which together account for €1.8 trillion, will be utilised towards achieving the 2030 climate targets (European Commission, 2020a). This means that until 2027 it is expected that more than half a trillion euros will flow towards a green transition. The NextGenerationEU is a financial instrument that aims to raise €750 billion from the capital market to establish the Recovery and Resilience Facility (RRF) (€672.5 billion) and bring additional funds to other EU programs like ReactEU (€47.5 billion), Horizon Europe (€5 billion), InvestEU (€5.6 billion), rural development (€7.5 billion), the Just Transition Fund (JTF) (€10 billion) and RescEU (€1.9 billion). The RRF is the centrepiece mechanism of the NextGenerationEU, which aims to provide Member States with grants and loans to support investments and reforms towards the recovery from the pandemic. Specifically, €360 billion will be available for loans and €312.5 will be offered in grants, which coupled with the previous amounts bring the total available funds in grants to €390 billion (European Commission, 2020b). To access these funds, Member States need to submit national recovery and resilience plans until April 2021, which will be assessed based on the integration of investments towards green and digital transformation. The Commission expects these plans to allocate at least 37% and 20% for green and digital investments and reforms respectively with emphasis on contributing to the seven flagship initiatives identified by the 2021 Annual Sustainable Growth for this twin transition: Power up, Renovate, Recharge and Refuel, Connect, Modernise, Scale-up, and Reskill and upskill (European Commission, 2020d). Specifically for the green transition, these initiatives should be aligned with the updated target of the European Green Deal of 55% emissions reduction by 2030 (Jäger-Waldau et al., 2020), which translates to integrating 40% of the 500GW of renewable energy required by 2030, the installation of 6 GW of electrolyser capacity, the production and transportation of 1 million tonnes of renewable hydrogen across the EU, doubling the renovation rate, as well as building one out of the three million charging points in 2030 and half of the 1,000 hydrogen stations needed (European Commission, 2020c). Considering these allocations, it can be expected that €250 billion will be used to support investments in clean energy and renewables, energy efficiency of buildings, and sustainable transport. However, the detailed breakdown of this budget in the three targets depends on the prioritisation of each Member State’s plan, expected by April 2021 at the latest.

In the context of the societal challenges emerging from COVID-19 and the EU pledges for an economic and sustainable recovery, this study aims to optimise the impact of the proposed fiscal program and the budget allocated towards the “green” transition in terms of jobs created in the energy sector and the reduction of GHG emissions. For this purpose, an extensive literature review is performed to identify the impact of sustainable technologies in terms of employment and then the GCAM model is employed to assess different levels of



subsidisation on these technologies. The results are fed into a portfolio analysis based on AUGMECON-R and a Monte Carlo simulation to handle uncertainty, in order to identify optimal strategies for the envisaged budget that maximise the creation of new jobs and the reduction of GHG emissions. We highlight that based on a provisional budget of €100-200 billion, about 230-432k new jobs can be created by 2025 and 50-233 MtCO_{2e} can be cut by 2030 on top of a current policies scenario, which will bring the EU targets slightly closer with significant co-benefits. These results are mainly driven by investments in biofuels, wind, and biogas and in smaller amounts in geothermal energy.

3.2 Methods

On the basis of the multiple-uncertainty analysis framework proposed in Section 1, here we present a two-level integrated assessment and portfolio modelling study, to investigate how to best allocate part of the announced recovery plans in renewable energy technologies. The renewable energy portfolios are optimised with the aim to maximise reductions in emissions, while at the same time maximising employment gains in the energy sector.

First, the GCAM model is run on top of a "Current Policies" (CP) scenario, as presented in PARIS REINFORCE Deliverable D7.4, meaning that results should be interpreted additionally to the established measures and targets. At this step, we retrieve GCAM outputs for different levels of subsidies in eight key technologies, including biofuels, biomass, CSP, geothermal, solar photovoltaics, electric vehicles, wind, and biogas, touching upon power generation, transport, buildings, etc. Given that the recovery and resilience funds have to be spent by 2024, it is assumed that the different subsidies are applied between 2021 and 2025 and affect the entire capital costs of the energy technologies, interpreting subsidy to lower initial investment costs. For GHGs, we calculate the cumulative emissions impacts from 2021 to 2030, abstracting GCAM results in 2030. We consider that green investments contribute to reducing emissions in the longer term, thereby extracting additional cumulative emissions reductions by 2030, while subsidies provided in 2021-2025 have an employment impact that is evident in the short-term (2025).

To calculate the jobs created per technology subsidisation, we perform an extensive literature review to identify the number of jobs per energy of unit produced (depending on the technology). Based on the GCAM simulation, we can then calculate the net impact of jobs compared to the reference (CP) scenario depending on the increase or decrease in the demand for each technology. The assumptions used in the analysis are presented in Table 15.

The jobs and energy produced (either TWh or TOE/kTOE) for Wind, PV, Biogas and Biofuels are directly drawn from EurObserverR (2020), which allowed us to calculate the jobs/unit of energy metric used in GCAM. For CSP, we focused on data from Spain for solar thermal energy, since most European CSP projects are located in Spain and the majority of solar thermal in the country refers to CSP. In that case, jobs are derived from EurObserver (2020) and energy data from IEA (2020), both of which corresponding to Spain. A similar approach was followed for geothermal energy, for which data for Italy were used since most of the EU geothermal production is in Italy.

For biomass, natural gas, and coal, we reviewed the literature to identify the conversion method, capacity factor, and lifetime of plants from Wei et al. (2010) and employment factors for Construction, Manufacturing, and O&M from Fragkos and Paroussos (2018) and Rutovitz et al. (2015), and then calculate the "jobs per energy unit produced" metric required. For oil, lifetime information was not available; we used considered that coal, gas, and oil share similar lifetimes (40 years) (Papapostolou et al., 2017), thereby assuming that oil and gas share a similar level of jobs required to produce one unit of energy, as hinted in Fragkos and Paroussos (2018).

A technology missing from the table yet examined in this study is electric vehicles (EVs): jobs associated with the labour-intensive charging infrastructure were not available at the moment of the analysis; the effect of EV subsidies on jobs is therefore only the net difference caused in the entire system due to the penetration of more EVs.



Table 15 Job Assumptions per technology

	Jobs	Electricity Production (TWh)	Jobs/TWh	Source
Wind	179,062	377.4	861.9	(EurObserverR, 2020)
PV	114,679.7	122.9	956.3	(EurObserverR, 2020)
CSP	8,200	4.9	1,683.8	(EurObserverR, 2020; IEA, 2020)
Geothermal	2,200	6.1	360.4	(EurObserverR, 2020; IEA, 2020)
Biomass	-	-	218.2	(Wei et al., 2010; Fragkos and Paroussos, 2018; Rutovitz et al., 2015)
Nuclear	1,133,400	822.3	1,378	(IEA, 2020; WNN, 2019)
Coal	-	-	132.9	(Wei et al., 2010; Fragkos and Paroussos, 2018; Rutovitz et al., 2015)
Oil	-	-	59.3	(Wei et al., 2010; Fragkos and Paroussos, 2018; Rutovitz et al., 2015; Papapostolou et al., 2017),
Natural Gas	-	-	59.3	(Wei et al., 2010; Fragkos and Paroussos, 2018; Rutovitz et al., 2015)
Biogas	68,800	16,838.7 (kTOE)	4.08 (Jobs/kTOE)	(EurObserverR, 2020)
Biofuels	248,200	16,658.2 (TOE of consumption for transport)	14.9 (Jobs/TOE of consumption for transport)	(EurObserverR, 2020)

On a simplified application of the methodology presented in Forouli et al. (2020), the outcomes of the GCAM analysis are fed into a portfolio optimisation model. The optimisation problem is modelled in GAMS and solved with the use of a bi-objective evaluation model for PA and of the AUGMECON-R method, as documented in Section 2. As stated above, the portfolios comprising any of eight renewable technologies (biofuels, biomass, CSP, geothermal, solar photovoltaics, electric vehicles, wind, and biogas) are evaluated based on their performance with regard to their contribution to the reduction of GHG emissions, and the positive consequences they may induce on jobs creation under different subsidy levels, forming two objecting functions:



$$\text{maximise } Z_1 = \sum_{i=1} \sum_{j=1} (\text{GHGred}_{i,j} \cdot b_{i,j}) \quad \forall i, j \quad (1)$$

$$\text{maximise } Z_2 = \sum_{i=1} \sum_{j=1} (\text{JobsCreat}_{i,j} \cdot b_{i,j}) \quad \forall i, j \quad (2)$$

where:

$\text{GHGred}_{i,j}$: emission reduction achieved by the i_{th} technology under budget option j

$\text{JobsCreat}_{i,j}$: impact on employment achieved by the i_{th} technology under budget option j

$i = 1, 2, \dots, 8$: for the eight renewable technologies examined

$j = 1, 2, \dots, 10$: for the ten levels of subsidisation considered, imposed as reduction in the initial investment costs of each technology

$b_{i,j}$: binary decision variable whose value is equal to 1, if the i_{th} technology under budget option j meets the criteria posed, and 0 otherwise.

It is noted here that the objective functions' coefficients, namely $\text{GHGred}_{i,j}$ and $\text{JobsCreat}_{i,j}$ are calculated based on the outcomes of the GCAM model.

To limit technology subsidisation into an amount consistent with the current EU policy, we trailed the proposed breakdown for the COVID recovery plan, looking at what part of the RRF could (theoretically at this point and prior to actual national requests expected by April 2021) be used for energy technology subsidies, and ended up with budgets between one and two hundred billion euros for the next five years. The reasoning behind these calculations is given in Section 3.1. Stemming from this analysis we selected three indicative budget levels within the range of one and two hundred billion (100, 150 and 200 billion Euros) as constraints for the portfolio optimisation and solved three optimisation problems, one for each budget constraint.

As a last step, and to deal with the inherent uncertainty characterising the basic parameters of the model, namely GHG emissions reduction and jobs impact, a Monte Carlo simulation is carried out in a plus or minus 5% range for both parameters per subsidy package. The Monte Carlo simulation is executed iteratively 1,000 times for each of the three portfolio analysis configurations. By doing so, the robustness of the obtained optimal energy technology portfolios can be evaluated, considering that the uncertainty in the model's parameters is of stochastic nature. More on the robustness evaluation approach used in this study can be found in Forouli et al. (2019a).

3.3 Results and Discussion

In the following, the optimal portfolios for the three assumed budgets are presented, also incorporating robustness information. The analysis shows that depending on the budget, the results change markedly in terms of portfolio mixes, but not substantially in terms of the qualitative synthesis.

3.3.1 Portfolios with budget of €100 billion

The final set of optimal portfolios is shown in Figure 16. The maximum impact on employment for the budget of €100 billion is 260 thousand jobs, while the best performance in emissions reduction is a reduction equal to 123 MtCO_{2e}. What is important to note here is how the technologies composing the optimal portfolios contribute to these goals. For that, we select two indicative portfolios, one that mainly contributes to emissions reductions (P1) and another with a higher potential for employment co-benefits (P2). The analysis shows that biofuels, wind, biogas, and geothermal subsidies dominate the portfolios. The decomposition of portfolios P1 and P2 also reveals the analysis' dynamics and most active trade-offs, which are next validated also for the other considered budgets: biofuels-heavy mixes can push emissions further down compared to other technologies, while wind-based portfolios can make the most impact in terms of employment.



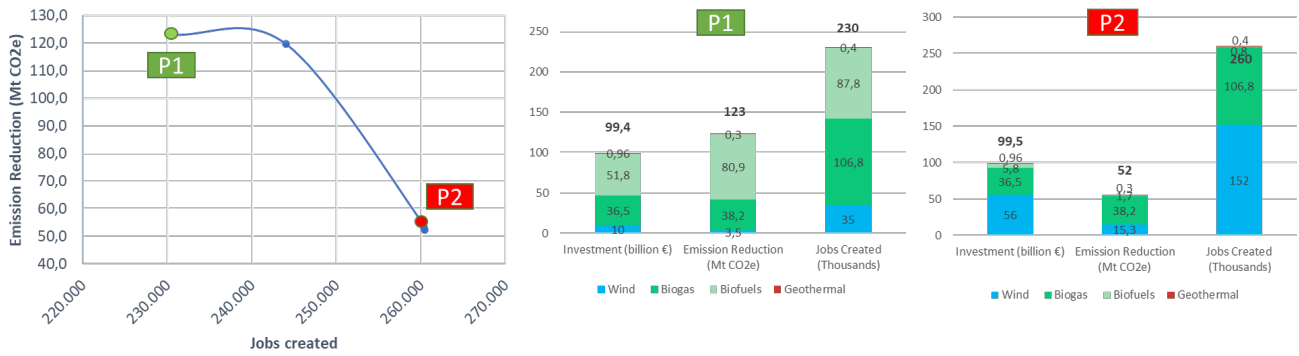


Figure 16: Optimal Portfolios and technologies participation (€100 billion)

The results of the Monte Carlo simulations provide further insights into the participation of technologies among the optimal portfolios. In Figure 17, we see the levels of subsidisation that each technology achieves among multiple Monte Carlo iterations. We confirm that the most frequent technologies are wind, biogas, biofuels, and geothermal, though subsidisation in geothermal is in most cases limited. It is noted that in some cases within the uncertainty spectrum considered, a limited budget is also invested in CSP. Solar photovoltaics, electric vehicles, and biomass are absent from (virtually) all portfolios. The dominant subsidisation levels for the technologies with higher potential, namely wind, biofuels and biogas, are €56, €52 and €37 billion respectively.

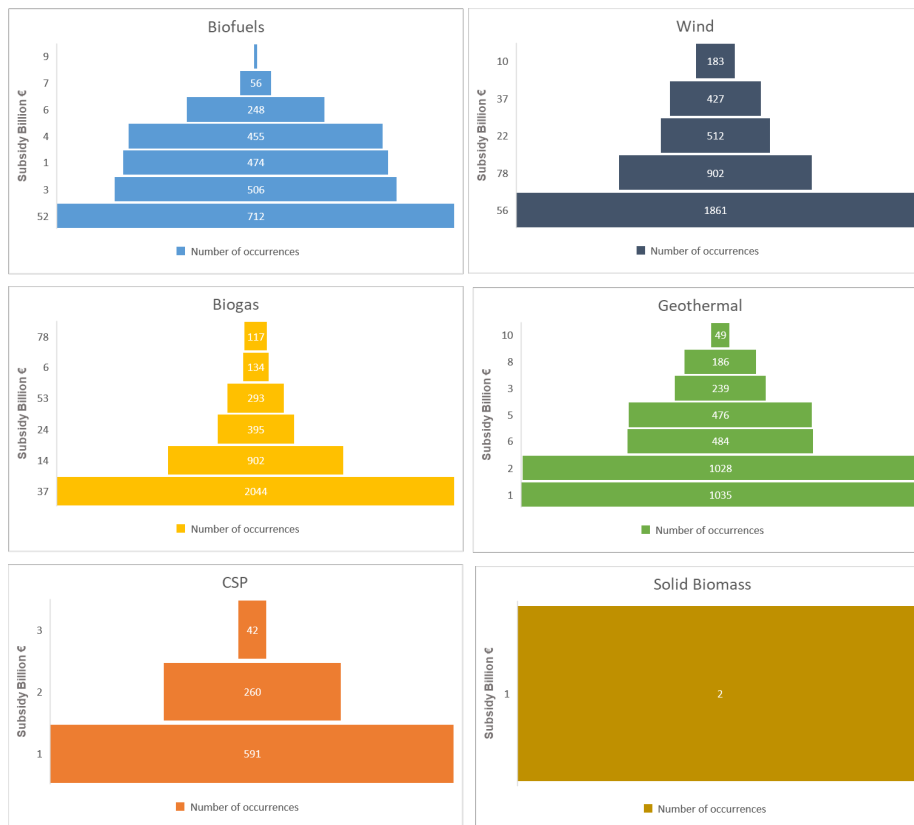


Figure 17: Technologies participation in the Monte Carlo simulations (€100 billion)

The robustness analysis performed through the Monte Carlo simulations also leads to the updated final set of optimal portfolios, with the most robust portfolios illustrated with bubbles of greater size (Figure 18).

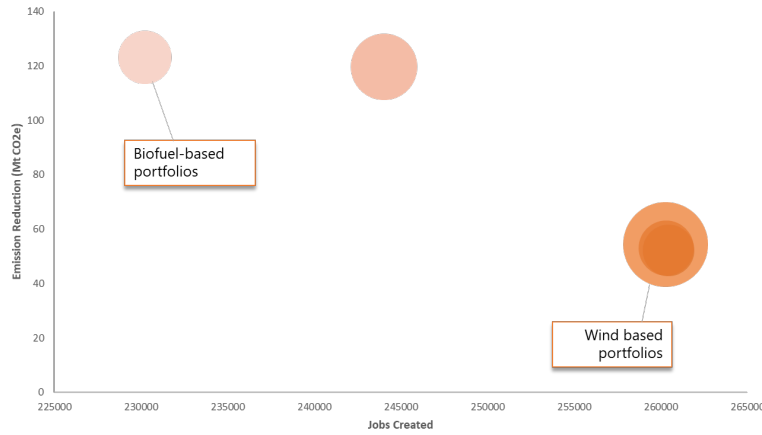


Figure 18: Pareto Front of robust portfolios (€100 billion)

3.3.2 Portfolios with budget of €150 billion

The final set of optimal portfolios is shown in Figure 19. The maximum impact on employment for the budget of €150 billion is 348 thousand jobs (a 34% increase compared to the €100 billion portfolios), while up to 160 MtCO_{2e} emissions cuts are achieved, on top of the CP scenario (30% increase compared to the €100 billion portfolios).

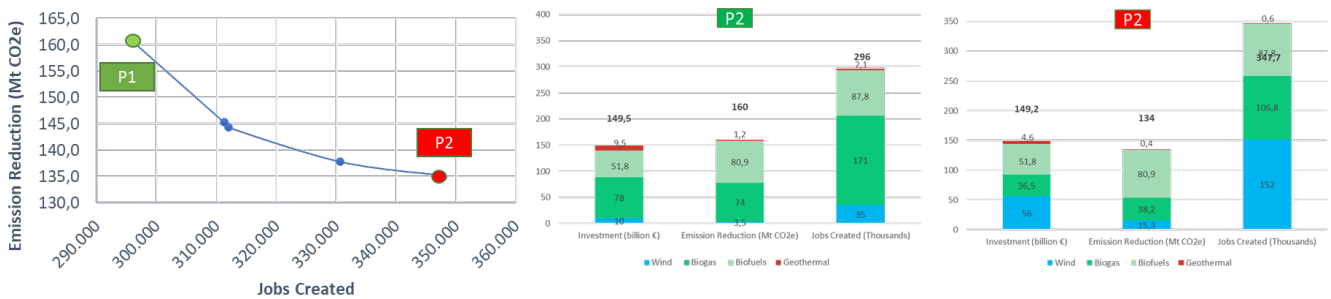


Figure 19: Optimal Portfolios and technologies participation (€150 billion)

Delving into the contribution of the technologies within the optimal portfolios and notice that, as in the €100 billion portfolios, biofuels, wind, biogas, and geothermal are again the dominant technologies. We highlight that, while we move towards a larger investment capacity, biogas breaks into the mix, essentially balancing portfolios, and biofuels keep maximising the emissions reductions potential. On the other end of the optimality front (portfolio P2), we observe that wind not only drastically improves the employment benefits of a 150-billion-euro subsidy, but as the Monte Carlo analysis indicates (Figure 21) it also makes up the most robust portfolios against uncertainties.

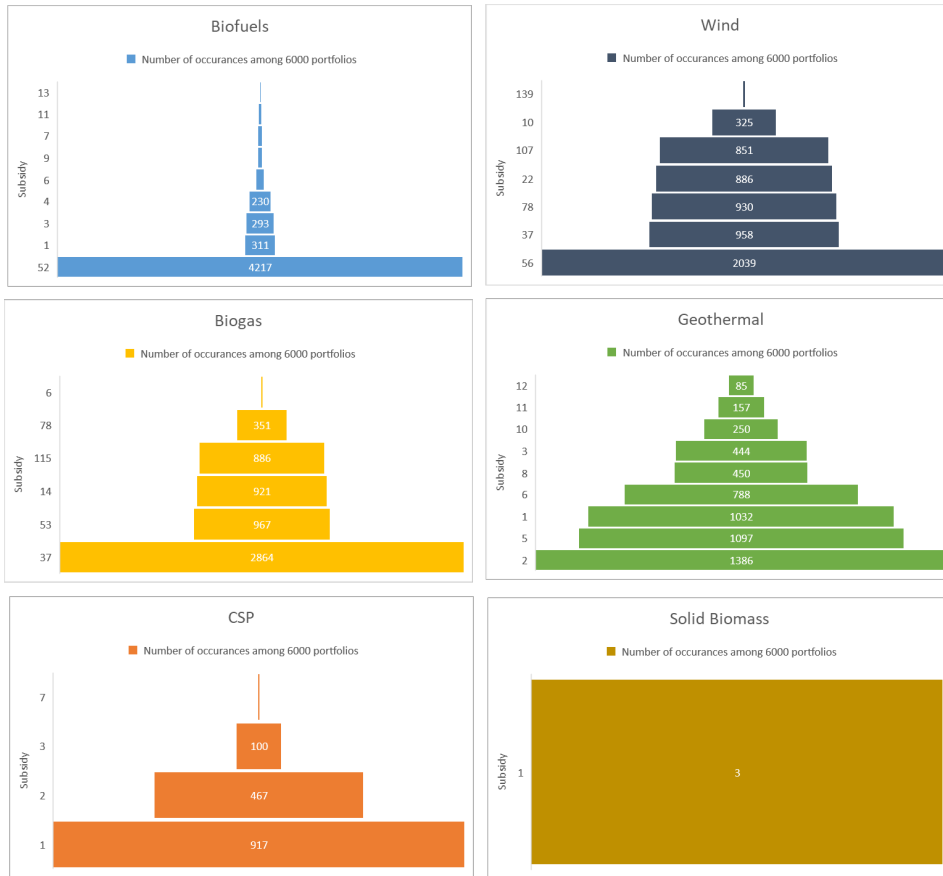


Figure 20: Technologies participation in the Monte Carlo simulations (€150 billion)

The results of the Monte Carlo simulations confirm again that the most robust technologies to subsidise are wind, biogas, biofuels, and geothermal energy. Wind and biogas are in most cases highly subsidised with investments from EUR 56 to 107 billion and EUR 37 to 115 billion, respectively. The different levels of subsidisation among these two technologies lead to a trade-off between emissions cuts (emphasised in case of biogas) and number of new jobs (higher in case of wind). The lower threshold to invest in biofuels is normally circa 50 billion. In the absence of investments in biofuels, the budget is distributed to wind and biogas to balance the two criteria. Subsidisation in geothermal energy is normally low, €1-10 billion depending on the investment mix of the main technologies, but this can be a reasonable investment that can yield to up to 1,500 new jobs; it is noteworthy that these small budget packages examined for geothermal energy partly reflect the overall potential of the source in the EU. CSP subsidies sometimes appear as complementary investments, across the uncertainty perturbations. Additional subsidies in photovoltaics and EVs on top of the current policies are neither here recommended.

The updated final set of optimal portfolios after the incorporation of robustness information is shown in the following figure.

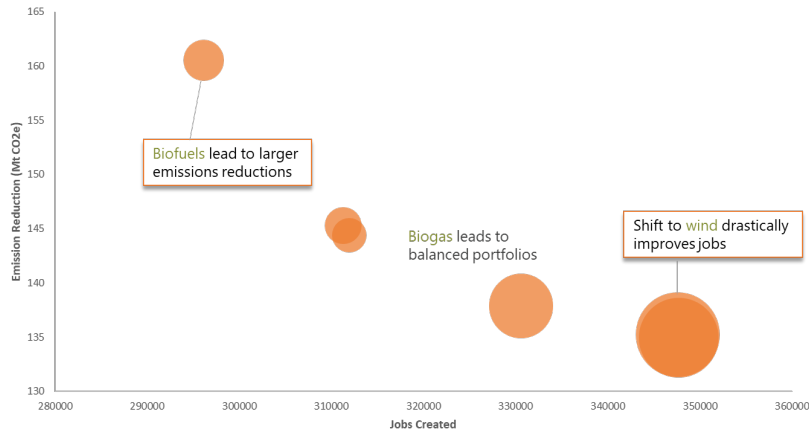


Figure 21: Pareto Front of robust portfolios (€150 billion)

3.3.3 Portfolios with budget of €200 billion

The final set of optimal portfolios is shown in Figure 22. The maximum impact on employment for the budget of €200 billion is 432 thousand jobs (24% increase compared to the €150 billion portfolios), while the largest potential of emissions reductions equals to 237 Mt CO₂e (48% increase compared to the €150 billion portfolios).

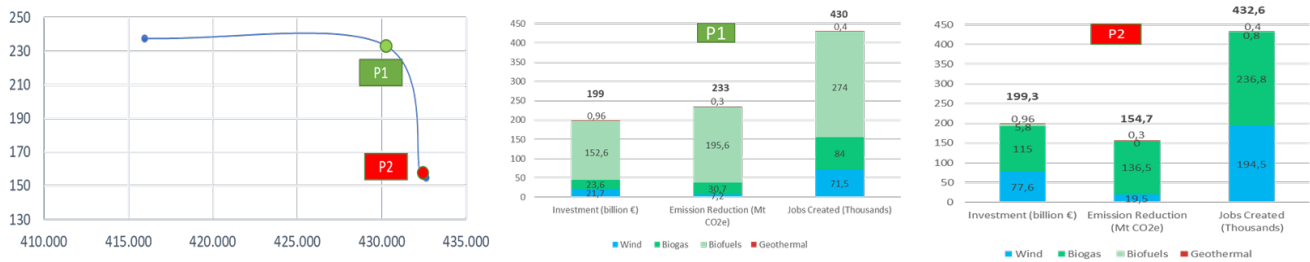


Figure 22: Optimal Portfolios and technologies participation (€200 billion)

As depicted in Figures 22 and 23, the main difference of the 200 billion-euro solution from the previous analyses is a larger investment in biofuels. This leads to solutions that achieve high emissions cuts and simultaneously create many new jobs in the entire energy sector, as the case is in portfolio P1. Biofuels are normally subsidised with up to €153 billion, while the most common investments in biogas are €37 billion and in wind €22 billion, which is a significant reduction compared to the high levels of subsidisation achieved by these technologies in the 100 and 150 billion-euro solutions. The remaining budget is allocated to geothermal energy and CSP and just in three portfolios in solid biomass.

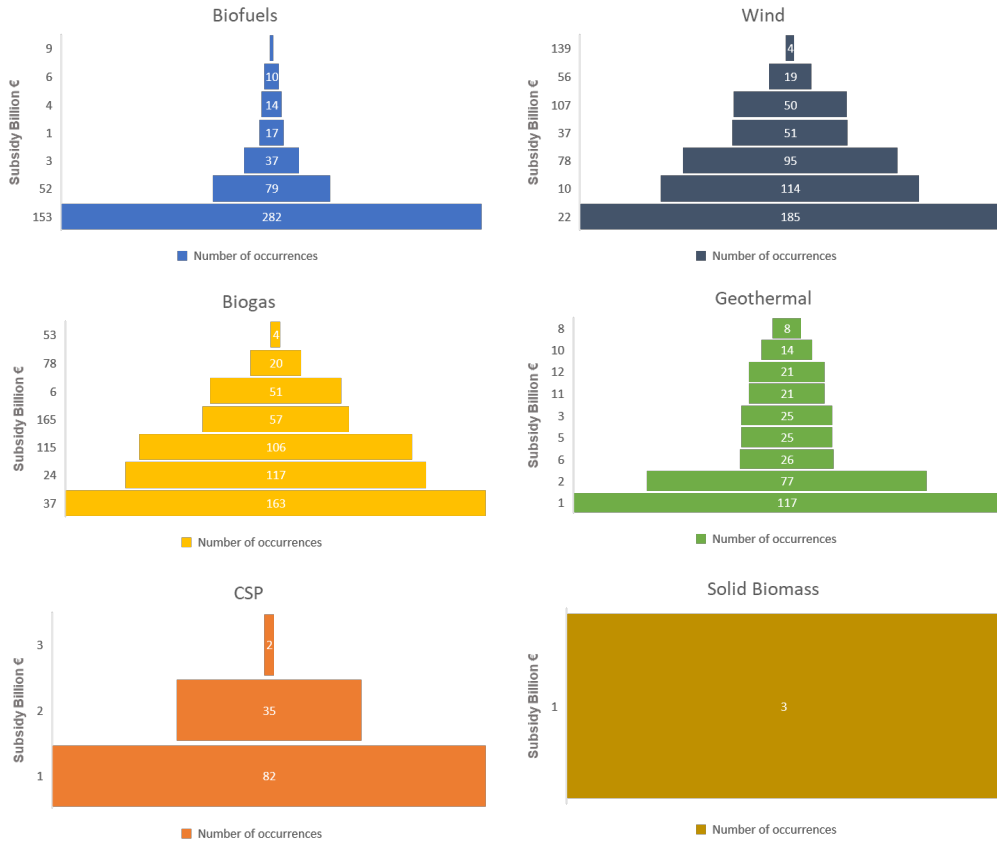


Figure 23: Technologies participation in the Monte Carlo simulations (€200 billion)

The updated, robust, set of optimal portfolios is given in the following figure.

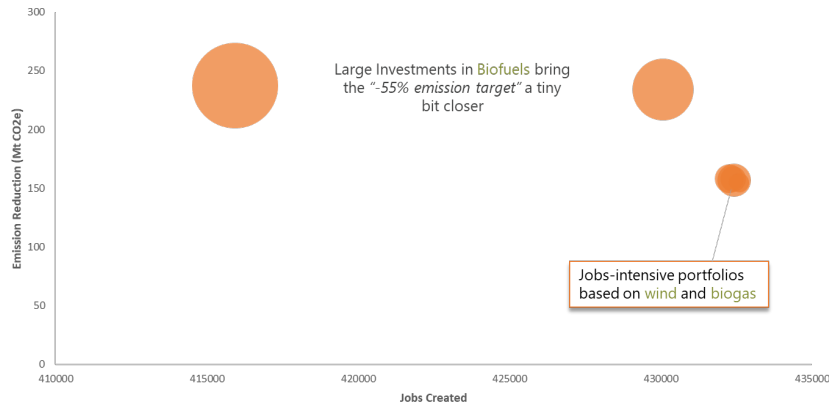


Figure 24: Pareto Front of robust portfolios (€200 billion)

In contrast to the robustness analysis results of 100 and 150 billion-euro portfolios, where wind intensive portfolios exhibited the higher level of robustness, the 200-billion-euro portfolio analysis shows that large investments in biofuels are the least sensitive way forward in terms of uncertainty perturbation. This could be partly attributed to the non-linearity of the budgets considered.

3.3.4 Discussion

The purpose of this study was to examine what would the benefits be in terms of jobs created and additional emissions reductions if the EU budget pledged for the economic recovery from the impact of COVID-19 was



largely used to fund subsidies for expanding renewable energy. The results should be interpreted as additional to the existing low-carbon measures and targets established.

The core finding of this study is that 100-to-200-billion-euro subsidies could achieve a further up-to-1% CO₂ emissions cuts. This may sound small, but at the same time such a strategy can create 230-432 thousand jobs in the energy sector, supporting the COVID-impacted employment as a side-effect of the green transition. It is also noteworthy that 2030 is the first year in the model that emissions impact of the subsidies is reflected, so a single-year or post-2030 comparison may reflect larger benefits. The main caveat is that this is still based on one of the many models of PARIS REINFORCE, so this is very much work in progress; but a first read of the modelling dynamics showed that we can in fact gain financially on these investments, in terms of pushing down costs of existing policies.

From a technological point of view, we can see that biofuels, wind, and biogas appear overall optimal, when considering both criteria, and that uncertainty plays out quite differently in terms of robust portfolio synthesis. Main caveats in this respect are the non-linearities in the budgets assumed in the analysis, as well as that the employment co-benefits for certain technologies do not capture the entire picture, with electric vehicles being the most prominent example: impacts of EV subsidies only trail net job changes throughout the entire energy sector, without accounting for associated labour-intensive activities like charging infrastructure. As a result, electric vehicles appear to lead to further emissions cuts, but these are expensive, and their employment impact is virtually negligible. We can also see that geothermal, for which smaller subsidy packages are considered to reflect the current potential in Europe (by proxy of the annualised costs of the technology in GCAM), is not that competitive compared to the three other optimal technologies. Nevertheless, it manages to break into all near-optimal solutions due to its low cost and positive impacts along both axes. What was very interesting also was that solar power appears to reach its tipping point in the base scenario, in the sense that there is already high penetration of photovoltaics in the electricity mix under a current policies scenario, meaning that additional subsidies seem to increase the resulting emissions (pointing to the need for gas to balance the grid load).

Furthermore, it is evident that the current policies already do a fine job in reducing emissions in the power sector (with the ETS and dropping capital costs), but this is not entirely true for other sectors (e.g. transport and buildings), in which subsidies turn out more cost-effective.

Clearly, emphasising emissions reductions by prioritising for example subsidies in biofuels, could possibly lead to some Land Use Change emissions outside the EU, especially in countries that are strong biofuel producers (e.g. USA, Brazil, Argentina, China; see PARIS REINFORCE Deliverable D4.1), which could also be why, for the same subsidies in GCAM, we see opposite-leaning impacts globally.

Next steps include extending the analysis to the broader modelling ensemble of PARIS REINFORCE, as well as adding more objectives, such as industrial value added, health co-benefits, etc.), and enhancing the level of detail in direct and indirect employment factors (including EVs). Furthermore, it will be useful to wait for the final RRF, in terms of investment capacity in subsidies (as finalised by the national recovery and resilience plans and financing requests to be submitted by April 2021), before examining the climate-employment co-benefits at both (EU- and Member State-) levels.

3.4 Key takeaways

The pandemic has had a significant impact on the European economy, with approximately 1.8 million EU citizens losing their jobs between September 2019 and September 2020. Towards facilitating a recovery, the EU launched the Recovery and Resilience Facility (RRF) to provide €672.5 billion of financial support to Member States in the coming years. In line with the European Green Deal and climate efforts, 37% of investments in national plans



requesting RRF financing must focus on a “green” transition. Integrated within the first PARIS REINFORCE model inter-comparison scenario logic of exploring “where the world is headed” based on current policies and pledges, we seek the optimal allocation of renewable energy subsidies from the COVID-19 recovery package in the EU. Towards further mitigating emissions and creating new jobs in the green transition, on top of a current policies scenario, we use budgets aligned with announced plans, and couple integrated assessment modelling with a technological portfolio analysis. We find that, for a €100-200 billion investment budget in 2021-2025, about 230-432k new jobs can be created by 2025 in the energy sector. The support package could also bring the EU (only slightly) closer to the new 2030 climate target: 50-233 MtCO_{2e} can be cut by 2030, corresponding to a 0.2-1% drop further down from the current policies scenario. Biofuels, wind, and biogas appear to be the most optimal technologies to subsidise against the two criteria, with small geothermal investments complementing portfolios. As solar energy already reaches high levels of penetration in a current policies scenario, additional subsidies push emissions higher due to increasing gas use for balancing grid load, while electric vehicles display expensive emissions cuts for negligible new jobs. Wind-based portfolios prioritising employment gains appear more robust against uncertainties; this shifts in favour of biofuels if larger investment capacity is assumed, maximising emissions reductions.



Bibliography

- Allan, G., Eromenko, I., McGregor, P., & Swales, K. (2011). The regional electricity generation mix in Scotland: A portfolio selection approach incorporating marine technologies. *Energy Policy*, 39(1), 6-22.
- Allen, M. R. (2003). Climate forecasting: Possible or probable?. *Nature*, 425(6955), 242-242.
- Alves Dias, P., Kanellopoulos, K., Medarac, H., Kapetaki, Z., Miranda-Barbosa, E., Shortall, R., ... & Tzimas, E. (2018). EU coal regions: opportunities and challenges ahead. European Union: Luxembourg. Retrieved from: <https://ec.europa.eu/jrc/en/publication/eur-scientific-and-technical-research-reports/eu-coal-regions-opportunities-and-challenges-ahead>
- Alves, M. J., & Costa, J. P. (2009). An exact method for computing the nadir values in multiple objective linear programming. *European Journal of Operational Research*, 198(2), 637-646.
- Antosiewicz, M., Nikas, A., Szpor, A., Witajewski-Baltvilks, J., & Doukas, H. (2020). Pathways for the transition of the Polish power sector and associated risks. *Environmental Innovation and Societal Transitions* 35, 271-291.
- Arancibia, A. L., Marques, G. F., & Mendes, C. A. B. (2016). Systems capacity expansion planning: Novel approach for environmental and energy policy change analysis. *Environmental modelling & software*, 85, 70-79.
- Aras, N., & Yurdakul, A. (2016). A new multi-objective mathematical model for the high-level synthesis of integrated circuits. *Applied Mathematical Modelling*, 40(3), 2274-2290.
- Arvesen, A., Luderer, G., Pehl, M., Bodirsky, B. L., & Hertwich, E. G. (2018). Deriving life cycle assessment coefficients for application in integrated assessment modelling. *Environmental modelling & software*, 99, 111-125.
- Attia, A. M., Ghaithan, A. M., & Duffuaa, S. O. (2019). A Multi-Objective Optimization Model for Tactical Planning of Upstream Oil & Gas Supply Chains. *Computers & Chemical Engineering*.
- Bababeik, M., Khademi, N., & Chen, A. (2018). Increasing the resilience level of a vulnerable rail network: The strategy of location and allocation of emergency relief trains. *Transportation Research Part E: Logistics and Transportation Review*, 119, 110-128.
- Baker, E., & Solak, S. (2011). Climate change and optimal energy technology R&D policy. *European Journal of Operational Research*, 213(2), 442-454.
- Bal, A., & Satoglu, S. I. (2018). A goal programming model for sustainable reverse logistics operations planning and an application. *Journal of cleaner production*, 201, 1081-1091.
- Baležentis, T., & Streimikiene, D. (2017). Multi-criteria ranking of energy generation scenarios with Monte Carlo simulation. *Applied energy*, 185, 862-871.
- Behmanesh, R., & Zandieh, M. (2019). Surgical case scheduling problem with fuzzy surgery time: An advanced bi-objective ant system approach. *Knowledge-Based Systems*, 104913.
- Ben-Tal, A., Bertsimas, D., & Brown, D. B. (2010). A soft robust model for optimization under ambiguity. *Operations research*, 58(4-part-2), 1220-1234.
- Bertsimas, D., & Brown, D. B. (2009). Constructing uncertainty sets for robust linear optimization. *Operations research*, 57(6), 1483-1495.
- Bertsimas, D., & Sim, M. (2004). The price of robustness. *Operations research*, 52(1), 35-53.



- Bezdek, R. H. (2020). The Jobs Impact of the USA New Green Deal. *American Journal of Industrial and Business Management*, 10(6), 1085-1106.
- Bistline, J. E. (2016). Energy technology R&D portfolio management: Modeling uncertain returns and market diffusion. *Applied energy*, 183, 1181-1196.
- Bootaki, B., Mahdavi, I., & Paydar, M. M. (2014). A hybrid GA-AUGMECON method to solve a cubic cell formation problem considering different worker skills. *Computers & Industrial Engineering*, 75, 31-40.
- Bootaki, B., Mahdavi, I., & Paydar, M. M. (2016). New criteria for configuration of cellular manufacturing considering product mix variation. *Computers & Industrial Engineering*, 98, 413-426.
- Calvin, K., & Bond-Lamberty, B. (2018). Integrated human-earth system modeling—state of the science and future directions. *Environmental Research Letters*, 13(6), 063006.
- Cambero, C., & Sowlati, T. (2016). Incorporating social benefits in multi-objective optimization of forest-based bioenergy and biofuel supply chains. *Applied Energy*, 178, 721-735.
- Cambero, C., Sowlati, T., & Pavel, M. (2016). Economic and life cycle environmental optimization of forest-based biorefinery supply chains for bioenergy and biofuel production. *Chemical Engineering Research and Design*, 107, 218-235.
- Canales-Bustos, L., Santibañez-González, E., & Candia-Véjar, A. (2017). A multi-objective optimization model for the design of an effective decarbonized supply chain in mining. *International Journal of Production Economics*, 193, 449-464.
- Carrizosa, E., Guerrero, V., & Morales, D. R. (2019). Visualization of complex dynamic datasets by means of mathematical optimization. *Omega*, 86, 125-136.
- Claeys, G., Tagliapietra, S., & Zachmann, G. (2019). How to make the European Green Deal work. *Bruegel Policy Contribution*, 13. Retrieved from: https://www.bruegel.org/wp-content/uploads/2019/11/PC-14_2019-041119.pdf
- Collins, W. D., Craig, A. P., Truesdale, J. E., Di Vittorio, A. V., Jones, A. D., Bond-Lamberty, B., ... & Patel, P. (2015). The integrated Earth system model version 1: formulation and functionality. *Geoscientific Model Development*, 8(7), 2203-2219.
- Crowe, K. A., & Parker, W. H. (2008). Using portfolio theory to guide reforestation and restoration under climate change scenarios. *Climatic Change*, 89(3-4), 355-370.
- Dabiri, N., Tarokh, M. J., & Alinaghian, M. (2017). New mathematical model for the bi-objective inventory routing problem with a step cost function: A multi-objective particle swarm optimization solution approach. *Applied Mathematical Modelling*, 49, 302-318.
- Dellink, R., Chateau, J., Lanzi, E., & Magné, B. (2017). Long-term economic growth projections in the Shared Socioeconomic Pathways. *Global Environmental Change*, 42, 200-214.
- del Granado, P. C., Skar, C., Doukas, H., & Trachanas, G. P. (2019). Investments in the EU Power System: A Stress Test Analysis on the Effectiveness of Decarbonisation Policies. In *Understanding Risks and Uncertainties in Energy and Climate Policy* (pp. 97-122). Springer, Cham.
- Domínguez-Ríos, M. Á., Chicano, F., Alba, E., del Águila, I., & del Sagrado, J. (2019). Efficient anytime algorithms to solve the bi-objective Next Release Problem. *Journal of Systems and Software*, 156, p. 217-231.
- Doukas, H., & Nikas, A. (2020). Decision support models in climate policy. *European Journal of Operational*



Research, 280(1), 1-24.

- Doukas, H., Nikas, A., González-Eguino, M., Arto, I., & Anger-Kraavi, A. (2018). From integrated to integrative: Delivering on the Paris Agreement. *Sustainability*, 10(7), 2299.
- Edmonds, J. A., Wise, M. A. and MacCracken, C. N. (1994) Advanced Energy Technologies and Climate Change: An Analysis Using the Global Change Assessment Model (gcam). PNL-9798. Pacific Northwest National Laboratory (PNNL), Richland, WA (United States).
- Ehrenstein, M., Wang, C. H., & Guillén-Gosálbez, G. (2019). Strategic planning of supply chains considering extreme events: Novel heuristic and application to the petrochemical industry. *Computers & Chemical Engineering*, 125, 306-323.
- Ehrgott, M., & Ryan, D. M. (2002). Constructing robust crew schedules with bicriteria optimization. *Journal of Multi - Criteria Decision Analysis*, 11(3), 139-150.
- Estrada, F., Tol, R. S., & Botzen, W. W. (2019). Extending integrated assessment models' damage functions to include adaptation and dynamic sensitivity. *Environmental Modelling & Software*, 121, 104504.
- EurObservER. (2019). The State of Renewable Energies in Europe, 2019 Edition, Paris. Retrieved from: <https://www.isi.fraunhofer.de/content/dam/isi/dokumente/ccx/2020/The-state-of-renewable-energies-in-Europe-2019.pdf>
- European Commission (EC). (2016). The roadmap for transforming the EU into a competitive, low-carbon economy by 2050. https://ec.europa.eu/clima/sites/clima/files/2050_roadmap_en.pdf.
- European Commission. (2020a). Annual Sustainable Growth Strategy 2021. Retrieved from: <https://eur-lex.europa.eu/legal-content/EN/TXT/PDF/?uri=CELEX:52020DC0575&from=en>
- European Commission. (2020b). Recovery plan for Europe. Retrieved from: https://ec.europa.eu/info/strategy/recovery-plan-europe_en
- European Commission. (2020c). Recovery and Resilience Plans. Retrieved from: https://ec.europa.eu/info/sites/info/files/3_en_document_travail_service_part1_v3_en_0.pdf
- European Commission. (2020d). The Recovery and Resilience Facility. Retrieved from: https://ec.europa.eu/info/business-economy-euro/recovery-coronavirus/recovery-and-resilience-facility_en
- European Council. (2020). COVID-19: the EU's response to the economic fallout. Retrieved from: <https://www.consilium.europa.eu/en/policies/coronavirus/covid-19-economy/>
- Eurostat. (2020). September2020 - Euro area unemployment at 8.3%. Retrieved from: <https://ec.europa.eu/eurostat/documents/2995521/10663786/3-30102020-CP-EN.pdf/f93787e0-0b9a-e10e-b897-c0a5f7502d4e>
- Ewert, F., Rötter, R. P., Bindi, M., Webber, H., Trnka, M., Kersebaum, K. C., ... & Semenov, M. A. (2015). Crop modelling for integrated assessment of risk to food production from climate change. *Environmental Modelling & Software*, 72, 287-303.
- Fauci, A. S., Lane, H. C., & Redfield, R. R. (2020). Covid-19—navigating the uncharted. *The New England Journal of Medicine*, 382, 1268-1269.
- Florios, K., & Mavrotas, G. (2014). Generation of the exact Pareto set in multi-objective traveling salesman and set covering problems. *Applied Mathematics and Computation*, 237, 1-19.



- Forouli, A., Doukas, H., Nikas, A., Sampedro, J., & Van de Ven, D. J. (2019a). Identifying optimal technological portfolios for European power generation towards climate change mitigation: A robust portfolio analysis approach. *Utilities Policy*, 57, 33-42.
- Forouli, A., Gkonis, N., Nikas, A., Siskos, E., Doukas, H., & Tourkolas, C. (2019b). Energy efficiency promotion in Greece in light of risk: Evaluating policies as portfolio assets. *Energy*, 170, 818-831.
- Forouli, A., Nikas, A., Van de Ven, D. J., Sampedro, J., & Doukas, H. (2020). A multiple-uncertainty analysis framework for integrated assessment modelling of several sustainable development goals. *Environmental Modelling & Software*, 131, 104795.
- Forouzanfar, M. H., Afshin, A., Alexander, L. T., Anderson, H. R., Bhutta, Z. A., Biryukov, S., ... & Cohen, A. J. (2016). Global, regional, and national comparative risk assessment of 79 behavioural, environmental and occupational, and metabolic risks or clusters of risks, 1990–2015: a systematic analysis for the Global Burden of Disease Study 2015. *The lancet*, 388(10053), 1659-1724.
- Fragkos, P., & Paroussos, L. (2018). Employment creation in EU related to renewables expansion. *Applied Energy*, 230, 935-945.
- Fuss, S., Szolgayová, J., Khabarov, N., & Obersteiner, M. (2012). Renewables and climate change mitigation: Irreversible energy investment under uncertainty and portfolio effects. *Energy Policy*, 40, 59-68.
- Gavranis, A., & Kozanidis, G. (2017). Mixed integer biobjective quadratic programming for maximum-value minimum-variability fleet availability of a unit of mission aircraft. *Computers & Industrial Engineering*, 110, 13-29.
- Geels, F. W., & Schot, J. (2007). Typology of sociotechnical transition pathways. *Research policy*, 36(3), 399-417.
- Geels, F. W., Berkhout, F., & van Vuuren, D. P. (2016). Bridging analytical approaches for low-carbon transitions. *Nature Climate Change*, 6(6), 576.
- Gidden, M. J., Fujimori, S., van den Berg, M., Klein, D., Smith, S. J., van Vuuren, D. P., & Riahi, K. (2018). A methodology and implementation of automated emissions harmonization for use in Integrated Assessment Models. *Environmental Modelling & Software*, 105, 187-200.
- Giupponi, C., Borsuk, M. E., De Vries, B. J., & Hasselmann, K. (2013). Innovative approaches to integrated global change modelling. *Environmental modelling & software*, 44, 1-9.
- Grübler, A., & Nakicenovic, N. (2001). Identifying dangers in an uncertain climate. *Nature*, 412(6842), 15-15.
- Habibi, F., Barzinpour, F., & Sadjadi, S. J. (2019). A mathematical model for project scheduling and material ordering problem with sustainability considerations: A case study in Iran. *Computers & industrial engineering*, 128, 690-710.
- Hajkowicz, S., Spencer, R., Higgins, A., & Marinoni, O. (2008). Evaluating water quality investments using cost utility analysis. *Journal of Environmental Management*, 88(4), 1601-1610.
- Hamilton, S. H., ElSawah, S., Guillaume, J. H., Jakeman, A. J., & Pierce, S. A. (2015). Integrated assessment and modelling: overview and synthesis of salient dimensions. *Environmental Modelling & Software*, 64, 215-229.
- Hanger-Kopp, S., Nikas, A., & Lieu, J. (2019). Framing risks and uncertainties associated with low-carbon pathways. In Hanger-Kopp, S., Lieu, A., & Nikas, A. (eds.) *Narratives of Low-Carbon Transitions*, pp. 10- 21. Routledge, Abingdon.



- He, H., & Harris, L. (2020). The impact of Covid-19 pandemic on corporate social responsibility and marketing philosophy. *Journal of Business Research*, 116, 176-182.
- Henry, M. S., Bazilian, M. D., & Markuson, C. (2020). Just transitions: Histories and futures in a post-COVID world. *Energy Research & Social Science*, 68, 101668.
- Hepburn, C., O'Callaghan, B., Stern, N., Stiglitz, J., & Zenghelis, D. (2020). Will COVID-19 fiscal recovery packages accelerate or retard progress on climate change?. *Oxford Review of Economic Policy*, 36, S359-S381.
- Hombach, L. E., & Walther, G. (2015). Pareto-efficient legal regulation of the (bio) fuel market using a bi-objective optimization model. *European Journal of Operational Research*, 245(1), 286-295.
- Huang, Y. H., & Wu, J. H. (2008). A portfolio risk analysis on electricity supply planning. *Energy policy*, 36(2), 627-641.
- Huppmann, D., Gidden, M., Fricko, O., Kolp, P., Orthofer, C., Pimmer, M., ... & Krey, V. (2019). The MESSAGEix Integrated Assessment Model and the ix modeling platform (ixmp): An open framework for integrated and cross-cutting analysis of energy, climate, the environment, and sustainable development. *Environmental modelling & software*, 112, 143-156.
- Hwang, C. L., Paidy, S. R., Yoon, K., & Masud, A. S. M. (1980). Mathematical programming with multiple objectives: A tutorial. *Computers & Operations Research*, 7(1-2), 5-31.
- IEA. (2018). *World Energy Outlook 2018*, IEA, Paris, <https://doi.org/10.1787/weo-2018-en>.
- IEA. (2020). Data and Statistics. Retrieved from: https://www.iea.org/data-and-statistics?country=***&fuel=Electricity%20and%20heat&indicator=ElecGenByFuel
- Inghels, D., Dullaert, W., & Bloemhof, J. (2016). A model for improving sustainable green waste recovery. *Resources, Conservation and Recycling*, 110, 61-73.
- Intergovernmental Panel on Climate Change. (2018). *Global Warming of 1.5° C: An IPCC Special Report on the Impacts of Global Warming of 1.5° C Above Pre-industrial Levels and Related Global Greenhouse Gas Emission Pathways, in the Context of Strengthening the Global Response to the Threat of Climate Change, Sustainable Development, and Efforts to Eradicate Poverty*. Intergovernmental Panel on Climate Change.
- IPBES. (2020). IPBES Workshop on Biodiversity and Pandemics. Retrieved from: <https://ipbes.net/pandemics>
- IRENA. (2020). *The post-COVID recovery: An agenda for resilience, development and equality*. Retrieved from: <https://www.irena.org/publications/2020/Jun/Post-COVID-Recovery>
- Jabbarzadeh, A., Azad, N., & Verma, M. (2019). An optimization approach to planning rail hazmat shipments in the presence of random disruptions. *Omega*.
- Jäger-Waldau, A., Kougias, I., Taylor, N., & Thiel, C. (2020). How photovoltaics can contribute to GHG emission reductions of 55% in the EU by 2030. *Renewable and Sustainable Energy Reviews*, 126, 109836.
- Jakeman, A. J., & Letcher, R. A. (2003). Integrated assessment and modelling: features, principles and examples for catchment management. *Environmental Modelling & Software*, 18(6), 491-501.
- Janssen, S., Ewert, F., Li, H., Athanasiadis, I. N., Wien, J. J. F., Théron, O., ... & Belhoucette, H. (2009). Defining assessment projects and scenarios for policy support: use of ontology in integrated assessment and modelling. *Environmental Modelling & Software*, 24(12), 1491-1500.
- Jenkins, P. R., Lunday, B. J., & Robbins, M. J. (2019). Robust, multi-objective optimization for the military medical



- evacuation location-allocation problem. *Omega*, 102088.
- JGCRI (2017) GCAM v4.4 Documentation. Available at: <http://jgcri.github.io/gcam-doc/v4.4/toc.html>.
- Jiang, L., & O'Neill, B. C. (2017). Global urbanization projections for the Shared Socioeconomic Pathways. *Global Environmental Change*, 42, 193-199.
- Kadziński, M., Labijak, A., & Napieraj, M. (2017). Integrated framework for robustness analysis using ratio-based efficiency model with application to evaluation of Polish airports. *Omega*, 67, 1-18.
- Kadziński, M., Tervonen, T., Tomczyk, M. K., & Dekker, R. (2017). Evaluation of multi-objective optimization approaches for solving green supply chain design problems. *Omega*, 68, 168-184.
- Khalili-Damghani, K., & Amiri, M. (2012). Solving binary-state multi-objective reliability redundancy allocation series-parallel problem using efficient epsilon-constraint, multi-start partial bound enumeration algorithm, and DEA. *Reliability Engineering & System Safety*, 103, 35-44.
- Khalili-Damghani, K., Abtahi, A. R., & Tavana, M. (2013). A new multi-objective particle swarm optimization method for solving reliability redundancy allocation problems. *Reliability Engineering & System Safety*, 111, 58-75.
- Khalili-Damghani, K., Tavana, M., & Sadi-Nezhad, S. (2012). An integrated multi-objective framework for solving multi-period project selection problems. *Applied Mathematics and Computation*, 219(6), 3122-3138.
- Kinzig, A., & Starrett, D. (2003). Coping with uncertainty: a call for a new science-policy forum. *AMBIO: A Journal of the Human Environment*, 32(5), 330-335.
- Krey, V. (2014). Global energy-climate scenarios and models: a review. *Wiley Interdisciplinary Reviews: Energy and Environment*, 3(4), 363-383.
- Lahtinen, T. J., Hämäläinen, R. P., & Liesiö, J. (2017). Portfolio decision analysis methods in environmental decision making. *Environmental modelling & software*, 94, 73-86.
- Laumanns, M., Thiele, L., & Zitzler, E. (2006). An efficient, adaptive parameter variation scheme for metaheuristics based on the epsilon-constraint method. *European Journal of Operational Research*, 169(3), 932-942.
- Le Quéré, C., Jackson, R. B., Jones, M. W., Smith, A. J., Abernethy, S., Andrew, R. M., Friedlingstein, P., Creutzig, F., & Peters, G. P. (2020). Temporary reduction in daily global CO₂ emissions during the COVID-19 forced confinement. *Nature Climate Change*, 1-7.
- Levoyannis C. (2021). The EU Green Deal and the Impact on the Future of Gas and Gas Infrastructure in the European Union. In: Mathioulakis M. (eds), *Aspects of the Energy Union. Energy, Climate and the Environment* (pp. 201-224). Cham: Palgrave Macmillan.
- Lin, Z., & Beck, M. B. (2012). Accounting for structural error and uncertainty in a model: An approach based on model parameters as stochastic processes. *Environmental modelling & software*, 27, 97-111.
- Liu, L., Hejazi, M., Iyer, G., & Forman, B. A. (2019). Implications of water constraints on electricity capacity expansion in the United States. *Nature Sustainability*, 2(3), 206.
- Liu, S., & Papageorgiou, L. G. (2013). Multiobjective optimisation of production, distribution and capacity planning of global supply chains in the process industry. *Omega*, 41(2), 369-382.
- Manzanedo, R. D., & Manning, P. (2020). COVID-19: Lessons for the climate change emergency. *Science of the Total Environment*, 742, 140563.



- Marinoni, O., Adkins, P., & Hajkowicz, S. (2011). Water planning in a changing climate: joint application of cost utility analysis and modern portfolio theory. *Environmental Modelling & Software*, 26(1), 18-29.
- Markowitz, H. (1952). Portfolio selection. *The journal of finance*, 7(1), 77-91.
- Martello, S., & Monaci, M. (2020). Algorithmic approaches to the multiple knapsack assignment problem. *Omega*, 90, 102004.
- Mastorakis, K., & Siskos, E. (2016). Value focused pharmaceutical strategy determination with multicriteria decision analysis techniques. *Omega*, 59, 84-96.
- Mavrotas, G. (2009). Effective implementation of the ϵ -constraint method in multi-objective mathematical programming problems. *Applied mathematics and computation*, 213(2), 455-465.
- Mavrotas, G., & Florios, K. (2013). An improved version of the augmented ϵ -constraint method (AUGMECON2) for finding the exact pareto set in multi-objective integer programming problems. *Applied Mathematics and Computation*, 219(18), 9652-9669.
- Mavrotas, G., Figueira, J. R., & Antoniadis, A. (2011). Using the idea of expanded core for the exact solution of bi-objective multi-dimensional knapsack problems. *Journal of Global Optimization*, 49(4), 589-606.
- Mavrotas, G., Figueira, J. R., & Siskos, E. (2015). Robustness analysis methodology for multi-objective combinatorial optimization problems and application to project selection. *Omega*, 52, 142-155.
- Mavrotas, G., Gakis, N., Skoulaxinou, S., Katsouros, V., & Georgopoulou, E. (2015). Municipal solid waste management and energy production: Consideration of external cost through multi-objective optimization and its effect on waste-to-energy solutions. *Renewable and Sustainable Energy Reviews*, 51, 1205-1222.
- Mavrotas, G., Skoulaxinou, S., Gakis, N., Katsouros, V., & Georgopoulou, E. (2013). A multi-objective programming model for assessment the GHG emissions in MSW management. *Waste Management*, 33(9), 1934-1949.
- Miles, D., Stedman, M., & Heald, A. (2020). Living with COVID-19: balancing costs against benefits in the face of the virus. *National Institute Economic Review*, 253, R60-R76.
- Mohammadi, M., Jula, P., & Tavakkoli-Moghaddam, R. (2019). Reliable single-allocation hub location problem with disruptions. *Transportation Research Part E: Logistics and Transportation Review*, 123, 90-120.
- Mohammadkhani, N., Sedighzadeh, M., & Esmaili, M. (2018). Energy and emission management of CCHPs with electric and thermal energy storage and electric vehicle. *Thermal Science and Engineering Progress*, 8, 494-508.
- Mohammed, A. M., & Duffuaa, S. O. (2020). A tabu search based algorithm for the optimal design of multi-objective multi-product supply chain networks. *Expert Systems with Applications*, 140, 112808.
- Mousazadeh, M., Torabi, S. A., Pishvae, M. S., & Abolhassani, F. (2018). Accessible, stable, and equitable health service network redesign: A robust mixed possibilistic-flexible approach. *Transportation Research Part E: Logistics and Transportation Review*, 111, 113-129.
- Muñoz, J. I., de la Nieta, A. A. S., Contreras, J., & Bernal-Agustín, J. L. (2009). Optimal investment portfolio in renewable energy: The Spanish case. *Energy Policy*, 37(12), 5273-5284.
- Musavi, M., & Bozorgi-Amiri, A. (2017). A multi-objective sustainable hub location-scheduling problem for perishable food supply chain. *Computers & Industrial Engineering*, 113, 766-778.
- Nicola, M., Alsafi, Z., Sohrabi, C., Kerwan, A., Al-Jabir, A., Iosifidis, C., ... & Agha, R. (2020). The socio-economic



- implications of the coronavirus pandemic (COVID-19): A review. *International journal of surgery*, 78, 185.
- Nikas, A., Doukas, H., & Papandreou, A. (2019). A detailed overview and consistent classification of climate-economy models. In *Understanding Risks and Uncertainties in Energy and Climate Policy* (pp. 1-54). Springer, Cham.
- Nikas, A., Forouli, A., Fountoulakis, A., & Doukas, H. (2020). A robust augmented ϵ -constraint method (AUGMECON-R) for finding exact solutions of multi-objective linear programming problems. *Operational Research*, in press.
- Nikas, A., Gambhir, A., Trutnevyte, E., Koasidis, K., Lund, H., Thellufsen, J. Z., Mayer, D., Zachmann, G., Miguel, L. J., Ferreras-Alonso, N., Sognaes, I., Peters, G., Colombo, E., Howells, M., Hawkes, A., van den Broek, M., Van de Ven, D. J., Gonzalez-Eguino, M., Flamos, A., & Doukas, H. (2021). Perspective of comprehensive and comprehensible multi-model energy and climate science in Europe. *Energy*, 215.
- Nikas, A., Lieu, J., Sorman, A., Gambhir, A., Turhan, E., Baptista, B. V., & Doukas, H. (2020). The desirability of transitions in demand: Incorporating behavioural and societal transformations into energy modelling. *Energy Research & Social Science*, 70, 101780.
- Nikas, A., Stavrakas, V., Arsenopoulos, A., Doukas, H., Antosiewicz, M., Witajewski-Baltvilks, J., & Flamos, A. (2020). Barriers to and consequences of a solar-based energy transition in Greece. *Environmental Innovation and Societal Transitions*, 35, 383-399.
- O'Neill, B. C., Kriegler, E., Ebi, K. L., Kemp-Benedict, E., Riahi, K., Rothman, D. S., ... & Levy, M. (2017). The roads ahead: Narratives for shared socioeconomic pathways describing world futures in the 21st century. *Global Environmental Change*, 42, 169-180.
- O'Neill, B. C., Kriegler, E., Riahi, K., Ebi, K. L., Hallegatte, S., Carter, T. R., ... & van Vuuren, D. P. (2014). A new scenario framework for climate change research: the concept of shared socioeconomic pathways. *Climatic change*, 122(3), 387-400.
- Odeh, R. P., Watts, D., & Negrete-Pincetic, M. (2018). Portfolio applications in electricity markets review: Private investor and manager perspective trends. *Renewable and Sustainable Energy Reviews*, 81, 192-204.
- Oke, O., & Siddiqui, S. (2015). Efficient automated schematic map drawing using multiobjective mixed integer programming. *Computers & Operations Research*, 61, 1-17.
- Ortega, M., del Río, P., Ruiz, P., Nijs, W., & Politis, S. (2020). Analysing the influence of trade, technology learning and policy on the employment prospects of wind and solar energy deployment: The EU case. *Renewable and Sustainable Energy Reviews*, 122, 109657.
- Pachauri, R. K. et al. (2015) IPCC, 2014: Climate Change 2014: Synthesis Report. Contribution of Working Groups I, II and III to the Fifth Assessment Report of the Intergovernmental Panel on Climate Change. IPCC.
- Papapostolou, A., Karakosta, C., Nikas, A., & Psarras, J. (2017). Exploring opportunities and risks for RES-E deployment under Cooperation Mechanisms between EU and Western Balkans: A multi-criteria assessment. *Renewable and Sustainable Energy Reviews*, 80, 519-530.
- Paul, N. R., Lunday, B. J., & Nurre, S. G. (2017). A multiobjective, maximal conditional covering location problem applied to the relocation of hierarchical emergency response facilities. *Omega*, 66, 147-158.
- Paydar, Z., & Qureshi, M. E. (2012). Irrigation water management in uncertain conditions—Application of Modern Portfolio Theory. *Agricultural water management*, 115, 47-54.



- Peters, G. P. (2016). The 'best available science' to inform 1.5 C policy choices. *Nature Climate Change*, 6(7), 646.
- Pietzcker, R. C., Ueckerdt, F., Carrara, S., De Boer, H. S., Després, J., Fujimori, S., ... & Luderer, G. (2017). System integration of wind and solar power in integrated assessment models: A cross-model evaluation of new approaches. *Energy Economics*, 64, 583-599.
- Pugh, G., Clarke, L., Marlay, R., Kyle, P., Wise, M., McJeon, H., & Chan, G. (2011). Energy R&D portfolio analysis based on climate change mitigation. *Energy Economics*, 33(4), 634-643.
- Qiu, R., Zhang, H., Gao, X., Zhou, X., Guo, Z., Liao, Q., & Liang, Y. (2019). A multi-scenario and multi-objective scheduling optimization model for liquefied light hydrocarbon pipeline system. *Chemical Engineering Research and Design*, 141, 566-579.
- Rabbani, M., Saravi, N. A., Farrokhi-Asl, H., Lim, S. F. W., & Tahaei, Z. (2018). Developing a sustainable supply chain optimization model for switchgrass-based bioenergy production: A case study. *Journal of cleaner production*, 200, 827-843.
- Rahimi, Y., Torabi, S. A., & Tavakkoli-Moghaddam, R. (2019). A new robust-possibilistic reliable hub protection model with elastic demands and backup hubs under risk. *Engineering Applications of Artificial Intelligence*, 86, 68-82.
- Rao, S. et al. (2017) 'Future air pollution in the Shared Socio-economic Pathways', *Global Environmental Change*, 42, pp. 346–358. doi: 10.1016/j.gloenvcha.2016.05.012.
- Rayat, F., Musavi, M., & Bozorgi-Amiri, A. (2017). Bi-objective reliable location-inventory-routing problem with partial backordering under disruption risks: A modified AMOSA approach. *Applied Soft Computing*, 59, 622-643.
- Razm, S., Nickel, S., & Sahebi, H. (2019). A multi-objective mathematical model to redesign of global sustainable bioenergy supply network. *Computers & Chemical Engineering*, 128, 1-20.
- Resat, H. G., & Turkay, M. (2015). Design and operation of intermodal transportation network in the Marmara region of Turkey. *Transportation Research Part E: Logistics and Transportation Review*, 83, 16-33.
- Resat, H. G., & Unsal, B. (2019). A novel multi-objective optimization approach for sustainable supply chain: A case study in packaging industry. *Sustainable Production and Consumption*, 20, 29-39.
- Riahi, K., Van Vuuren, D. P., Kriegler, E., Edmonds, J., O'Neill, B. C., Fujimori, S., ... & Lutz, W. (2017). The shared socioeconomic pathways and their energy, land use, and greenhouse gas emissions implications: an overview. *Global Environmental Change*, 42, 153-168.
- Roshan, M., Tavakkoli-Moghaddam, R., & Rahimi, Y. (2019). A two-stage approach to agile pharmaceutical supply chain management with product substitutability in crises. *Computers & Chemical Engineering*, 127, 200-217.
- Rutovitz, J., Dominish, E., & Downes, J. (2015). Calculating global energy sector jobs: 2015 methodology.
- Saadat, S., Rawtani, D., & Hussain, C. M. (2020). Environmental perspective of COVID-19. *Science of The Total Environment*, 138870.
- Saedinia, R., Vahdani, B., Etebari, F., & Nadjafi, B. A. (2019). Robust gasoline closed loop supply chain design with redistricting, service sharing and intra-district service transfer. *Transportation Research Part E: Logistics and Transportation Review*, 123, 121-141.
- Şakar, C. T., & Köksalan, M. (2013). A stochastic programming approach to multicriteria portfolio optimization.



- Journal of Global Optimization, 57(2), 299-314.
- Samir, K. C., & Lutz, W. (2017). The human core of the shared socioeconomic pathways: Population scenarios by age, sex and level of education for all countries to 2100. *Global Environmental Change*, 42, 181-192.
- Sazvar, Z., Rahmani, M., & Govindan, K. (2018). A sustainable supply chain for organic, conventional agro-food products: The role of demand substitution, climate change and public health. *Journal of cleaner production*, 194, 564-583.
- Schaeffer, S. E., & Cruz-Reyes, L. (2016). Static R&D project portfolio selection in public organizations. *Decision support systems*, 84, 53-63.
- Schneider, S. H. (2003). Imaginable surprise. In Potter, T. D., & Colman, B. R. (eds) *Handbook of weather, climate, and water* (pp. 947-954). Wiley Interscience, New Jersey.
- Schwanitz, V. J. (2013). Evaluating integrated assessment models of global climate change. *Environmental modelling & software*, 50, 120-131.
- Scott, M. J., Sands, R. D., Edmonds, J., Liebetrau, A. M., & Engel, D. W. (1999). Uncertainty in integrated assessment models: modeling with MiniCAM 1.0. *Energy Policy*, 27(14), 855-879.
- Sedighzadeh, M., Esmaili, M., & Mohammadkhani, N. (2018). Stochastic multi-objective energy management in residential microgrids with combined cooling, heating, and power units considering battery energy storage systems and plug-in hybrid electric vehicles. *Journal of cleaner production*, 195, 301-317.
- Shah, R., & Reed, P. (2011). Comparative analysis of multiobjective evolutionary algorithms for random and correlated instances of multiobjective d-dimensional knapsack problems. *European Journal of Operational Research*, 211(3), 466-479.
- Shekarian, M., Nooraie, S. V. R., & Parast, M. M. (2019). An examination of the impact of flexibility and agility on mitigating supply chain disruptions. *International Journal of Production Economics*.
- Shi, W., Ou, Y., Smith, S. J., Ledna, C. M., Nolte, C. G., & Loughlin, D. H. (2017). Projecting state-level air pollutant emissions using an integrated assessment model: GCAM-USA. *Applied energy*, 208, 511-521.
- Shmelev, S. E., & van den Bergh, J. C. (2016). Optimal diversity of renewable energy alternatives under multiple criteria: An application to the UK. *Renewable and Sustainable Energy Reviews*, 60, 679-691.
- Steuer, R. (1989) *Multiple criteria optimization: theory, computation and application*. Malabar, Fla: Krieger.
- Sylva, J., & Crema, A. (2007). A method for finding well-dispersed subsets of non-dominated vectors for multiple objective mixed integer linear programs. *European Journal of Operational Research*, 180(3), 1011-1027.
- Tartibu, L. K., Sun, B. O. H. U. A., & Kaunda, M. A. E. (2015). Optimal design study of thermoacoustic regenerator with lexicographic optimization method. *Journal of engineering, design and technology*, 13(3), 499-519.
- Tollefson, J. (2020). Why deforestation and extinctions make pandemics more likely. *Nature*, 584(7820), 175-176.
- Torabi, S. A., Hamed, M., & Ashayeri, J. (2013). A new optimization approach for nozzle selection and component allocation in multi-head beam-type SMD placement machines. *Journal of Manufacturing Systems*, 32(4), 700-714.
- Trachanas, G. P., Forouli, A., Gkonis, N., & Doukas, H. (2018). Hedging uncertainty in energy efficiency strategies: a minimax regret analysis. *Operational Research*, 1-16.
- Turnheim, B., Berkhout, F., Geels, F., Hof, A., McMeekin, A., Nykvist, B., & van Vuuren, D. (2015). Evaluating



sustainability transitions pathways: Bridging analytical approaches to address governance challenges. *Global Environmental Change*, 35, 239-253.

Uusitalo, L., Lehikoinen, A., Helle, I., & Myrberg, K. (2015). An overview of methods to evaluate uncertainty of deterministic models in decision support. *Environmental Modelling & Software*, 63, 24-31.

Vafaenezhad, T., Tavakkoli-Moghaddam, R., & Cheikhrouhou, N. (2019). Multi-objective mathematical modeling for sustainable supply chain management in the paper industry. *Computers & Industrial Engineering*.

Van de Ven, D. J., Sampedro, J., Johnson, F. X., Bailis, R., Forouli, A., Nikas, A., Yu, S., Pardo, G., de Jalón, S.G., Wise, M., & Doukas, H. (2019). Integrated policy assessment and optimisation over multiple sustainable development goals in Eastern Africa. *Environmental Research Letters*, 14(9), 094001.

Van Dingenen, R., Dentener, F., Crippa, M., Leitao, J., Marmer, E., Rao-Skirbekk, S., Solazzo, E., & Valentini, L. (2018). TM5-FASST: a global atmospheric source-receptor model for rapid impact analysis of emission changes on air quality and short-lived climate pollutants.

Van Groenendaal, W. J., & Kleijnen, J. P. (2002). Deterministic versus stochastic sensitivity analysis in investment problems: an environmental case study. *European Journal of Operational Research*, 141(1), 8-20.

Van Ruijven, B. J., Levy, M. A., Agrawal, A., Biermann, F., Birkmann, J., Carter, T. R., Ebi, K.L., Garschagen, M., Jones, B., Jones, R., & Kemp-Benedict, E. (2014). Enhancing the relevance of Shared Socioeconomic Pathways for climate change impacts, adaptation and vulnerability research. *Climatic Change*, 122(3), 481-494.

Van Vliet, O.P.R., Hanger-Kopp, S., Nikas, A., Spijker, E., Carlsen, H., Doukas, H., & Lieu, J. (2020). The importance of stakeholders in scoping risk assessments – lessons from low-carbon transitions. *Environmental Innovation and Societal Transitions* 35, 400-413.

Vieira, M., Pinto-Varela, T., & Barbosa-Póvoa, A. P. (2017). Production and maintenance planning optimisation in biopharmaceutical processes under performance decay using a continuous-time formulation: A multi-objective approach. *Computers & Chemical Engineering*, 107, 111-139.

Vilkkumaa, E., Salo, A., & Liesiö, J. (2014). Multicriteria portfolio modeling for the development of shared action agendas. *Group decision and negotiation*, 23(1), 49-70.

Wang, S., Wang, X., Yu, J., Ma, S., & Liu, M. (2018). Bi-objective identical parallel machine scheduling to minimize total energy consumption and makespan. *Journal of cleaner production*, 193, 424-440.

Warren, R. F., Edwards, N. R., Babonneau, F., Bacon, P. M., Dietrich, J. P., Ford, R. W., ... & Hiscock, K. (2019). Producing policy-relevant science by enhancing robustness and model integration for the assessment of global environmental change. *Environmental modelling & software*, 111, 248-258.

Wei, M., Patadia, S., & Kammen, D. M. (2010). Putting renewables and energy efficiency to work: How many jobs can the clean energy industry generate in the US?. *Energy policy*, 38(2), 919-931.

Weyant, J. (2017). Some contributions of integrated assessment models of global climate change. *Review of Environmental Economics and Policy*, 11(1), 115-137.

Wiedemann, P. (1978). Planning with multiple objectives. *Omega*, 6(5), 427-432.

Witting, K., Ober-Blöbaum, S., & Dellnitz, M. (2013). A variational approach to define robustness for parametric multiobjective optimization problems. *Journal of Global Optimization*, 57(2), 331-345.

World Bank (2015) 'Beyond Connections: Energy Access Redefined', Technical Report, 008/15, pp. 1–244. Available at: <http://www.worldbank.org/content/dam/Worldbank/Topics/Energy> and



Extract/Beyond_Connections_Energy_Access_Redefined_Exec_ESMAP_2015.pdf.

- World Nuclear News (WNN). (2019). Study highlights nuclear's value to EU employment. Retrieved from: <https://www.world-nuclear-news.org/Articles/Study-highlights-nuclears-value-to-EU-employment>
- Wyrwa, A. (2015). An optimization platform for Poland's power sector considering air pollution and health effects. *Environmental Modelling & Software*, 74, 227-237.
- Xidonas, P., Mavrotas, G., & Psarras, J. (2010). Equity portfolio construction and selection using multiobjective mathematical programming. *Journal of Global Optimization*, 47(2), 185-209.
- Xidonas, P., Mavrotas, G., Zopounidis, C., & Psarras, J. (2011). IPSSIS: An integrated multicriteria decision support system for equity portfolio construction and selection. *European Journal of Operational Research*, 210(2), 398-409.
- Xin, S., Liang, Y., Zhou, X., Li, W., Zhang, J., Song, X., ... & Zhang, H. (2019). A two-stage strategy for the pump optimal scheduling of refined products pipelines. *Chemical Engineering Research and Design*, 152, 1-19.
- Xiong, B., Chen, H., An, Q., & Wu, J. (2019). A multi-objective distance friction minimization model for performance assessment through data envelopment analysis. *European Journal of Operational Research*.
- Yu, L., Zhang, C., Yang, H., & Miao, L. (2018). Novel methods for resource allocation in humanitarian logistics considering human suffering. *Computers & Industrial Engineering*, 119, 1-20.
- Yu, S., Eom, J., Zhou, Y., Evans, M., & Clarke, L. (2014). Scenarios of building energy demand for China with a detailed regional representation. *Energy*, 67, 284-297.
- Zhang, S., Zhao, T., & Xie, B. C. (2018). What is the optimal power generation mix of China? An empirical analysis using portfolio theory. *Applied energy*, 229, 522-536.
- Zhang, W., & Reimann, M. (2014). A simple augmented ϵ -constraint method for multi-objective mathematical integer programming problems. *European Journal of Operational Research*, 234(1), 15-24.
- Zhang, Y., Masuku, C. M., & Biegler, L. T. (2019). An MPCC reactive distillation optimization model for multi-objective Fischer-Tropsch synthesis. In *Computer Aided Chemical Engineering* (Vol. 46, pp. 451-456). Elsevier.
- Zhou, L., Geng, N., Jiang, Z., & Wang, X. (2018). Multi-objective capacity allocation of hospital wards combining revenue and equity. *Omega*, 81, 220-233.



Appendix A: Source code of AUGMECON-R

Set

```
I 'constraints' / i1* i4 /
J 'decision variables' / j1*j40 /
K 'objective functions' / k1* k4 /
;
```

Parameter

```
dir(k) 'direction of the objective functions 1 for max and -1 for min' / k1 1,
k2 1, k3 1, k4 1 /
b(I) 'RHS of the constraints' / i1 1570, i2 1210 , i3 1355, i4 1035/;
```

Table c(J,K) 'matrix of objective function coefficients C'

	k1	k2	k3	k4
j1	7	22	17	5
j2	13	10	11	25
j3	16	20	5	8
j4	19	20	11	18
j5	24	20	3	20
j6	24	3	7	10
j7	23	24	4	7
j8	6	7	19	20
j9	5	24	8	17
j10	20	16	8	11
j11	10	24	3	10
j12	7	14	7	15
j13	23	20	9	2
j14	3	8	15	20
j15	7	3	16	23
j16	20	19	19	18
j17	9	10	10	10
j18	13	4	12	5
j19	20	2	12	4
j20	18	17	13	11
j21	17	10	12	23
j22	6	10	7	24
j23	7	15	19	8
j24	10	7	11	15
j25	11	12	24	12
j26	5	7	22	8
j27	22	10	5	3
j28	16	17	21	21
j29	16	7	13	16
j30	3	10	14	5
j31	8	23	24	11
j32	3	11	4	19
j33	20	10	5	2
j34	18	15	7	9
j35	10	4	5	19
j36	22	9	8	21
j37	6	19	13	8
j38	20	10	10	3



j39	12	24	17	6
j40	11	24	16	21

;

Table a(J,I) 'matrix of technological coefficients A'

	i1	i2	i3	i4
j1	78	59	53	76
j2	94	67	75	51
j3	97	88	117	88
j4	116	107	101	102
j5	50	65	77	90
j6	62	77	88	114
j7	66	93	52	107
j8	110	89	64	94
j9	63	107	118	57
j10	59	110	87	71
j11	118	95	66	58
j12	104	77	101	114
j13	117	111	116	106
j14	120	97	105	94
j15	65	100	65	109
j16	102	95	97	73
j17	100	69	84	81
j18	97	99	55	77
j19	61	66	99	53
j20	102	113	103	85
j21	71	89	115	71
j22	86	73	91	99
j23	53	85	98	56
j24	110	88	64	84
j25	58	84	113	101
j26	87	58	60	50
j27	69	76	83	69
j28	69	79	111	83
j29	71	96	81	113
j30	83	75	64	94
j31	85	112	110	84
j32	88	81	80	75
j33	109	63	61	71
j34	115	103	56	80
j35	106	112	69	105
j36	95	68	75	76
j37	98	71	71	83
j38	87	52	52	80
j39	102	94	109	54
j40	56	107	63	101



;

Variable

Z(K) 'objective function variables'
X(J) 'decision variables';

Binary Variable X;**Equations**

objfun(K) objective functions
con(I) constraints

;

objfun(K) .. sum(J, c(J,K) *X(J)) =e= Z(K);
con(I) .. sum(J, a(J,I) *X(J)) =l= b(I);

Model example / all /;

\$STitle eps-constraint method

Set k1(k) the first element of k, kml(k) all but the first elements of k;
k1(k)\$(ord(k)=1) = **yes**; kml(k)=**yes**; kml(k1) = **no**;
Set kk(k) active objective function in constraint allobj ;

Parameter

rhs(k) right hand side of the constrained obj functions in eps-constraint
maxobj(k) maximum value from the payoff table
minobj(k) minimum value from the payoff table
numk(k) ordinal value of k starting with 1
range(k) maxobj-minobj ;

Scalar

iter total number of iterations
infeas total number of infeasibilities
elapsed_time elapsed time for payoff and e-constraint
start start time
finish finish time ;

Variables

a_objval auxiliary variable for the objective function
obj auxiliary variable during the construction of the payoff table ;

Positive Variables

sl(k) slack or surplus variables for the eps-constraints ;

Equations

con_obj(k) constrained objective functions
augm_obj augmented objective function to avoid weakly efficient solutions
allobj all the objective functions in one expression;

con_obj(kml) .. z(kml) - dir(kml) *sl(kml) =e= rhs(kml);

** We optimize the first objective function and put the others as constraints*



```

* the second term is for avoiding weakly efficient points

* objfun=max z1 + 0.001*(s1/r1+0.1 s2/r2+ 0.01*s3/r3+...)
augm_obj..
    sum(k1,dir(k1)*z(k1))+1.0e-3*sum(km1,power(10,-(numk(km1)-
1))*s1(km1)/(maxobj(km1)-minobj(km1))) =e= a_objval;

allobj..    sum(kk, dir(kk)*z(kk)) =e= obj;

Model mod_payoff      / example, allobj / ;
Model mod_epsmethod / example, con_obj, augm_obj / ;

Parameter
    payoff(k,k)  payoff tables entries;
Alias (k, kp);

option optcr=0.0;
option limrow=0, limcol=0, solprint=off, solveLink = %solveLink.LoadLibrary% ;
$offlisting;
$offsymxref;
$offsymlist;
$offuelxref;
$offuelist;
*,solveLink = %solveLink.LoadLibrary%
*file cplexopt /cplex.opt/;
*put cplexopt;
*put 'threads 4'/;
*put 'parallelmode 1'/;
*putclose cplexopt;
*mod_epsmethod.optfile=1;
*option optca=0.;
*mod_payoff.optfile=1;
*mod_epsmethod.optfile=1;

* Generate payoff table applying lexicographic optimization
loop(kp,
    kk(kp)=yes;
    repeat
        solve mod_payoff using mip maximizing obj;
        payoff(kp,kk) = z.l(kk);
        z.fx(kk) = z.l(kk);
        kk(k++1) = kk(k);
    until kk(kp); kk(kp) = no;
* release the fixed values of the objective functions for the new iteration
    z.up(k) = inf; z.lo(k) =-inf;
);
if (mod_payoff.modelstat<>1 and mod_payoff.modelstat<>8, abort 'no optimal
solution for mod_payoff');

File fx / 4kp40_uncorrelated_nadir.txt /;

PUT fx ' PAYOFF TABLE' / ;
loop (kp,

```



```

        loop(k, put payoff(kp,k):12:2);
        put /;
    );
put fx /;

*display payoff;
*minobj(k)=smin(kp,payoff(kp,k));
**$ontext
*Ideally minobj(k) could be set to zero value minobj(k)=0;
minobj(k)=floor(0.088*smin(kp,payoff(kp,k)));
maxobj(k)=smax(kp,payoff(kp,k));
range(k)=(maxobj(k)-minobj(k));
*$ontext
*$set fname h.%scrext.dat%

*gridpoints=max integer of km1

$if not set gridpoints_1 $set gridpoints_1 1000
$if not set gridpoints_2 $set gridpoints_2 1000
$if not set gridpoints_3 $set gridpoints_3 1000
*Generally speaking gridpoints are set to a very large value
Set g grid points /g0*g%gridpoints%/
    grid(k,g) 'grid '
    q    /q0*q%gridpoints_1%/
    r    /r0*r%gridpoints_2%/
    s    /s0*s%gridpoints_3%/

;

```

Parameter

gridrhs(k,g)
 maxg(k) maximum point in grid for objective
 posg(k) grid position of objective
 firstOffMax, lastZero, current1, current2, current3, synthiki, b2, b3, b4,
 terminal1, terminal2, terminal3, controll1, control2, range1, range2, range3 some
 counters

* numk(k) ordinal value of k starting with 1
 numg(g) 'ordinal value of g starting with 0 '
 step(k) step of grid points in objective functions
 jump(k) jumps in the grid points' traversing only for the first objective
 function

numq(q) ordinal value of q starting with zero
 numr(r) ordinal value of r starting with zero
 nums(s) ordinal value of s starting with zero
 flag(q,r,s) memory matrix

```

;

lastZero=1; loop(km1, numk(km1)=lastZero; lastZero=lastZero+1); numg(g) = ord(g) -

```



```

1;
numq(q) = ord(q)-1;
numr(r) = ord(r)-1;
nums(s) = ord(s)-1;
range1=sum(k$(ord(k)=2),range(k));
range2=sum(k$(ord(k)=3),range(k));
range3=sum(k$(ord(k)=4),range(k));

loop(q$(numq(q)<range1+1),
      loop(r$(numr(r)<range2+1),
            loop(s$(nums(s)<range3+1), flag(q,r,s)=0);)););

grid(km1,g) = yes;
maxg(k)=range(k);
step(km1) = 1;
gridrhs(grid(km1,g))$(dir(km1)=-1) = maxobj(km1) - numg(g)/maxg(km1)*(maxobj(km1) -
minobj(km1));
gridrhs(grid(km1,g))$(dir(km1)=1) = minobj(km1) + numg(g)*step(km1);
*display gridrhs;

*PUT fx ' Grid points' / ;
*loop (g,
*      loop(km1, put gridrhs(km1,g):12:2);
*      put /;
*      );
put fx /;
put fx 'Efficient solutions' /;

* Walk the grid points and take shortcuts if the model becomes infeasible
posg(km1) = 0;

iter=0;
infeas=0;
terminal1=0;
terminal2=0;
terminal3=0;
terminal1=sum(km1$(numk(km1)=1),maxg(km1));
terminal2=sum(km1$(numk(km1)=2),maxg(km1));
terminal3=sum(km1$(numk(km1)=3),maxg(km1));
synthiki=0;
controll=0;
start=jnow;

repeat
rhs(km1) = sum(grid(km1,g)$(numg(g)=posg(km1)), gridrhs(km1,g));
current1=0;
current2=0;
current3=0;
current1=sum(km1$(numk(km1)=1),posg(km1)) ;
current2=sum(km1$(numk(km1)=2),posg(km1)) ;

```




```

current3=sum(km1$(numk(km1)=3),posg(km1)) ;
loop(q$(numq(q)=current1),
  loop(r$(numr(r)=current2),
    loop(s$(nums(s)=current3), synthiki=flag(q,r,s));));
if(synthiki=0, solve mod_epsmethod maximizing a_objval using mip);
iter=iter+1;
if (synthiki=0 and mod_epsmethod.modelstat<>1 and mod_epsmethod.modelstat<>8,
  infeas=infeas+1;
put fx iter:5:0, ' infeasible'//;
lastZero = 0; loop(km1$(posg(km1)>0 and lastZero=0), lastZero=numk(km1));
posg(km1)$(numk(km1)<=lastZero) = maxg(km1);
  loop(s$(nums(s)>=current3 and nums(s)<=terminal3),
    loop(r$(numr(r)>=current2 and numr(r)<=terminal2),
      loop(q$(numq(q)=current1), flag(q,r,s)=terminal1-current1+1));));

else if(synthiki=0 ,
  put fx iter:5:0;
  loop(k, put fx z.l(k):12:2);
  put fx ' *** ';
  loop(km1, put fx sl.l(km1):12:2, put fx posg(km1):6:0);
  put fx ' *** ';
  loop(km1$(numk(km1)=1),b2=floor(sl.l(km1)/step(km1)));
  loop(km1$(numk(km1)=2),b3=floor(sl.l(km1)/step(km1)));
  loop(km1$(numk(km1)=3),b4=floor(sl.l(km1)/step(km1)));
    loop(s$(nums(s)>=current3 and nums(s)<=current3+b4),
      loop(r$(numr(r)>=current2 and numr(r)<=current2+b3),
        loop(q$(numq(q)=current1) , flag(q,r,s)=b2+1));));

  jump(km1)=1;

* calculate only for the first constrained objective function jump(km1)
  put fx ' * ';
* loop(km1$(numk(km1)=1), jump(km1)=1+floor(sl.l(km1)/step(km1)));
jump(km1)$(numk(km1)=1)=1+floor(sl.l(km1)/step(km1));
loop(km1, put fx jump(km1):5:0) ;
loop(km1$(jump(km1)> 1), put ' jump')
put /;
);
);

jump(km1)$(numk(km1)>1)=1 ;
* Proceed forward in the grid
controll=0;
firstOffMax = 0;
loop(km1$(posg(km1)<maxg(km1) and firstOffMax=0 and numk(km1)=1 and
synthiki>0),control2=posg(km1)+synthiki;
posg(km1)=min(posg(km1)+synthiki,maxg(km1)); firstOffMax=numk(km1) );
loop(km1$(posg(km1)=maxg(km1) and numk(km1)=1 and synthiki>0 and firstOffMax>0
and control2>maxg(km1)), controll=1);
loop(km1$(posg(km1)<maxg(km1) and firstOffMax=0 and numk(km1)=1 and synthiki=0),

```



```
posg(km1)=min((posg(km1)+jump(km1)),maxg(km1)); firstOffMax=numk(km1));
  loop(km1$(posg(km1)<maxg(km1) and firstOffMax=0 and numk(km1)>1),
posg(km1)=min((posg(km1)+jump(km1)),maxg(km1)); firstOffMax=numk(km1));

  loop(km1$(posg(km1)<maxg(km1) and controll>0 and numk(km1)>1 ),
posg(km1)=min((posg(km1)+jump(km1)),maxg(km1)); firstOffMax=numk(km1);
controll=0);

      posg(km1)$(numk(km1)<firstOffMax) = 0 ;

until sum(km1$(posg(km1)=maxg(km1)),1)= card(km1) and firstOffMax=0;

finish=jnow;
elapsed_time=(finish-start)*86400;

put /;
put 'Infeasibilities = ', infeas:5:0 /;
put 'Elapsed time: ',elapsed_time:10:2, ' seconds' / ;
*$offtext
putclose fx;
**$offtext
```



Appendix B: Datasets used for the complex problems

B.1 Dataset of the 4kp40 problem

Table $c(J,K)$ 'matrix of objective function coefficients C'

	k2	k4	k3	k1
j1	7	22	17	5
j2	13	10	11	25
j3	16	20	5	8
j4	19	20	11	18
j5	24	20	3	20
j6	24	3	7	10
j7	23	24	4	7
j8	6	7	19	20
j9	5	24	8	17
j10	20	16	8	11
j11	10	24	3	10
j12	7	14	7	15
j13	23	20	9	2
j14	3	8	15	20
j15	7	3	16	23
j16	20	19	19	18
j17	9	10	10	10
j18	13	4	12	5
j19	20	2	12	4
j20	18	17	13	11
j21	17	10	12	23
j22	6	10	7	24
j23	7	15	19	8
j24	10	7	11	15
j25	11	12	24	12
j26	5	7	22	8
j27	22	10	5	3
j28	16	17	21	21
j29	16	7	13	16
j30	3	10	14	5
j31	8	23	24	11
j32	3	11	4	19
j33	20	10	5	2
j34	18	15	7	9
j35	10	4	5	19



j36	22	9	8	21
j37	6	19	13	8
j38	20	10	10	3
j39	12	24	17	6
j40	11	24	16	21

Table a(J, I) 'matrix of constraint coefficients A'

	i1	i2	i3	i4
j1	78	59	53	76
j2	94	67	75	51
j3	97	88	117	88
j4	116	107	101	102
j5	50	65	77	90
j6	62	77	88	114
j7	66	93	52	107
j8	110	89	64	94
j9	63	107	118	57
j10	59	110	87	71
j11	118	95	66	58
j12	104	77	101	114
j13	117	111	116	106
j14	120	97	105	94
j15	65	100	65	109
j16	102	95	97	73
j17	100	69	84	81
j18	97	99	55	77
j19	61	66	99	53
j20	102	113	103	85
j21	71	89	115	71
j22	86	73	91	99
j23	53	85	98	56
j24	110	88	64	84
j25	58	84	113	101
j26	87	58	60	50
j27	69	76	83	69
j28	69	79	111	83
j29	71	96	81	113
j30	83	75	64	94
j31	85	112	110	84
j32	88	81	80	75



j33	109	63	61	71
j34	115	103	56	80
j35	106	112	69	105
j36	95	68	75	76
j37	98	71	71	83
j38	87	52	52	80
j39	102	94	109	54
j40	56	107	63	101

B.2 Dataset of the 4kp50 binary problem

Table c(J,K) 'matrix of objective function coefficients C'

	k1	k3	k2	k4
j1	68	65	65	66
j2	66	50	63	69
j3	59	53	57	62
j4	55	68	69	68
j5	57	51	58	60
j6	67	56	63	70
j7	55	62	53	56
j8	54	64	53	59
j9	57	67	59	65
j10	64	50	62	66
j11	68	59	58	54
j12	62	70	69	50
j13	53	60	67	65
j14	70	62	60	58
j15	52	64	51	63
j16	55	64	53	53
j17	64	56	61	53
j18	52	61	57	57
j19	65	63	70	57
j20	57	69	63	67
j21	61	56	57	61
j22	54	68	61	59
j23	50	64	52	68
j24	57	67	64	52
j25	57	65	57	57
j26	58	67	66	58
j27	63	64	60	57



j28	55	69	70	64
j29	64	69	63	53
j30	67	60	55	55
j31	68	69	60	67
j32	63	69	66	60
j33	57	62	67	62
j34	67	57	67	56
j35	67	58	68	56
j36	68	56	52	60
j37	56	65	70	68
j38	52	69	52	59
j39	54	62	51	52
j40	55	69	64	69
j41	50	52	64	57
j42	63	63	62	69
j43	67	54	68	61
j44	68	64	57	61
j45	58	67	57	53
j46	52	52	67	53
j47	63	62	55	60
j48	53	53	65	63
j49	52	54	53	69
j50	67	67	58	66

Table a(J,I) 'matrix of constraint coefficients A'

	i1	i2	i3	i4
j1	0	1	0	0
j2	1	1	1	1
j3	1	0	1	1
j4	0	0	1	1
j5	1	1	0	1
j6	0	0	0	0
j7	1	1	1	0
j8	1	1	0	0
j9	1	0	1	1
j10	0	1	0	1
j11	1	0	1	1
j12	1	0	0	0
j13	0	0	0	1



j14	1	1	0	0
j15	1	0	1	0
j16	1	0	0	1
j17	1	1	1	1
j18	1	0	1	1
j19	0	1	1	0
j20	1	1	0	0
j21	0	1	1	0
j22	1	1	0	1
j23	1	0	1	0
j24	0	0	0	0
j25	1	1	0	1
j26	0	1	1	1
j27	1	1	1	1
j28	1	1	0	1
j29	1	1	0	1
j30	1	1	0	0
j31	0	0	1	1
j32	1	0	1	1
j33	1	1	0	0
j34	0	0	0	1
j35	0	0	0	1
j36	1	1	1	1
j37	1	0	0	1
j38	1	1	1	0
j39	0	0	0	1
j40	1	0	0	1
j41	1	1	0	0
j42	0	0	1	1
j43	1	1	1	1
j44	1	1	1	0
j45	1	1	1	0
j46	1	1	1	1
j47	0	0	0	0
j48	1	1	1	1
j49	1	1	0	0
j50	0	0	1	0



B.3 Dataset of the 5kp40 binary problem

Table c(J,K) 'matrix of objective function coefficients C'

	k1	k2	k3	k4	k5
j1	3	10	4	9	10
j2	5	4	8	9	4
j3	5	5	6	6	7
j4	5	3	3	4	5
j5	8	2	2	9	7
j6	5	5	9	6	4
j7	9	5	3	6	7
j8	4	3	3	6	2
j9	4	2	8	3	4
j10	3	9	7	5	7
j11	7	9	8	5	9
j12	8	3	5	4	3
j13	6	9	7	6	9
j14	8	7	9	5	4
j15	4	5	4	6	6
j16	5	2	8	3	8
j17	5	5	6	5	2
j18	5	2	5	5	3
j19	3	7	5	8	7
j20	3	7	4	6	5
j21	9	5	10	6	3
j22	5	7	8	10	4
j23	9	7	8	6	9
j24	4	8	4	4	2
j25	4	4	10	7	4
j26	5	3	5	8	7
j27	2	7	4	5	6
j28	7	6	5	6	7
j29	9	6	9	8	3
j30	9	3	8	4	7
j31	3	8	10	4	10
j32	9	9	5	10	9
j33	5	3	7	5	3
j34	5	6	7	4	7
j35	7	6	7	4	8
j36	3	9	3	8	4
j37	8	2	7	4	4



j38	5	7	7	3	9
j39	8	10	9	8	5
j40	8	4	8	10	7

Table a (J,I) 'matrix of constraint coefficients A'

	i1	i2	i3	i4	i5
j1	285	153	237	204	217
j2	308	192	345	162	289
j3	124	150	72	154	298
j4	131	262	227	299	370
j5	290	130	245	255	155
j6	315	71	134	270	253
j7	101	179	359	213	325
j8	323	52	57	189	398
j9	252	244	186	146	358
j10	232	389	324	232	155
j11	370	382	220	270	194
j12	232	79	202	284	184
j13	265	183	199	277	146
j14	355	62	60	79	344
j15	141	80	161	68	208
j16	163	174	139	135	286
j17	152	371	215	208	148
j18	346	192	130	389	225
j19	397	305	386	124	143
j20	135	299	107	248	259
j21	305	178	303	121	239
j22	201	357	138	145	190
j23	75	234	155	212	156
j24	369	350	318	102	94
j25	390	109	276	287	300
j26	115	260	263	79	368
j27	378	66	226	116	150
j28	80	146	349	197	65
j29	380	144	323	266	385
j30	386	265	389	238	286
j31	63	148	98	245	235
j32	324	208	334	101	347
j33	163	251	399	85	222
j34	152	131	95	252	189



j35	94	341	125	250	215
j36	360	297	164	361	199
j37	111	140	135	195	240
j38	290	337	316	151	53
j39	187	305	185	238	352
j40	272	159	74	269	186

B.4 Dataset of the 6kp50 binary problem

Table c(J,K) 'matrix of objective function coefficients C'

	k1	k2	k3	k4	k5	k6
j1	2	2	5	3	0	1
j2	5	3	3	4	4	3
j3	0	3	0	1	0	2
j4	0	2	1	3	5	4
j5	5	4	5	4	3	4
j6	4	3	1	4	5	5
j7	2	0	1	3	3	5
j8	3	1	4	1	0	2
j9	2	2	2	1	5	5
j10	0	5	3	0	1	4
j11	1	4	4	3	1	2
j12	2	0	1	0	5	4
j13	5	4	1	2	1	3
j14	2	0	4	2	3	3
j15	1	4	2	4	1	2
j16	4	1	3	1	4	2
j17	2	1	2	4	4	2
j18	0	4	2	4	4	4
j19	4	4	3	3	0	4
j20	3	2	0	0	2	3
j21	1	3	2	5	1	1
j22	3	1	2	3	0	1
j23	4	1	1	3	0	1
j24	4	4	3	5	1	0
j25	4	5	4	2	4	2
j26	4	3	4	0	4	4
j27	1	4	1	3	1	2
j28	3	4	0	0	2	4
j29	2	4	1	0	4	1



j30	3	2	3	3	5	1
j31	5	4	0	2	4	0
j32	4	4	3	4	0	1
j33	3	2	1	2	5	2
j34	0	3	5	0	3	2
j35	3	1	4	3	3	1
j36	4	4	2	2	3	1
j37	2	2	1	3	1	2
j38	2	4	2	5	1	3
j39	5	5	3	0	4	1
j40	0	2	5	2	1	3
j41	4	0	5	1	1	3
j42	3	2	5	2	4	3
j43	4	2	4	5	4	5
j44	3	4	4	3	3	0
j45	1	4	2	4	3	3
j46	3	4	1	5	2	2
j47	1	3	2	2	5	2
j48	4	4	4	3	3	0
j49	1	1	4	3	4	2
j50	1	3	2	3	3	5

Table a (J,I) 'matrix of constraint coefficients A'

	i1	i2	i3	i4	i5	i6
j1	1	0	0	0	0	1
j2	0	1	1	0	0	1
j3	0	0	0	1	1	0
j4	1	1	0	0	1	1
j5	0	0	1	0	1	1
j6	1	1	1	1	0	0
j7	1	1	0	1	0	1
j8	0	1	0	1	0	1
j9	1	1	1	0	0	1
j10	0	0	1	1	0	0
j11	0	0	0	1	0	1
j12	0	1	1	1	1	0
j13	1	0	0	1	1	1
j14	1	1	1	0	1	1
j15	0	1	1	0	1	1
j16	0	1	1	1	1	0



j17	0	0	1	0	0	1
j18	0	1	1	0	0	0
j19	0	1	1	0	1	0
j20	0	0	0	1	0	1
j21	0	0	0	1	1	0
j22	0	0	0	1	0	1
j23	1	0	1	0	0	1
j24	0	0	0	0	1	0
j25	1	0	1	0	0	0
j26	0	0	1	0	0	1
j27	0	0	1	1	0	1
j28	0	1	1	1	1	1
j29	0	0	1	1	0	1
j30	0	0	0	1	1	1
j31	1	1	0	1	1	1
j32	1	0	1	1	1	0
j33	0	0	1	0	1	1
j34	1	0	1	1	1	1
j35	1	0	0	1	1	0
j36	0	0	1	1	0	0
j37	1	0	0	0	1	0
j38	0	1	1	0	1	0
j39	0	0	1	1	0	0
j40	0	0	0	1	0	0
j41	1	0	1	1	0	0
j42	1	0	0	1	0	1
j43	0	0	0	0	1	1
j44	1	1	0	0	0	1
j45	0	0	0	1	0	1
j46	1	0	1	1	0	1
j47	1	1	1	0	1	0
j48	0	1	1	1	1	0
j49	1	0	1	0	0	0
j50	0	1	1	0	1	0

